A second-order accurate, original energy dissipative numerical scheme for chemotaxis and its convergence analysis

Jie Ding* Cheng Wang[†] Shenggao Zhou[‡]
May 22, 2025

Abstract

This paper proposes a second-order accurate numerical scheme for the Patlak–Keller–Segel system with various mobilities for the description of chemotaxis. Formulated in a variational structure, the entropy part is novelly discretized by a modified Crank-Nicolson approach so that the solution to the proposed nonlinear scheme corresponds to a minimizer of a convex functional. A careful theoretical analysis reveals that the unique solvability and positivity-preserving property could be theoretically justified. More importantly, such a second order numerical scheme is able to preserve the dissipative property of the original energy functional, instead of a modified one. To the best of our knowledge, the proposed scheme is the first second-order accurate one in literature that could achieve both the numerical positivity and original energy dissipation. In addition, an optimal rate convergence estimate is provided for the proposed scheme, in which rough and refined error estimate techniques have to be included to accomplish such an analysis. Ample numerical results are presented to demonstrate robust performance of the proposed scheme in preserving positivity and original energy dissipation in blowup simulations.

Keywords: Patlak–Keller–Segel system; second-order accuracy; unique solvability; positivity preservation; original energy dissipation; optimal rate convergence analysis **AMS subject classification**: 35K35, 35K61, 65M06, 65M12, 92C17

1 Introduction

As a classical chemotaxis model, the Patlak–Keller–Segel (PKS) system is often used to describe the evolution of living organisms interacting with environmental signals [34, 43]:

$$\begin{cases} \partial_t \rho = \gamma \Delta \rho - \chi \nabla \cdot (\eta(\rho) \nabla \phi), \\ \theta \partial_t \phi = \mu \Delta \phi - \alpha \phi + \chi \rho. \end{cases}$$
 (1.1)

Here ρ is the density distribution of living organisms, ϕ stands for the density of the chemical signals, γ , μ , and α are three positive constants, χ denotes the chemotactic sensitivity, $\eta(\rho)$

^{*}School of Science, Jiangnan University, Wuxi, Jiangsu, 214122, China. E-mail: jding@jiangnan.edu.cn.

 $^{^\}dagger Department$ of Mathematics, University of Massachusetts, North Dartmouth, MA 02747, USA. E-mail: cwang1@umassd.edu.

[‡]School of Mathematical Sciences, MOE-LSC, and CMA-Shanghai, Shanghai Jiao Tong University, Shanghai, 200240, China. E-mail: sgzhou@sjtu.edu.cn.

is the density-dependent mobility, and $\theta \geq 0$ describes how fast chemical signals respond to living organisms. To address the confinement effect in a bounded domain Ω , the PKS system is prescribed with homogeneous Neumann boundary condition:

$$\nabla \rho \cdot \mathbf{n} = \nabla \phi \cdot \mathbf{n} = 0, \quad \text{on } \partial \Omega. \tag{1.2}$$

The PKS system describes the diffusion of living organisms and aggregation induced by chemical signals. In particular, the nonlinear term $-\chi\nabla\cdot(\eta(\rho)\nabla\phi)$ models organism movement towards higher density of chemical signals. It is well-known that the solution of the classical PKS system (1.1) with $\eta(\rho) = \rho$ may blow up in finite time. Many efforts have been devoted to mathematical analysis on blowup solutions [5, 29, 30, 41, 42, 44]. According to the homogeneous Neumann boundary condition (1.2), the total mass is conserved in the PKS system. There exists a certain critical threshold value for initial total mass, by which the finite-time blow up solution and globally existent solution can be distinguished [5,7,8,33,40,42]. In fact, the 2D solution exhibits a critical-mass $(8\pi/\chi)$ phenomenon: initial data with subcritical mass lead to global existence, while initial data with supercritical mass may cause finite-time blowup [7, 8, 17, 31]. Meanwhile, in the 3D case, the solution existence becomes more subtle: blowup can occur for any positive initial mass dependent on the initial concentration, with no universal threshold [51,52], although global existence and boundedness can be established if the initial data is sufficiently small [35]. However, the density of living organisms does not blow up in reality, rather exhibiting density peaks with difference of several orders in magnitude. Modified models with various $\eta(\rho)$ have been proposed to capture such a phenomenon [36].

Many numerical methods have been proposed for the PKS system in various chemotaxis applications [2-4,21,24,39,45,50,56]. The solution to the PKS system has several properties of great physical significance, such as mass conservation, positivity for cell density, and energy dissipation. Shen and Xu develop unconditionally energy-stable schemes that preserve positivity/bounds for the PKS equations [45]. Based on the scalar auxiliary variable (SAV) approach, a high-order, linear, positivity/bound preserving and unconditionally energy-stable scheme has also been developed in [32]. Based on the Slotboom formulation, a positivity-preserving and asymptotic preserving scheme has also been constructed for the PKS system in 2D [39]. On the other hand, second-order positivity-preserving central-upwind schemes have been developed for chemotaxis models, by using the finite volume method [12] and discontinuous Galerkin approach [22, 23]. An implicit finite volume scheme has been proposed in [24], in which the existence of a positive solution is established under certain restrictions. Bessemoulin-Chatard and Jüngel have also constructed a finite volume scheme for the PKS model [4], with an additional cross-diffusion term in the second equation of (1.1). The positivity-preserving, mass conservation, entropy stability, and the well-posedness of the nonlinear scheme have been proved in the work. Zhou and Saito have introduced a linear finite volume scheme that satisfies both positivity and mass conservation requirements [56].

Because of the non-constant mobilities, the numerical design of a second order accurate in time, energy-stable algorithm for the PKS system turns out to be very challenging. In this work, we propose a novel second-order (in time) numerical scheme for the PKS equations. The standard Crank-Nicolson approximation is applied to the chemoattractant evolution equation, while the variational structure of the density equation is used to facilitate the numerical design. In more details, the mobility function is computed by an explicit second order extrapolation formula, and such an explicit treatment will be useful in the unique solvability analysis. On the other hand, a

singular logarithmic term appears in the chemical potential, and poses a great challenge for secondorder temporal discretization to ensure the theoretical properties at a discrete level. To overcome
this subtle difficulty, we approximate the logarithmic term by a careful Taylor expansion, up to the
second order accuracy. The unique solvability and positivity-preserving property of such a highly
nonlinear and singular numerical system is theoretically established, in which the convex and
singular nature of the implicit terms play a very important role in the theoretical analysis; see the
related works for various gradient flow models with singular energy potential [9–11,18–20,54,55].
This approach also avoids a nonlinear artificial regularization term in the numerical design. More
importantly, a careful nonlinear analysis reveals a dissipation property of the original free energy
functional, instead of a modified energy reported in many existing works for multi-step numerical
schemes [32,45]. This turns out to be a remarkable theoretical result for a second order accurate
scheme.

It is observed that, a highly nonlinear formulation in the numerical system, which is designed to accomplish certain structure-preserving properties at a discrete level, often poses a challenging task for a rigorous convergence analysis. In this work, an optimal rate convergence analysis is performed for the proposed second-order numerical scheme. Due to the non-constant mobility nature, together with the highly nonlinear and singular properties of the logarithmic terms, such an optimal rate convergence analysis for the PKS equations turns out to be a very complicated issue. To overcome this difficulty, several highly non-standard techniques have to be introduced. A careful linearization expansion is required for the higher-order asymptotic analysis of the numerical solution, up to the fourth order accuracy in both time and space. Such a higher-order asymptotic expansion enables one to derive a maximum norm bound for the density variable, based on a rough error estimate. Subsequently, the corresponding inner product between the discrete temporal derivative of the numerical error function and the numerical error associated with the logarithmic terms becomes a discrete derivative of certain nonlinear, non-negative functional in terms of the numerical error functions, along with a few numerical perturbation terms. Consequently, all the major challenges in the nonlinear analysis of the second-order accurate scheme could be overcome, and the associated error estimate could be carefully derived. To our knowledge, this is the first work to combine three theoretical properties for second-order accurate numerical schemes for the PKS system: positivity-preservation, original energy dissipation, and optimal rate convergence analysis.

The rest of the paper is organized as follows. In Section 2, the PKS system for chemotaxis is introduced, and the associated physical properties are recalled. Subsequently, a second-order accurate numerical scheme is proposed in Section 3. Afterwards, the structure-preserving properties of the proposed numerical scheme, such as mass conservation, unique solvability, positivity-preserving property, and the original energy dissipation, are proved in Section 4. In addition, the optimal rate convergence analysis is presented in Section 5. Some numerical results are provided in Section 6. Finally, some concluding remarks are given in Section 7.

2 Chemotaxis models

For the PKS system (1.1), the following free energy is considered:

$$F(\rho,\phi) = \int_{\Omega} \left[\gamma f(\rho) - \chi \rho \phi + \frac{\mu}{2} |\nabla \phi|^2 + \frac{\alpha}{2} \phi^2 \right] d\mathbf{x}. \tag{2.1}$$

For simplicity of presentation, the notation $\eta(\rho) = \frac{1}{f''(\rho)}$ is introduced. With an alternate representation formula $\Delta \rho = \nabla \cdot (\frac{1}{f''(\rho)} \nabla f'(\rho))$ [45], the PKS system could be rewritten as

$$\begin{cases} \partial_t \rho = \nabla \cdot \left(\frac{1}{f''(\rho)} \nabla \left[\gamma f'(\rho) - \chi \phi \right] \right) = \nabla \cdot \left(\frac{1}{f''(\rho)} \nabla \frac{\delta F}{\delta \rho} \right), \\ \theta \partial_t \phi = \mu \Delta \phi - \alpha \phi + \chi \rho = -\frac{\delta F}{\delta \phi}. \end{cases}$$
(2.2)

The homogeneous Neumann boundary condition (1.2) is imposed for both physical variables.

In this work, we consider three typical choices of the entropy function $f(\rho)$ and the corresponding mobility function $\eta(\rho)$ (see the related examples in [28, 44, 45]):

• (i) The classical PKS system:

$$\eta(\rho) = \rho, \quad f(\rho) = \rho(\ln \rho - 1), \quad \text{for } \rho \in \mathbb{I} = (0, \infty);$$
(2.3)

• (ii) PKS system with a bounded mobility [47, 48]:

$$\eta(\rho) = \frac{\rho}{\kappa \rho + 1} (\kappa > 0), \quad f(\rho) = \rho(\ln \rho - 1) + \kappa \rho^2 / 2, \quad \text{for } \rho \in \mathbb{I} = (0, \infty); \tag{2.4}$$

• (iii) PKS system with a saturation density [16, 27]:

$$\eta(\rho) = \rho(1 - \rho/M)(M > 0), \ f(\rho) = \rho \ln \rho + (M - \rho) \ln(1 - \rho/M), \ \text{for } \rho \in \mathbb{I} = (0, M), \ (2.5)$$

where M is the saturation density.

For cases (i) and (ii), the solution of the PKS equations requires the positivity of the density variable, while in the case (iii), a bound $0 < \rho < M$ is needed.

With homogeneous Neumann boundary condition, the analytical solution to (1.1) has three properties of physical importance:

• Mass conservation: the total density remains constant over time, i.e.,

$$\int_{\Omega} \rho(t, \boldsymbol{x}) d\boldsymbol{x} = \int_{\Omega} \rho(0, \boldsymbol{x}) d\boldsymbol{x}, \quad \forall t > 0;$$

• Bound/Positivity: the organism density is positive, i.e.,

$$\rho(t, \boldsymbol{x}) \in \mathbb{I}$$
, if $\rho(0, \boldsymbol{x}) \in \mathbb{I}$, for $\boldsymbol{x} \in \Omega$, $\forall t > 0$;

• Free-energy dissipation: the free-energy (2.1) decays in time [6, 13]

$$\frac{dF}{dt} = -\int_{\Omega} \left[\frac{1}{f''(\rho)} \left(\nabla \frac{\delta F}{\delta \rho} \right)^2 + \frac{1}{\theta} \left(\frac{\delta F}{\delta \phi} \right)^2 \right] d\boldsymbol{x} \le 0, \text{ for } \theta > 0.$$

3 The numerical scheme

3.1 Some notations

For simplicity, a cubic rectangular computational domain $\Omega = (a, b)^3$ is considered, with homogeneous Neumann boundary condition. Let $N \in \mathbb{N}^*$ be the number of grid points along each dimension, and h = (b - a)/N be the uniform grid spacing size. The computational domain is covered by the cell-centered grid points

$$\{x_i, y_j, z_k\} = \left\{a + (i - \frac{1}{2})h, a + (j - \frac{1}{2})h, a + (k - \frac{1}{2})h\right\},\,$$

for $i, j, k = 1, \dots, N$. Denote by $\rho_{i,j,k}$ and $\phi_{i,j,k}$ the discrete approximations of $\rho(x_i, y_j, z_k, \cdot)$ and $\phi(x_i, y_j, z_k, \cdot)$, respectively.

The standard discrete operators and notations are recalled in the finite difference discretization [49,53]. We define a uniform mesh with grid spacing h > 0: $P = \{p_i \mid i = 1, 2, \dots, N\}$, where $p_i := a + (i - \frac{1}{2})h$. The following grid function spaces, with homogeneous Neumann boundary conditions, are introduced:

$$\mathcal{C} := \{ u : P \times P \times P \to \mathbb{R} \mid u_{mN,j,k} = u_{1+mN,j,k}, \ u_{i,mN,k} = u_{i,1+mN,k}, \ u_{i,j,mN} = u_{i,j,1+mN}, \forall i, j, k = 1, 2, \dots, N, m = 0, 1 \},$$

$$\mathring{\mathscr{C}} := \left\{ u \in \mathscr{C} \mid \overline{u} := \frac{h^3}{|\Omega|} \sum_{i,j,k=1}^N u_{i,j,k} = 0 \right\},\,$$

in which $u_{i,j,k} = u(p_i, p_j, p_k)$ is taken. Meanwhile, the average and difference operators in the x-direction are given by

$$A_x f_{i+1/2,j,k} := \frac{1}{2} \left(f_{i+1,j,k} + f_{i,j,k} \right), \quad D_x f_{i+1/2,j,k} := \frac{1}{h} \left(f_{i+1,j,k} - f_{i,j,k} \right),$$

$$a_x f_{i,j,k} := \frac{1}{2} \left(f_{i+1/2,j,k} + f_{i-1/2,j,k} \right), \quad d_x f_{i,j,k} := \frac{1}{h} \left(f_{i+1/2,j,k} - f_{i-1/2,j,k} \right).$$

Average and difference operators in y and z directions, denoted by A_y , A_z , D_y , D_z , a_y , a_z , d_y , and d_z , could be analogously defined. The discrete gradient and discrete divergence become

$$\nabla_h f_{i,j,k} = \left(D_x f_{i+1/2,j,k}, D_y f_{i,j+1/2,k}, D_z f_{i,j,k+1/2} \right),$$

$$\nabla_h \cdot \vec{f}_{i,j,k} = d_x f_{i,j,k}^x + d_y f_{i,j,k}^y + d_z f_{i,j,k}^z,$$

where $\vec{f} = (f^x, f^y, f^z)$, with f^x , f^y and f^z evaluated at (i+1/2, j, k), (i, j+1/2, k), (i, j, k+1/2), respectively. The standard discrete Laplacian turns out to be

$$\Delta_h f_{i,j,k} := \nabla_h \cdot (\nabla_h f)_{i,j,k} = d_x (D_x f)_{i,j,k} + d_y (D_y f)_{i,j,k} + d_z (D_z f)_{i,j,k}.$$

Similarly, for a scalar function $\mathfrak D$ that is defined at face center points, we have

$$\nabla_h \cdot \left(\mathfrak{D} \vec{f} \right)_{i,j,k} = d_x \left(\mathfrak{D} f^x \right)_{i,j,k} + d_y \left(\mathfrak{D} f^y \right)_{i,j,k} + d_z \left(\mathfrak{D} f^z \right)_{i,j,k}.$$

If $f \in \mathcal{C}$, then $\nabla_h \cdot (\mathfrak{D} \nabla_h \cdot) : \mathcal{C} \to \mathcal{C}$ becomes

$$\nabla_h \cdot (\mathfrak{D}\nabla_h f)_{i,j,k} = d_x (\mathfrak{D}D_x f)_{i,j,k} + d_y (\mathfrak{D}D_y f)_{i,j,k} + d_z (\mathfrak{D}D_z f)_{i,j,k}.$$

For $f, \xi \in \mathcal{C}$, the discrete L^2 inner product is defined as

$$\langle f, \xi \rangle := h^3 \sum_{i,j,k=1}^N f_{i,j,k} \, \xi_{i,j,k}, \quad f, \, \xi \in \mathscr{C}.$$

Similarly, for two vector grid functions $\vec{f_s} = (f_s^x, f_s^y, f_s^z)$, s = 1, 2, evaluated at (i+1/2, j, k), (i, j + 1/2, k), (i, j, k + 1/2), respectively, the corresponding discrete inner product is given by

$$[f,\xi]_{\mathbf{x}} := \langle a_x(f\xi), 1 \rangle, \quad [f,\xi]_{\mathbf{y}} := \langle a_y(f\xi), 1 \rangle,$$

 $[f,\xi]_{\mathbf{z}} := \langle a_z(f\xi), 1 \rangle, \quad [\vec{f}_1, \vec{f}_2] := [f_1^x, f_2^x]_{\mathbf{x}} + [f_1^y, f_2^y]_{\mathbf{y}} + [f_1^z, f_2^z]_{\mathbf{z}}.$

In turn, the following norms could be introduced for $f \in \mathcal{C}$: $||f||_2^2 := \langle f, f \rangle$, $||f||_p^p := \langle |f|^p, 1 \rangle$, with $1 \le p < \infty$, and $||f||_{\infty} := \max_{1 \le i,j,k \le N} |f_{i,j,k}|$. The gradient norms are defined as

$$\|\nabla_{h}f\|_{2}^{2} := [\nabla_{h}f, \nabla_{h}f] = [D_{x}f, D_{x}f]_{x} + [D_{y}f, D_{y}f]_{y} + [D_{z}f, D_{z}f]_{z}, \quad \forall f \in \mathscr{C},$$

$$\|\nabla_{h}f\|_{p}^{p} := [|D_{x}f|^{p}, 1]_{x} + [|D_{y}f|^{p}, 1]_{y} + [|D_{z}f|^{p}, 1]_{z}, \quad \forall f \in \mathscr{C}, \quad 1 \le p < \infty.$$

The higher-order norms could be similarly introduced:

$$||f||_{H_h^1}^2 := ||f||_2^2 + ||\nabla_h f||_2^2, \quad ||f||_{H_h^2}^2 := ||f||_{H_h^1}^2 + ||\Delta_h f||_2^2, \quad \forall f \in \mathscr{C}.$$

We now define a discrete analogue of the space $H^{-1}(\Omega)$. Consider a positive, scalar function \mathfrak{D} . For any $g \in \mathring{\mathfrak{C}}$, there exists a unique solution $f \in \mathring{\mathfrak{C}}$ to the equation

$$\mathbb{Q}_{\mathfrak{D}}f:=-\nabla_h\cdot(\mathfrak{D}\nabla_hf)=g,$$

with discrete homogeneous Neumann boundary condition

$$f_{mN,j,k} = f_{1+mN,j,k}, f_{i,mN,k} = f_{i,1+mN,k}, f_{i,j,mN} = f_{i,j,1+mN}$$
 for $i,j,k=1,\cdots,N, m=0,1$.

Then the following discrete norm could be introduced:

$$\|g\|_{\mathbb{Q}_{\mathfrak{D}}^{-1}} = \sqrt{\langle g, \mathbb{Q}_{\mathfrak{D}}^{-1}(g) \rangle}.$$

In particular, if $\mathfrak{D}=1$, we have $\mathfrak{Q}_1f=-\Delta_hf$, and a discrete $\|\cdot\|_{-1,h}$ norm becomes

$$||g||_{-1,h} = \sqrt{\langle g, (-\Delta_h)^{-1}(g)\rangle}.$$

Lemma 3.1 [25, 49, 53] For any ϕ_1 , ϕ_2 , ϕ_3 , $g \in \mathcal{C}$, and any $\vec{f} = (f^x, f^y, f^z)$, with f^x , f^y and f^z evaluated at (i + 1/2, j, k), (i, j + 1/2, k), (i, j, k + 1/2), respectively, the following summation-by-parts formulas are valid:

$$\left\langle \phi_1, \nabla_h \cdot \vec{f} \right\rangle = - [\nabla_h \phi_1, \vec{f}], \quad \left\langle \phi_2, \nabla_h \cdot (g \nabla_h \phi_3) \right\rangle = - [\nabla_h \phi_2, \mathcal{A}_h(g) \nabla_h \phi_3],$$

where the vector $\mathcal{A}_h(g)\nabla_h\phi_3=(A_xgD_x\phi_3,A_ygD_y\phi_3,A_zgD_z\phi_3).$

Second-order accurate numerical scheme

We consider uniform temporal discretization with a time step size Δt , and define time steps $t_n = n\Delta t, \ t_{n+\frac{1}{2}} = n\Delta t + \frac{\Delta t}{2}$. Denote by $\rho_{i,j,k}^n$ and $\phi_{i,j,k}^n$ the approximations of $\rho(n\Delta t, x_i, y_j, z_k)$ and $\phi(n\Delta t, x_i, y_j, z_k)$ for $i, j, k = 1, \dots, N$. Moreover, denote by ρ^n and ϕ^n the approximate grid

To derive second-order temporal discretization, we start with the following approximation

$$\left. \frac{\delta F}{\delta \rho} \right|_{t=t_{n+1/2}} \approx \gamma \frac{f(\rho^{n+1}) - f(\rho^n)}{\rho^{n+1} - \rho^n} - \chi \phi^{n+1/2}.$$

By a third order Taylor expansion, one obtains

$$\left. \frac{\delta F}{\delta \rho} \right|_{t=t_{n+1/2}} \approx \gamma S^{n+\frac{1}{2}} - \chi \phi^{n+1/2},$$

where

$$S^{n+\frac{1}{2}} = f'(\rho^{n+1}) - \frac{1}{2}f''(\rho^{n+1})(\rho^{n+1} - \rho^n) + \frac{1}{6}f'''(\rho^{n+1})(\rho^{n+1} - \rho^n)^2.$$

A third order expansion brings several crucial advantages in preserving structure properties of the analytical solution to the PKS system. With such an approximation, we propose the following

$$\frac{\rho^{n+1} - \rho^n}{\Delta t} = \nabla_h \cdot \left[\frac{1}{f''(\hat{\rho}^{n+\frac{1}{2}})} \nabla_h \left(\gamma S^{n+\frac{1}{2}} - \chi \phi^{n+\frac{1}{2}} + \frac{\chi^2 \Delta t}{4\theta} (\rho^{n+1} - \rho^n) \right) \right], \tag{3.1}$$

$$\theta \frac{\phi^{n+1} - \phi^n}{\Delta t} = \mu \Delta_h \phi^{n+\frac{1}{2}} - \alpha \phi^{n+\frac{1}{2}} + \chi \rho^{n+\frac{1}{2}}, \tag{3.2}$$

where the mobility function at $t_{n+\frac{1}{2}}$, namely $\frac{1}{f''(\hat{\rho}^{n+\frac{1}{2}})}$, is approximated by using

$$\hat{\rho}^{n+\frac{1}{2}} = \left(\left(\frac{3}{2} \rho^n - \frac{1}{2} \rho^{n-1} \right)^2 + \Delta t^8 \right)^{\frac{1}{2}},\tag{3.3}$$

to ensure both the positivity and a higher order consistency, and the stabilization term $\frac{\chi^2 \Delta t}{4\theta} (\rho^{n+1} - 1)$ ρ^n) is introduced to establish the unique existence of the solution to the nonlinear scheme. See Section 4 for more details.

Define two linear operators

$$\mathscr{L}_1 = \frac{\theta}{\Delta t} + \frac{\alpha}{2} - \frac{\mu}{2} \Delta_h, \quad \mathscr{L}_2 = \frac{\theta}{\Delta t} - \frac{\alpha}{2} + \frac{\mu}{2} \Delta_h,$$

where \mathcal{L}_1 is invertible. In turn, the proposed numerical scheme could be rewritten as

Is invertible. In turn, the proposed numerical scheme could be rewritten as
$$\begin{cases}
\frac{\rho^{n+1} - \rho^n}{\Delta t} = \nabla_h \cdot \left[\frac{1}{f''(\hat{\rho}^{n+\frac{1}{2}})} \nabla_h \left(\gamma S^{n+\frac{1}{2}} - \left(\frac{\chi}{2} \mathcal{L}_1^{-1} \mathcal{L}_2 \phi^n + \frac{\chi^2}{4} \mathcal{L}_1^{-1} \rho^n + \frac{\chi}{2} \phi^n + \frac{\chi^2 \Delta t}{4\theta} \rho^n \right) + \mathcal{G}_h \rho^{n+1} \right) \right], \\
+ \frac{\chi^2 \Delta t}{4\theta} \rho^n + \frac{\chi}{2} (\rho^{n+1} + \rho^n),
\end{cases} (3.4)$$

with $\mathscr{G}_h := \frac{\chi^2 \Delta t}{4\theta} - \frac{\chi^2}{4} \mathscr{L}_1^{-1}$. The nonlinear scheme supplemented with homogeneous boundary conditions results in a nonlinear system.

Remark 3.2 A stabilization term $\frac{\chi^2 \Delta t}{4\theta + 2\alpha \Delta t}(\rho^{n+1} - \rho^n)$, instead of $\frac{\chi^2 \Delta t}{4\theta}(\rho^{n+1} - \rho^n)$ in (3.1), could be used in the numerical scheme for a small positive θ , and the theoretical analysis on structure-preserving properties and convergence could still go through. In the case with $\theta = 0$, the stabilization term becomes $\frac{\chi^2}{2\alpha}(\rho^{n+1} - \rho^n)$, and the proposed numerical scheme is reduced to a first-order accurate one with provable structure-preserving properties.

Remark 3.3 Since the proposed numerical scheme is a three-level algorithm, we need an accurate approximation to the living organism density variable at a temporally "ghost" point approximation, namely ρ^{-1} , which such an approximation to the chemical signal density variable is not required. A careful application of predictor-correction approach could be applied to accomplish this goal. For instance, a rough predictive numerical solution at the first time step by using the two-level semi-implicit scheme [45]:

$$\begin{split} &\frac{\hat{\rho}^{1} - \rho^{0}}{\Delta t} = \nabla_{h} \cdot \left(\frac{1}{f''(\rho^{0})} \nabla_{h} \left[\gamma f'(\hat{\rho}^{1}) - \frac{\chi}{2} (\phi^{0} + \hat{\phi}^{1}) + \frac{\chi}{2} (\hat{\rho}^{1} - \rho^{0}) \right] \right), \\ &\theta \frac{\hat{\phi}^{1} - \phi^{0}}{\Delta t} = \mu \Delta_{h} \hat{\phi}^{1} - \alpha \hat{\phi}^{1} + \frac{\chi}{2} (\rho^{0} + \hat{\rho}^{1}) - \frac{\chi}{2} (\hat{\phi}^{1} - \phi^{0}), \end{split}$$

where $\rho_{i,j,k}^0 = \rho(0,x_i,y_j,z_k)$, $\phi_{i,j,k}^0 = \phi(0,x_i,y_j,z_k)$, $i,j,k=1,\cdots,N$. In fact, $(\hat{\rho}^1,\hat{\phi}^1)$ is an $O(\Delta t^2 + h^2)$ approximation to the exact solution at time instant $t^1 = \Delta t$, which comes from a single-step numerical approximation. Subsequently, a more accurate correction process is carried out: we take an average of $\hat{\rho}^1$ and ρ^0 to approximate $\hat{\rho}^{\frac{1}{2}}$, and implement numerical scheme (3.1-3.2) at n=0 to obtain $(\hat{\rho}^1,\hat{\phi}^1)$, and use $\frac{3}{2}\hat{\rho}^1 - \frac{1}{2}\rho^0$ to approximate $\hat{\rho}^{\frac{3}{2}}$, and implement numerical scheme (3.1-3.2) at n=1 to obtain $(\hat{\rho}^2,\hat{\phi}^2)$. Again, since these computations correspond to finite time step algorithm, we see that $(\hat{\rho}^j,\hat{\phi}^j)$ are indeed $O(\Delta t^3 + \Delta t h^2)$ approximation to the exact solution at t^j , j=1,2. In turn, a third order extrapolation formula, $\rho^{-1}=3\rho^0-3\hat{\rho}^1-3\hat{\rho}^2$, $\rho^{-2}=6\rho^0-8\hat{\rho}^1+3\hat{\rho}^2$, gives an $O(\Delta t^3+\Delta th^2)$ approximation to the living organism density variable at t^{-1} , t^{-2} , respectively. Such an approximation will be useful in the later convergence analysis. Of course, with an accurate approximation to ρ^{-1} , the initialization process for the proposed three-level numerical scheme (3.1-3.2) is completed, and the numerical values of (ρ^j,ϕ^j) $(j\geq 1)$ could be obtained by the solution of the numerical algorithm.

4 Structure-preserving properties

In this section, we prove the mass conservation, unique solvability, positivity-preserving properties of the second-order numerical scheme, as well as an unconditional dissipation of the original free energy functional, at the discrete level.

Theorem 4.1 (Mass conservation) The second-order accurate numerical scheme (3.1-3.2) respects a discrete mass conservation law:

$$\langle \rho^{n+1}, 1 \rangle = \langle \rho^n, 1 \rangle.$$

Such a mass conservation identity is obtained by applying the summation on both sides, and the discrete homogeneous Neumann boundary conditions have been used.

The free energy is discretized as

$$F_h(\rho^n, \phi^n) = \gamma \langle f(\rho^n), 1 \rangle - \chi \langle \rho^n, \phi^n \rangle + \frac{\mu}{2} \|\nabla_h \phi^n\|_2^2 + \frac{\alpha}{2} \|\phi^n\|_2^2, \tag{4.1}$$

which turns out to be a second-order approximation to the continuous version of the energy.

Meanwhile, the following monotonicity property is needed in the unique solvability analysis.

Lemma 4.2 The linear operator \mathcal{G}_h satisfies the monotonicity condition:

$$\langle \mathcal{G}_h(\eta_1) - \mathcal{G}_h(\eta_2), \eta_1 - \eta_2 \rangle \ge 0, \quad \text{for } \eta_1, \eta_2 \in \mathscr{C}.$$
 (4.2)

Furthermore, the equality is valid if and only if $\tilde{\eta} = 0$, i.e., $\eta_1 = \eta_2$, if $\overline{\eta_1} = \overline{\eta_2} = 0$ is required. Therefore, the operator \mathcal{G}_h is invertible.

Proof Denote a difference function $\tilde{\eta} = \eta_1 - \eta_2 \in \mathring{\mathscr{C}}$. Since \mathscr{G}_h is a linear operator, we have

$$\mathcal{G}_h(\eta_1) - \mathcal{G}_h(\eta_2) = \mathcal{G}_h(\tilde{\eta}) = \frac{\chi^2 \Delta t}{4\theta} \tilde{\eta} - \frac{\chi^2}{4} \mathcal{L}_1^{-1} \tilde{\eta}. \tag{4.3}$$

Taking a discrete inner product with (4.3) by $\tilde{\eta}$ yields

$$\langle \mathcal{G}_h(\tilde{\eta}), \tilde{\eta} \rangle = \frac{\chi^2 \Delta t}{4\theta} \|\tilde{\eta}\|_2^2 - \frac{\chi^2}{4} \left\langle \mathcal{L}_1^{-1} \tilde{\eta}, \tilde{\eta} \right\rangle. \tag{4.4}$$

From Appendix B, we have

$$\frac{\chi^2}{4} \left\langle \tilde{\eta}, \mathcal{L}_1^{-1} \tilde{\eta} \right\rangle \le \frac{\chi^2 \Delta t}{4\theta} \|\tilde{\eta}\|_2^2. \tag{4.5}$$

Consequently, a combination of (4.4) and (4.5) leads to

$$\langle \mathcal{G}_h(\tilde{\eta}), \tilde{\eta} \rangle \ge 0.$$
 (4.6)

In addition, the equality is valid if and only if $\tilde{\eta} = 0$, i.e., $\eta_1 = \eta_2$. The proof is complete.

Moreover, a discrete maximum norm bound of the operator \mathbb{Q}_f^{-1} is also needed in the later analysis.

Lemma 4.3 Assume that $\nu \in \mathring{\mathfrak{C}}$, $\|\nu\|_{\infty} \leq C_2$, and $f \in \mathfrak{C}$ satisfies $f \geq f_0 > 0$ (at a point-wise level). The following estimate is available:

$$\|\mathbb{Q}_f^{-1}\nu\|_{\infty} \le C_3 f_0^{-1} h^{-\frac{1}{2}},$$

where $C_3 > 0$ only depends on Ω and C_2 .

Such an estimate has been established in Lemma 3.2 of the work [11] for periodic boundary conditions. The proof is omitted for brevity. Interested readers are referred to another previous work [15] for the details involving homogeneous Neumann boundary conditions.

The positivity-preserving and unique solvability properties are proved in the following theorem. For simplicity of presentation, the classical PKS system, with $f(\rho) = \rho(\ln \rho - 1)$ (as given by (2.3)), is considered in the theoretical analysis. In turn, we get $f'(\rho) = \ln \rho$, $f''(\rho) = \frac{1}{\rho}$ and $f'''(\rho) = -\frac{1}{\rho^2}$. An extension to the PKS system with a bounded mobility (2.4) and a saturation density (2.5) would be straightforward.

Theorem 4.4 (Existence, uniqueness, and positivity-preserving property) Define $C_{\min}^n := \min_{1 \leq i,j,k \leq N} \rho_{i,j,k}^n$, $C_{\max}^n := \max_{1 \leq i,j,k \leq N} \rho_{i,j,k}^n$ and $\|\phi^n\|_{\infty} \leq M_{\max}^n$. Given $C_{\min}^n > 0$, there exists a unique solution to the second-order accurate scheme (3.1-3.2), such that

$$\rho_{i,i,k}^{n+1} > 0$$
, for $i, j, k = 1, 2, \dots, N$. (4.7)

Proof The numerical solution to the proposed algorithm (3.1-3.2) is equivalent to the minimizer of the discrete energy functional:

$$\mathcal{J}^{n}(\rho) = \frac{1}{2\Delta t} \|\rho - \rho^{n}\|_{\mathbb{Q}^{-1}_{\hat{\rho}^{n+\frac{1}{2}}}}^{2} + \gamma \left\langle \rho + \frac{5}{6}\rho^{n}, \ln \rho - 1 \right\rangle + \gamma \left\langle (\rho^{n})^{2}, \frac{1}{6\rho} \right\rangle - \frac{2}{3}\gamma \left\langle \rho, 1 \right\rangle
- \frac{\chi^{2}}{8} \left\langle \rho, \mathcal{L}_{1}^{-1}\rho \right\rangle + \frac{\chi^{2}\Delta t}{8\theta} \|\rho\|_{2}^{2}
- \left\langle \frac{\chi}{2} \mathcal{L}_{1}^{-1} \mathcal{L}_{2}\phi^{n} + \frac{\chi^{2}}{4} \mathcal{L}_{1}^{-1}\rho^{n} + \frac{\chi}{2}\phi^{n} + \frac{\chi^{2}\Delta t}{4\theta}\rho^{n}, \rho \right\rangle,$$
(4.8)

over the admissible set

$$\mathbb{K}_h := \left\{ \rho \middle| 0 < \rho_{i,j,k} < \xi, \ \frac{1}{|\Omega|} \langle \rho, 1 \rangle = Q^0, \quad i, j, k = 1, \cdots, N \right\}, \ Q^0 = \frac{1}{|\Omega|} \left\langle \rho^0, 1 \right\rangle, \ \xi := \frac{Q^0 |\Omega|}{h^3}.$$

Consider a closed subset $\mathbb{K}_{h,\delta} \subset \mathbb{K}_h$:

$$\mathbb{K}_{h,\delta} := \left\{ \rho \middle| \delta \le \rho_{i,j,k} \le \xi - \delta, \ \frac{1}{|\Omega|} \left\langle \rho, 1 \right\rangle = Q^0, \quad i, j, k = 1, \cdots, N \right\}, \quad \delta \in (0, \frac{\xi}{2}).$$

Obviously, $\mathbb{K}_{h,\delta}$ is a bounded, convex, and compact subset of \mathbb{K}_h . By the convexity of \mathcal{J}^n , there exists a unique minimizer of \mathcal{J}^n in $\mathbb{K}_{h,\delta}$.

Suppose that the minimizer of \mathcal{F}^n , ρ^* , touches the boundary of $\mathbb{K}_{h,\delta}$. Assume that there exists a grid point $\vec{\alpha}_0 = (i_0, j_0, k_0)$ such that $\rho_{\vec{\alpha}_0}^* = \delta$, and a grid point $\vec{\alpha}_1 = (i_1, j_1, k_1)$ such that the maximum of ρ^* is achieved. It is clear that the maximum value $\rho_{\vec{\alpha}_1}^*$ is larger than the mean value Q^0 , and the minimum value $\rho_{\vec{\alpha}_0}^*$ is less than Q^0 , i.e.,

$$\rho_{\vec{\alpha}_1}^* \ge Q^0, \quad \rho_{\vec{\alpha}_0}^* \le Q^0.$$

Consider the following directional derivative

$$\lim_{t \to 0^{+}} \frac{\mathcal{J}^{n}(\rho^{*} + td) - \mathcal{J}^{n}(\rho^{*})}{t}$$

$$= \frac{1}{\Delta t} \left\langle \mathbb{Q}_{\hat{\rho}^{n+\frac{1}{2}}}^{-1}(\rho^{*} - \rho^{n}), d \right\rangle + \gamma \left\langle \ln \rho^{*} + \frac{5\rho^{n}}{6\rho^{*}} - \frac{(\rho^{n})^{2}}{6(\rho^{*})^{2}} - \frac{2}{3}, d \right\rangle$$

$$+ \left\langle \mathcal{G}_{h}\rho^{*}, d \right\rangle - \left\langle \frac{\chi}{2}\mathcal{L}_{1}^{-1}\mathcal{L}_{2}\phi^{n} + \frac{\chi^{2}}{4}\mathcal{L}_{1}^{-1}\rho^{n} + \frac{\chi}{2}\phi^{n} + \frac{\chi^{2}\Delta t}{4\theta}\rho^{n}, d \right\rangle,$$

with the direction

$$d = \delta_{i,i_0} \delta_{j,j_0} \delta_{k,k_0} - \delta_{i,i_1} \delta_{j,j_1} \delta_{k,k_1},$$

where $\delta_{l,k}$ is the Kronecker symbol. Clearly, $d \in \mathring{\mathscr{C}}$. In turn, the directional derivative becomes

$$\frac{1}{h^{3}} \lim_{t \to 0^{+}} \frac{\mathcal{J}^{n}(\rho^{*} + td) - \mathcal{J}^{n}(\rho^{*})}{t}$$

$$= \frac{1}{\Delta t} \mathcal{Q}_{\hat{\rho}^{n+\frac{1}{2}}}^{-1}(\rho^{*} - \rho^{n})_{\vec{\alpha}_{0}} - \frac{1}{\Delta t} \mathcal{Q}_{\hat{\rho}^{n+\frac{1}{2}}}^{-1}(\rho^{*} - \rho^{n})_{\vec{\alpha}_{1}} + (\mathcal{G}_{h}\rho^{*})_{\vec{\alpha}_{0}} - (\mathcal{G}_{h}\rho^{*})_{\vec{\alpha}_{1}}$$

$$+ \gamma \left(\ln \rho^{*} + \frac{5\rho^{n}}{6\rho^{*}} - \frac{(\rho^{n})^{2}}{6(\rho^{*})^{2}}\right)_{\vec{\alpha}_{0}} - \gamma \left(\ln \rho^{*} + \frac{5\rho^{n}}{6\rho^{*}} - \frac{(\rho^{n})^{2}}{6(\rho^{*})^{2}}\right)_{\vec{\alpha}_{1}}$$

$$- \left(\frac{\chi}{2} \mathcal{L}_{1}^{-1} \mathcal{L}_{2} \phi^{n} + \frac{\chi^{2}}{4} \mathcal{L}_{1}^{-1} \rho^{n} + \frac{\chi}{2} \phi^{n} + \frac{\chi^{2} \Delta t}{4\theta} \rho^{n}\right)_{\vec{\alpha}_{0}}$$

$$+ \left(\frac{\chi}{2} \mathcal{L}_{1}^{-1} \mathcal{L}_{2} \phi^{n} + \frac{\chi^{2}}{4} \mathcal{L}_{1}^{-1} \rho^{n} + \frac{\chi}{2} \phi^{n} + \frac{\chi^{2} \Delta t}{4\theta} \rho^{n}\right)_{\vec{\alpha}_{1}}.$$
(4.9)

Define $C_{\max}^n = \max_{i,j,k=1,\cdots,N} \rho_{i,j,k}^n$ and $C_{\min}^n = \min_{i,j,k=1,\cdots,N} \rho_{i,j,k}^n$. Since $\rho_{\vec{\alpha}_0}^* = \delta$ and $\rho_{\vec{\alpha}_1}^* \geq Q^0$, we have

$$\gamma \left[\ln(\rho^*) + \frac{5\rho^n}{6\rho^*} - \frac{(\rho^n)^2}{6(\rho^*)^2} \right]_{\vec{\alpha}_0} - \gamma \left[\ln(\rho^*) + \frac{5\rho^n}{6\rho^*} - \frac{(\rho^n)^2}{6(\rho^*)^2} \right]_{\vec{\alpha}_1} \\
\leq \gamma \ln \delta + \frac{5\gamma C_{\text{max}}^n}{6\delta} - \frac{\gamma (C_{\text{min}}^n)^2}{6\delta^2} - \gamma \ln Q^0 + \frac{\gamma (C_{\text{max}}^n)^2}{6(Q^0)^2}. \tag{4.10}$$

With a similar analysis technique as in Lemma 4.3, one can derive that $\|\mathcal{G}_h\rho^*\|_{\infty} \leq M_1/2$ with $\|\rho^*\|_{\infty} \leq \xi$, where M_1 is a constant independent of δ . Then we have

$$(\mathcal{G}_h \rho^*)_{\vec{\alpha}_0} - (\mathcal{G}_h \rho^*)_{\vec{\alpha}_1} \le M_1. \tag{4.11}$$

On the other hand, the operator $\frac{\chi}{2}\mathcal{L}_1^{-1}\mathcal{L}_2\phi^n + \frac{\chi^2}{4}\mathcal{L}_1^{-1}\rho^n + \frac{\chi}{2}\phi^n + \frac{\chi^2\Delta t}{4\theta}\rho^n$ is linear with respect to ϕ^n and ρ^n . Subsequently, the a-priori assumptions $\|\rho^n\|_{\infty} \leq C_{\max}^n$ and $\|\phi^n\|_{\infty} \leq M_{\max}^n$ indicate that

$$\left(\frac{\chi}{2}\mathcal{L}_{1}^{-1}\mathcal{L}_{2}\phi^{n} + \frac{\chi^{2}}{4}\mathcal{L}_{1}^{-1}\rho^{n} + \frac{\chi}{2}\phi^{n} + \frac{\chi^{2}}{4\theta}\rho^{n}\right)_{\vec{\alpha}_{1}} - \left(\frac{\chi}{2}\mathcal{L}_{1}^{-1}\mathcal{L}_{2}\phi^{n} + \frac{\chi^{2}}{4}\mathcal{L}_{1}^{-1}\rho^{n} + \frac{\chi}{2}\phi^{n} + \frac{\chi^{2}}{4\theta}\rho^{n}\right)_{\vec{\alpha}_{0}} \leq M_{2}, \tag{4.12}$$

where M_2 is another constant independent of δ . By the bound $\|\rho^* - \rho^n\|_{\infty} \leq \xi + C_{\max}^n$, we get

$$\mathbb{Q}_{\hat{\rho}^{n+\frac{1}{2}}}^{-1}(\rho^* - \rho^n)_{\vec{\alpha}_0} - \mathbb{Q}_{\hat{\rho}^{n+\frac{1}{2}}}^{-1}(\rho^* - \rho^n)_{\vec{\alpha}_1} \le 2M_3, \tag{4.13}$$

where M_3 is a constant dependent on C_{\max}^n , Δt , h, Ω , ξ , and Lemma 4.3 has been applied. Substituting (4.10), (4.11), (4.12), and (4.13) into (4.9), we obtain

$$\frac{1}{h^3} \lim_{t \to 0^+} \frac{\mathcal{J}^n(\rho^* + td) - \mathcal{J}^n(\rho^*)}{t} \le 2(\Delta t)^{-1} M_3 + \gamma \ln \delta + \frac{5\gamma C_{\text{max}}^n}{6\delta} + M_1 + M_2
- \frac{\gamma (C_{\text{min}}^n)^2}{6\delta^2} - \gamma \ln Q^0 + \frac{\gamma (C_{\text{max}}^n)^2}{6(Q^0)^2}.$$
(4.14)

For any fixed Δt and h, the value of δ could be chosen sufficiently small so that

$$2(\Delta t)^{-1}M_3 + \gamma \ln \delta + \frac{5\gamma C_{\text{max}}^n}{6\delta} - \frac{\gamma (C_{\text{min}}^n)^2}{6\delta^2} - \gamma \ln Q^0 + \frac{\gamma (C_{\text{max}}^n)^2}{6(Q^0)^2} + M_1 + M_2 < 0.$$
 (4.15)

Therefore, the following inequality is valid:

$$\lim_{t \to 0^+} \frac{\mathcal{J}^n(\rho^* + td) - \mathcal{J}^n(\rho^*)}{t} < 0. \tag{4.16}$$

This is contradictory to the assumption that ρ^* is the minimizer of \mathcal{J}^n .

Similarly, we are able to prove that the minimizer of \mathcal{J}^n cannot occur at the upper boundary of $\mathbb{K}_{h,\delta}$. In fact, if this occurs, there must be a grid point, at which the value of ρ^* approaches zero. A contradiction could be obtained in the same manner as above. Therefore, the global minimum of \mathcal{J}^n could only possibly achieve at an interior point, i.e., $\rho^* \in \mathring{\mathbb{K}}_{h,\delta} \subset \mathring{\mathbb{K}}_h$ as $\delta \to 0$. Since \mathcal{J}^n is a smooth functional, there must exist a solution $\rho^* \in \mathring{\mathbb{K}}_{h,\delta} \subset \mathring{\mathbb{K}}_h$, satisfying

$$\lim_{t \to 0^+} \frac{\mathcal{F}^n(\rho^* + td) - \mathcal{F}^n(\rho^*)}{t} = 0. \tag{4.17}$$

As a result, there exists a positive numerical solution ρ^* to the numerical system (3.1-3.2). The uniqueness of the numerical solution is a direct consequence of the strict convexity of the discrete energy functional $\mathcal{J}^n(\rho)$.

Theorem 4.5 (The original energy dissipation) The second-order numerical scheme (3.1-3.2) respects a dissipation law of the discrete free energy (4.1):

$$F_h^{n+1} - F_h^n \le -\Delta t \left[\frac{1}{f''(\hat{\rho}^{n+\frac{1}{2}})} \nabla_h v^{n+\frac{1}{2}}, \nabla_h v^{n+\frac{1}{2}} \right] - \frac{\theta}{\Delta t} \|\phi^{n+1} - \phi^n\|_2^2 - \frac{\chi^2 \Delta t}{4\theta} \|\rho^{n+1} - \rho^n\|_2^2 \le 0,$$

$$with \ v^{n+\frac{1}{2}} = \gamma S^{n+\frac{1}{2}} - \frac{\chi}{2} (\phi^{n+1} + \phi^n) + \frac{\chi^2 \Delta t}{4\theta} (\rho^{n+1} - \rho^n).$$

$$(4.18)$$

Proof Taking a discrete inner product with (3.1) by $\Delta t v^{n+\frac{1}{2}}$, we get

$$\left\langle \rho^{n+1} - \rho^n, v^{n+\frac{1}{2}} \right\rangle = -\Delta t \left[\frac{1}{f''(\hat{\rho}^{n+\frac{1}{2}})} \nabla_h v^{n+\frac{1}{2}}, \nabla_h v^{n+\frac{1}{2}} \right].$$
 (4.19)

For any function $H(\cdot) \in C^4(\mathbb{R})$, the following Taylor expansion is valid:

$$H(x) = H(y) + H^{(1)}(y)(x - y) + \frac{1}{2}H^{(2)}(y)(x - y)^{2} + \frac{1}{6}H^{(3)}(y)(x - y)^{3} + \frac{1}{24}H^{(4)}(\eta)(x - y)^{4}, \ \forall x, y \in \mathbb{R},$$

where η is between x and y, and $H^{(p)}(y) = \frac{\partial^p H}{\partial y^p}$ for p = 1, 2, 3, 4. If $H^{(4)}(\eta) > 0$, one has

$$H(y) - H(x) \le \left(H^{(1)}(y) - \frac{1}{2}H^{(2)}(y)(y-x) + \frac{1}{6}H^{(3)}(y)(y-x)^2\right)(y-x).$$

Choosing $H(\rho) = f(\rho)$, we have

$$\left\langle \rho^{n+1} - \rho^{n}, v^{n+\frac{1}{2}} \right\rangle \ge \gamma \left\langle f(\rho^{n+1}) - f(\rho^{n}), 1 \right\rangle - \frac{\chi}{2} \left\langle \rho^{n+1} - \rho^{n}, \phi^{n+1} + \phi^{n} \right\rangle + \frac{\chi^{2} \Delta t}{4\theta} \|\rho^{n+1} - \rho^{n}\|_{2}^{2}.$$

$$(4.20)$$

On the other hand, taking a discrete inner product with (3.2) by $-(\phi^{n+1} - \phi^n)$, we have

$$-\frac{\theta}{\Delta t} \|\phi^{n+1} - \phi^{n}\|_{2}^{2} = \frac{\mu}{2} \left(\|\nabla_{h}\phi^{n+1}\|^{2} - \|\nabla_{h}\phi^{n}\|^{2} \right) + \frac{\alpha}{2} \left(\|\phi^{n+1}\|^{2} - \|\phi^{n}\|^{2} \right) - \frac{\chi}{2} \left\langle \rho^{n} + \rho^{n+1}, \phi^{n+1} - \phi^{n} \right\rangle.$$

$$(4.21)$$

Moreover, the following equality is valid:

$$-\frac{\chi}{2}\left\langle \rho^{n+1} - \rho^n, \phi^{n+1} + \phi^n \right\rangle - \frac{\chi}{2}\left\langle \rho^n + \rho^{n+1}, \phi^{n+1} - \phi^n \right\rangle = -\chi\left(\left\langle \rho^{n+1}, \phi^{n+1} \right\rangle - \left\langle \rho^n, \phi^n \right\rangle\right). \tag{4.22}$$

A combination of (4.19)-(4.22) leads to the energy dissipation inequality (4.18).

Remark 4.6 Structure-preserving properties, such as the unique solvability of positive numerical solution (4.7) and the original energy dissipation (4.18), can be analogously proved for the PKS system with a bounded mobility (2.4) or a saturation density (2.5).

Remark 4.7 If the free energy contains both the convex and concave parts, some existing works have reported a modified energy stability analysis for various second order accurate, multi-step numerical schemes [10,20,32]. However, these reported stability analysis is in terms of a modified discrete energy. In comparison, the stability estimate (4.18) is in terms of the original free energy (4.1), which turns out to be a remarkable theoretical result that has been rarely reported.

5 Convergence analysis

Let (ϕ_e, ρ_e) be the exact solution to the PKS system (2.2) [7, 26, 51, 52]. In fact, for a gradient flow equation with a logarithmic energy potential, its regularity relies heavily on the separation property, i.e., a uniform distance between the solution away from the singular limit value of 0, namely $\rho_e \geq \varepsilon^* > 0$ in the PKS system. For example, in terms of the 2D Flogy-Huggins-Cahn-Hilliard equation, in which the energy potential takes a very similar form as (2.5), the separation property for the phase variable has been justified at a theoretical level [1, 14]. As a result, the higher order regularity estimate (in addition to the free energy regularity) for the 2D Flogy-Huggins-Cahn-Hilliard equation could be easily derived with the help of this separation property, so that the global-in-time smooth solution becomes a straightforward consequence. On the other hand, such a uniform-in-time analysis for the PKS system (2.2) is expected to be much more challenging than that of the Cahn-Hilliard equation, due to the lack of a regular surface diffusion part in the free energy expansion. In turn, a global-in-time separation property and the smooth solution analysis have not been theoretically established. Meanwhile, although a global-in-time solution has not been theoretically available, one could always derive a local-in-time smooth solution with a sufficient regular initial data, with the help of local-in-time analytic tools. Since the convergence analysis and error estimate are always local-in-time, it is natural to assume a local-in-time exact solution with sufficient regularity, as well as its separation property.

The following regularity assumption is made for the exact solution:

$$\phi_e, \rho_e \in \Re := H^6(0, T; C(\Omega)) \cap H^5(0, T; C^2(\Omega)) \cap L^{\infty}(0, T; C^6(\Omega)).$$

In addition, the following separation property is assumed for the exact solution, for the convenience of the analysis:

$$\rho_e \geq \varepsilon^*$$
, for some $\varepsilon^* > 0$, at a point-wise level.

Define $\rho_N := \mathcal{P}_N \rho_e(\cdot, t)$ and $\phi_N := \mathcal{P}_N \phi_e(\cdot, t)$ as the Fourier Cosine projection of the exact solution into \mathcal{P}^K , which is the space of trigonometric polynomials spanned by cosine functions in x, y, and z, with degree up to K (with K = N - 1) defined by

$$\mathcal{P}^K = \operatorname{span}\left\{\cos(\frac{k_x\pi x}{b-a})\cos(\frac{k_y\pi y}{b-a})\cos(\frac{k_z\pi z}{b-a}) \mid 0 \le k_x, k_y, k_z \le K\right\}.$$

See more details in our previous work [15]. The following projection approximation is standard, for $(\phi_e, \rho_e) \in L^{\infty}(0, T; H^m(\Omega))$, with $m \in \mathbb{N}$, $0 \le k \le m$:

$$\|\phi_N - \phi_e\|_{L^{\infty}(0,T;H^k)} \le Ch^{m-k} \|\phi_e\|_{L^{\infty}(0,T;H^m)},$$

$$\|\rho_N - \rho_e\|_{L^{\infty}(0,T;H^k)} \le Ch^{m-k} \|\rho_e\|_{L^{\infty}(0,T;H^m)}.$$
(5.1)

Notice that the Fourier Cosine projection estimate does not preserve the positivity of the variables, while we are always able to take h sufficiently small (corresponding to a large N) so that

$$\rho_N \ge \frac{1}{2}\varepsilon^*.$$

Denote by $\phi_N^n = \phi_N(\cdot, t_n)$ and $\rho_N^n = \rho_N(\cdot, t_n)$, with $t_n = n\Delta t$. Since $\rho_N^n \in \mathcal{P}^K$, the mass conservative property is available at the discrete level:

$$\overline{\rho^n} = \frac{1}{|\Omega|} \int_{\Omega} \rho(\cdot, t_n) d\boldsymbol{x} = \frac{1}{|\Omega|} \int_{\Omega} \rho(\cdot, t_{n-1}) d\boldsymbol{x} = \overline{\rho^{n-1}} \text{ for } n \in \mathbb{N}^*.$$

On the other hand, the numerical solution of the second-order scheme (3.1-3.2) is also mass conservative at the discrete level:

$$\overline{\rho^{n-1}} = \overline{\rho^n} \text{ for } n \in \mathbb{N}^*.$$

In turn, the mass conservative projection is made for the initial data:

$$\phi^{0} = \mathcal{P}_{h}\phi_{N}(\cdot, t = 0) := \phi_{N}(p_{i}, p_{j}, p_{k}, t = 0),$$

$$\rho^{0} = \mathcal{P}_{h}\rho_{N}(\cdot, t = 0) := \rho_{N}(p_{i}, p_{j}, p_{k}, t = 0),$$

where \mathcal{P}_h is an interpolation operator that restricts a continuous function in \mathcal{P}^K onto its value on the discrete grid (x_i, y_j, z_k) . Accordingly, the error grid functions are defined as

$$e_{\phi}^{n} := \mathcal{P}_{h}\phi_{N}^{n} - \phi^{n}, \quad e_{\rho}^{n} := \mathcal{P}_{h}\rho_{N}^{n} - \rho^{n}, \quad n \in \mathbb{N}^{*}.$$
 (5.2)

As indicated above, one can verify that $\bar{e}_{\phi}^{n}=0$, $\bar{e}_{\rho}^{n}=0$, for $n\in\mathbb{N}$, so that the discrete norm $\|\cdot\|_{-1,h}$ is well defined for the error grid functions.

The following theorem is the main result of this section.

Theorem 5.1 Given initial data $\phi_e(\cdot, t = 0), \rho_e(\cdot, t = 0) \in C^6(\Omega)$, suppose the exact solution for the PKS system (2.2) is of regularity class \Re . Let e^n_{ϕ} and e^n_{ρ} be the error grid functions

defined in (5.2). Then, under the linear refinement requirement $\lambda_1 h \leq \Delta t \leq \lambda_2 h$, the following convergence result is available as $\Delta t, h \to 0$:

$$\begin{aligned} \left\| e_{\rho}^{n} \right\|_{2} + \left(\Delta t \sum_{k=0}^{n-1} \left\| \nabla_{h} (e_{\rho}^{k} + e_{\rho}^{k+1}) \right\|_{2}^{2} \right)^{\frac{1}{2}} \\ + \left\| e_{\phi}^{n} \right\|_{2} + \left\| \nabla_{h} e_{\phi}^{n} \right\|_{2} + \left(\Delta t \sum_{k=0}^{n-1} \left\| \Delta_{h} (e_{\phi}^{k} + e_{\phi}^{k+1}) \right\|_{2}^{2} \right)^{\frac{1}{2}} \leq C(\Delta t^{2} + h^{2}), \ n \in \mathbb{N}, \end{aligned}$$

$$(5.3)$$

where $t_n = n\Delta t \leq T$ and the constant C > 0 is independent of Δt and h.

5.1 Higher-order consistency analysis

The leading local truncation error will not be sufficient to recover an ℓ^{∞} bound of the discrete temporal derivative of the numerical solution, which is needed in the nonlinear convergence analysis. To overcome this subtle difficulty, we apply a higher order consistency estimate via a perturbation analysis [37, 38]. Such a higher order consistency result is stated below, and the detailed proof follows a similar idea as in [38]. The technical details are skipped for the sake of brevity.

Proposition 5.2 Let (ϕ_e, ρ_e) be the exact solution to the PKS system (1.1) and (ϕ_N, ρ_N) be its Fourier Cosine projection. There exists auxiliary variables, $\phi_{\Delta t,1}$, $\phi_{\Delta t,2}$, $\phi_{h,1}$, $\rho_{\Delta t,1}$, $\rho_{\Delta t,2}$, $\rho_{h,1}$, so that the following expansion profiles

$$\dot{\phi} = \phi_N + \mathcal{P}_N \left(\Delta t^2 \phi_{\Delta t, 1} + \Delta t^3 \phi_{\Delta t, 2} + h^2 \phi_{h, 1} \right),
\dot{\rho} = \rho_N + \mathcal{P}_N \left(\Delta t^2 \rho_{\Delta t, 1} + \Delta t^3 \rho_{\Delta t, 2} + h^2 \rho_{h, 1} \right),$$
(5.4)

satisfy the numerical scheme up to an $O(\Delta t^4 + h^4)$ consistency:

$$\frac{\check{\rho}^{n+1} - \check{\rho}^{n}}{\Delta t} = \nabla_{h} \cdot \left[\left(\frac{3}{2} \check{\rho}^{n} - \frac{1}{2} \check{\rho}^{n-1} \right) \nabla_{h} \left(\gamma \check{S}^{n+\frac{1}{2}} - \frac{\chi}{2} (\check{\phi}^{n} + \check{\phi}^{n+1}) \right) \right. \\
\left. + \frac{\chi^{2} \Delta t}{4\theta} (\check{\rho}^{n+1} - \check{\rho}^{n}) \right) \right] + \tau_{\rho}^{n+\frac{1}{2}}, \\
\check{S}^{n+\frac{1}{2}} = \ln(\check{\rho}^{n+1}) - \frac{1}{2\check{\rho}^{n+1}} (\check{\rho}^{n+1} - \check{\rho}^{n}) - \frac{1}{6(\check{\rho}^{n+1})^{2}} (\check{\rho}^{n+1} - \check{\rho}^{n})^{2}, \\
\theta \frac{\check{\phi}^{n+1} - \check{\phi}^{n}}{\Delta t} = \frac{\mu}{2} \Delta_{h} (\check{\phi}^{n+1} + \check{\phi}^{n}) - \frac{\alpha}{2} (\check{\phi}^{n+1} + \check{\phi}^{n}) + \frac{\chi}{2} (\check{\rho}^{n+1} + \check{\rho}^{n}) + \tau_{\phi}^{n+\frac{1}{2}}, \tag{5.5}$$

with $\|\tau_{\rho}^{n+\frac{1}{2}}\|_2$, $\|\tau_{\phi}^{n+\frac{1}{2}}\|_2 \leq C(\Delta t^4 + h^4)$. The constructed variables $\phi_{\Delta t,1}$, $\phi_{\Delta t,2}$, $\phi_{h,1}$, $\rho_{\Delta t,1}$, $\rho_{\Delta t,2}$, $\rho_{h,1}$ solely depend on the exact solution (ϕ_e, ρ_e) , and their derivatives are bounded.

(1) The following mass conservative identities and zero-mean property for the local truncation error are available:

$$\rho^{0} \equiv \check{\rho}^{0}, \quad \overline{\rho^{n}} = \overline{\rho^{0}}, \quad n \in \mathbb{N},$$

$$\overline{\check{\rho}^{n}} = \frac{1}{|\Omega|} \int_{\Omega} \check{\rho}(\cdot, t_{n}) d\boldsymbol{x} = \frac{1}{|\Omega|} \int_{\Omega} \check{\rho}^{0} d\boldsymbol{x} = \overline{\check{\rho}^{0}}, \quad n \in \mathbb{N},$$

$$\overline{\tau_{\rho}^{n+\frac{1}{2}}} = 0, \quad n \in \mathbb{N}.$$
(5.6)

(2) A similar phase separation property is valid for the constructed $\check{\rho}$, for some $\varepsilon^* > 0$:

$$\tilde{\rho} \ge \varepsilon^* > 0.$$
(5.7)

(3) A discrete $W^{1,\infty}$ bound for the constructed profile $\check{\rho}$, as well as its discrete temporal derivative, is available at any time step t^k :

$$\|\check{\rho}^{k}\|_{\infty} \le C^{*}, \quad \|\nabla_{h}\check{\rho}^{k}\|_{\infty} \le C^{*}, \quad \|\check{\rho}^{k} - \check{\rho}^{k-1}\|_{\infty} \le C^{*}\Delta t, \quad \|\nabla_{h}(\check{\rho}^{k} - \check{\rho}^{k-1})\|_{\infty} \le C^{*}\Delta t. \quad (5.8)$$

5.2 A rough error estimate

Instead of analyzing the original numerical error functions defined in (5.2), we consider the following ones

$$\tilde{\phi}^n := \mathcal{P}_h \check{\phi}^n - \phi^n, \quad \tilde{\rho}^n := \mathcal{P}_h \check{\rho}^n - \rho^n, \quad n \in \mathbb{N}. \tag{5.9}$$

For the convenience of the notation, the following average numerical error functions are introduced at the intermediate time instant $t_{n+\frac{1}{3}}$:

$$\begin{split} \check{\rho}^{n+\frac{1}{2}} &= \frac{3}{2} \check{\rho}^n - \frac{1}{2} \check{\rho}^{n-1}, \\ \hat{\bar{\rho}}^{n+\frac{1}{2}} &= \check{\rho}^{n+\frac{1}{2}} - \hat{\rho}^{n+\frac{1}{2}} = \frac{3}{2} \check{\rho}^n - \frac{1}{2} \check{\rho}^{n-1} - \left((\frac{3}{2} \rho^n - \frac{1}{2} \rho^{n-1})^2 + \Delta t^8 \right)^{\frac{1}{2}}. \end{split}$$

Subtracting the numerical scheme (3.1-3.2) from the consistency estimate (5.5) yields

$$\frac{\tilde{\rho}^{n+1} - \tilde{\rho}^n}{\Delta t} = \nabla_h \cdot \left(\hat{\rho}^{n+\frac{1}{2}} \nabla_h \tilde{v}^{n+\frac{1}{2}} + \tilde{\tilde{\rho}}^{n+\frac{1}{2}} \nabla_h \mathcal{V}^{n+\frac{1}{2}} \right) + \tau_{\rho}^{n+\frac{1}{2}}, \tag{5.10}$$

$$\theta \frac{\tilde{\phi}^{n+1} - \tilde{\phi}^n}{\Delta t} = \frac{\mu}{2} \Delta_h(\tilde{\phi}^n + \tilde{\phi}^{n+1}) - \frac{\alpha}{2} (\tilde{\phi}^{n+1} + \tilde{\phi}^n) + \frac{\chi}{2} (\tilde{\rho}^{n+1} + \tilde{\rho}^n) + \tau_{\phi}^{n+\frac{1}{2}}, \tag{5.11}$$

where

$$\tilde{v}^{n+\frac{1}{2}} = \gamma \tilde{S}^{n+\frac{1}{2}} - \frac{\chi}{2} (\tilde{\phi}^{n+1} + \tilde{\phi}^{n}) + \frac{\chi^{2} \Delta t}{4\theta} (\tilde{\rho}^{n+1} - \tilde{\rho}^{n}),
\tilde{S}^{n+\frac{1}{2}} = \ln(\check{\rho}^{n+1}) - \ln(\rho^{n+1}) - \frac{1}{2\rho^{n+1}} (\tilde{\rho}^{n+1} - \tilde{\rho}^{n}) + \frac{\tilde{\rho}^{n+1}}{2\check{\rho}^{n+1}\rho^{n+1}} (\check{\rho}^{n+1} - \check{\rho}^{n})
- \frac{\check{\rho}^{n+1} - \check{\rho}^{n} + \rho^{n+1} - \rho^{n}}{6(\rho^{n+1})^{2}} (\tilde{\rho}^{n+1} - \tilde{\rho}^{n}) + \frac{(\check{\rho}^{n+1} + \rho^{n+1})\tilde{\rho}^{n+1}}{6(\check{\rho}^{n+1})^{2} (\rho^{n+1} - \check{\rho}^{n})^{2}},
\mathcal{V}^{n+\frac{1}{2}} = \gamma \check{S}^{n+\frac{1}{2}} - \frac{\chi}{2} (\check{\phi}^{n+1} + \check{\phi}^{n}) + \frac{\chi^{2} \Delta t}{4\theta} (\check{\rho}^{n+1} - \check{\rho}^{n}).$$
(5.12)

A discrete $W_h^{1,\infty}$ bound could be assumed for $\mathcal{V}^{n+\frac{1}{2}}$, due to the fact that it only depends on the exact solution and the constructed profiles:

$$\|\mathcal{V}^{n+\frac{1}{2}}\|_{W_{b}^{1,\infty}} \le C^{*}. \tag{5.13}$$

In addition, we make the following a-prior assumption at the previous time steps:

$$\|\tilde{\rho}^n\|_2, \ \|\tilde{\phi}^n\|_2 \le \Delta t^{\frac{15}{4}} + h^{\frac{15}{4}}, \ \|\tilde{\rho}^{n-1}\|_2, \ \|\tilde{\rho}^{n-2}\|_2 \le \Delta t^{\frac{11}{4}} + h^{\frac{11}{4}}.$$
 (5.14)

Such an a-priori assumption is valid at n=0, as indicated by Remark 3.3. In addition, this assumption will be recovered by the optimal rate convergence analysis at the next time step, as will be proved later. Thanks to the inverse inequality, the $W_h^{1,\infty}$ bound for the numerical error function is available at the previous time steps:

$$\|\tilde{\rho}^{k}\|_{\infty} \leq \frac{C\|\tilde{\rho}^{k}\|_{2}}{h^{\frac{3}{2}}} \leq \frac{C(\Delta t^{\frac{11}{4}} + h^{\frac{11}{4}})}{h^{\frac{3}{2}}} \leq C(\Delta t^{\frac{5}{4}} + h^{\frac{5}{4}}) \leq \frac{\varepsilon^{*}}{2},$$

$$\|\nabla_{h}\tilde{\rho}^{k}\|_{\infty} \leq \frac{2\|\tilde{\rho}^{k}\|_{\infty}}{h} \leq \frac{C(\Delta t^{\frac{5}{4}} + h^{\frac{5}{4}})}{h} \leq C(\Delta t^{\frac{1}{4}} + h^{\frac{1}{4}}) \leq 1,$$

$$(5.15)$$

where the linear refinement constraint $\lambda_1 h \leq \Delta t \leq \lambda_2 h$ has been used. Subsequently, combined with the regularity assumption (5.8), a $W_h^{1,\infty}$ bound for the numerical solution could be derived at the previous time steps:

$$\|\rho^{k}\|_{\infty} \leq \|\check{\rho}^{k}\|_{\infty} + \|\tilde{\rho}^{k}\|_{\infty} \leq C^{*} + \frac{\varepsilon^{*}}{2} := \check{C}_{0}, \quad k = n, n - 1, n - 2,$$

$$\|\nabla_{h}\rho^{k}\|_{\infty} \leq \|\nabla_{h}\check{\rho}^{k}\|_{\infty} + \|\nabla_{h}\tilde{\rho}^{k}\|_{\infty} \leq C^{*} + 1 := \tilde{C}_{0}.$$
(5.16)

Its combination with the separation estimate for $\check{\rho}$ results in a similar separation property for the numerical solution at the previous time steps:

$$\rho^k \ge \check{\rho}^n - \|\tilde{\rho}^k\|_{\infty} \ge \frac{\varepsilon^*}{2} \quad k = n, n - 1, n - 2. \tag{5.17}$$

Moreover, the discrete temporal derivative of the numerical solution at the previous time steps has to be bounded, for k = n, n - 1, n - 2, and such a bound will be useful in the later analysis:

$$\|\tilde{\rho}^{k} - \tilde{\rho}^{k-1}\|_{\infty} \leq \|\tilde{\rho}^{k}\|_{\infty} + \|\tilde{\rho}^{k-1}\|_{\infty} \leq C(\Delta t^{\frac{5}{4}} + h^{\frac{5}{4}}) \leq \Delta t,$$

$$\|\rho^{k} - \rho^{k-1}\|_{\infty} \leq \|\check{\rho}^{k} - \check{\rho}^{k-1}\|_{\infty} + \|\tilde{\rho}^{k} - \tilde{\rho}^{k-1}\|_{\infty} \leq (C^{*} + 1)\Delta t = \tilde{C}_{0}\Delta t, \text{ (by (5.8))}.$$

$$(5.18)$$

The following preliminary estimate will be used in the later analysis; its proof is based on direct calculations. The details are left to interested readers.

Lemma 5.3 The following bounds are valid at the intermediate time instant $t_{n+\frac{1}{2}}$:

$$\frac{\varepsilon^*}{2} \le \hat{\rho}^{n+\frac{1}{2}} \le \check{C}_0, \quad \|\tilde{\hat{\rho}}^{n+\frac{1}{2}}\|_2 \le \frac{3}{2} \|\tilde{\rho}^n\|_2 + \frac{1}{2} \|\tilde{\rho}^{n-1}\|_2 + \Delta t^4,
\|\hat{\rho}^{n+\frac{1}{2}} - \hat{\rho}^{n-\frac{1}{2}}\|_{\infty} \le \frac{3}{2} \|\rho^n - \rho^{n-1}\|_{\infty} + \frac{1}{2} \|\rho^{n-1} - \rho^{n-2}\|_{\infty} + 2\Delta t^4 \le 2\tilde{C}_0 \Delta t.$$
(5.19)

Before proceeding into the error estimate, a rough bound control of the nonlinear error inner products, namely, $\langle \tilde{\rho}^{n+1}, \gamma \tilde{S}^{n+\frac{1}{2}} \rangle$, is necessary. A preliminary estimate is stated in the following lemma; the detailed proof is provided in Appendix A.

Lemma 5.4 Suppose the assumptions of the regularity requirement (5.8), phase separation (5.7) for the constructed approximate solution $(\check{\phi}, \check{\rho})$, and the a-priori assumption (5.14) hold. In addition, let $\tilde{\psi}^n$ be an another error function with $\|\tilde{\psi}^n\|_{\infty} \leq h$. Define the following set

$$\mathbb{K} = \{(i, j, k) : \rho_{i,j,k} \ge 2C^* + 1\},$$
(5.20)

and denote $L^* := |\mathbb{K}|$, the number of grid points in \mathbb{K} . Then there exists a constant \check{C}_2 dependent only on ε^* , γ , \check{C}_0 and C^* such that

$$\langle \tilde{\rho}^{n+1}, \gamma \tilde{S}^{n+\frac{1}{2}} + \tilde{\psi}^n \rangle \ge \frac{C^*}{6} \gamma L^* h^3 - \check{C}_2(\gamma^2 \| \tilde{\rho}^n \|_2^2 + \| \tilde{\psi}^n \|_2^2). \tag{5.21}$$

In addition, if $L^* = 0$, i.e., \mathbb{K} is an empty set, there exists a constant \check{C}_3 dependent on C^* and γ such that

$$\langle \tilde{\rho}^{n+1}, \gamma \tilde{S}^{n+\frac{1}{2}} + \tilde{\psi}^n \rangle \ge \check{C}_3 \|\tilde{\rho}^{n+1}\|_2^2 - \check{C}_2(\gamma^2 \|\tilde{\rho}^n\|_2^2 + \|\tilde{\psi}^n\|_2^2). \tag{5.22}$$

The following proposition states a rough error estimate.

Proposition 5.5 Based on the regularity requirement assumption (5.13) for the constructed profile $\mathcal{V}^{n+\frac{1}{2}}$, as well as the a-priori assumption (5.14) for the numerical solution at the previous time steps, a rough error estimate is available:

$$\|\tilde{\rho}^{n+1}\|_2 \le \Delta t^3 + h^3. \tag{5.23}$$

Proof We divide the proof into three steps: (1) establish an upper bound for $\langle \tilde{\rho}^{n+1}, \tilde{v}^{n+\frac{1}{2}} \rangle$; (2) establish a lower bound for $\langle \tilde{\rho}^{n+1}, \tilde{v}^{n+\frac{1}{2}} \rangle$; and (3) combine the bounds obtained in steps 1 and 2 to get the rough estimate (5.23).

Step 1. Taking a discrete inner product with (5.10) by $\tilde{v}^{n+\frac{1}{2}}$ leads to

$$\langle \tilde{\rho}^{n+1}, \tilde{v}^{n+\frac{1}{2}} \rangle + \Delta t \langle \hat{\rho}^{n+\frac{1}{2}} \nabla_h \tilde{v}^{n+\frac{1}{2}}, \nabla_h \tilde{v}^{n+\frac{1}{2}} \rangle = \langle \tilde{\rho}^n, \tilde{v}^{n+\frac{1}{2}} \rangle + \Delta t \langle \tau_{\rho}^{n+\frac{1}{2}}, \tilde{v}^{n+\frac{1}{2}} \rangle - \Delta t \langle \tilde{\hat{\rho}}^{n+\frac{1}{2}} \nabla_h \mathcal{V}^{n+\frac{1}{2}}, \nabla_h \tilde{v}^{n+\frac{1}{2}} \rangle.$$

$$(5.24)$$

Applying the separation estimate (5.19) for the mobility functions $\hat{\rho}^{n+\frac{1}{2}}$, we obtain the following inequality:

$$\langle \hat{\rho}^{n+\frac{1}{2}} \nabla_h \tilde{v}^{n+\frac{1}{2}}, \nabla_h \tilde{v}^{n+\frac{1}{2}} \rangle \ge \frac{\varepsilon^*}{2} \| \nabla_h \tilde{v}^{n+\frac{1}{2}} \|_2^2.$$
 (5.25)

By the mean-free property for the local truncation error terms, the following estimate is obvious:

$$\langle \tau_{\rho}^{n+\frac{1}{2}}, \tilde{v}^{n+\frac{1}{2}} \rangle \leq \| \tau_{\rho}^{n+\frac{1}{2}} \|_{-1,h} \cdot \| \nabla_{h} \tilde{v}^{n+\frac{1}{2}} \|_{2} \leq \frac{2}{\varepsilon^{*}} \| \tau_{\rho}^{n+\frac{1}{2}} \|_{-1,h}^{2} + \frac{\varepsilon^{*}}{8} \| \nabla_{h} \tilde{v}^{n+\frac{1}{2}} \|_{2}^{2}.$$
 (5.26)

An application of the Cauchy inequality reveals that

$$\langle \tilde{\rho}^{n}, \tilde{v}^{n+\frac{1}{2}} \rangle \leq \|\tilde{\rho}^{n}\|_{-1,h} \cdot \|\nabla_{h}\tilde{v}^{n+\frac{1}{2}}\|_{2} \leq \frac{2}{\varepsilon^{*}\Lambda_{t}} \|\tilde{\rho}^{n}\|_{-1,h}^{2} + \frac{\varepsilon^{*}}{8} \Delta t \|\nabla_{h}\tilde{v}^{n+\frac{1}{2}}\|_{2}^{2}.$$
 (5.27)

Using discrete Hölder and Young's inequalities for the last term on the right hand side of (5.24), we have

$$-\left\langle \tilde{\rho}^{n+\frac{1}{2}} \nabla_{h} \mathcal{V}^{n+\frac{1}{2}}, \nabla_{h} \tilde{v}^{n+\frac{1}{2}} \right\rangle \leq \|\nabla_{h} \mathcal{V}^{n+\frac{1}{2}}\|_{\infty} \cdot \|\tilde{\rho}^{n+\frac{1}{2}}\|_{2} \cdot \|\nabla_{h} \tilde{v}^{n+\frac{1}{2}}\|_{2}$$

$$\leq C^{*} \|\tilde{\rho}^{n+\frac{1}{2}}\|_{2} \cdot \|\nabla_{h} \tilde{v}^{n+\frac{1}{2}}\|_{2}$$

$$\leq C^{*} \left(\frac{3}{2} \|\tilde{\rho}^{n}\|_{2} + \frac{1}{2} \|\tilde{\rho}^{n-1}\|_{2} + \Delta t^{4} \right) \cdot \|\nabla_{h} \tilde{v}^{n+\frac{1}{2}}\|_{2}$$

$$\leq \hat{C}_{1} \left(3 \|\tilde{\rho}^{n}\|_{2}^{2} + \|\tilde{\rho}^{n-1}\|_{2}^{2} + \Delta t^{8} \right) + \frac{\varepsilon^{*}}{8} \|\nabla_{h} \tilde{v}^{n+\frac{1}{2}}\|_{2}^{2},$$

$$(5.28)$$

where $\hat{C}_1 = \frac{4(C^*)^2}{\varepsilon^*}$. Therefore, a substitution of (5.25-5.28) into (5.24) gives

$$\langle \tilde{\rho}^{n+1}, \tilde{v}^{n+\frac{1}{2}} \rangle + \frac{\varepsilon^* \Delta t}{8} \| \nabla_h \tilde{v}^{n+\frac{1}{2}} \|_2^2 \le \frac{2}{\varepsilon^* \Delta t} \| \tilde{\rho}^n \|_{-1,h}^2 + \frac{2\Delta t}{\varepsilon^*} \| \tau_{\rho}^{n+\frac{1}{2}} \|_{-1,h}^2 + \hat{C}_1 \Delta t (3 \| \tilde{\rho}^n \|_2^2 + \| \tilde{\rho}^{n-1} \|_2^2 + \Delta t^8).$$
(5.29)

Step 2. The numerical error for the evolutionary equation (5.11) is equivalent to $\mathcal{L}_1\tilde{\phi}^{n+1} = \mathcal{L}_2\tilde{\phi}^n + \frac{\chi}{2}(\tilde{\rho}^{n+1} + \tilde{\rho}^n) + \tau_{\phi}^{n+\frac{1}{2}}$, so that the linear error terms could be rewritten as

$$\tilde{\phi}^{n+1} = \mathcal{L}_1^{-1} \mathcal{L}_2 \tilde{\phi}^n + \frac{\chi}{2} \mathcal{L}_1^{-1} (\tilde{\rho}^{n+1} + \tilde{\rho}^n) + \mathcal{L}_1^{-1} \tau_{\phi}^{n+\frac{1}{2}}.$$

This in turn gives

$$-\frac{\chi}{2}(\tilde{\phi}^{n+1}+\tilde{\phi}^n)+\frac{\chi^2}{4\theta}\Delta t(\tilde{\rho}^{n+1}-\tilde{\rho}^n)=\tilde{\psi}^n+\mathcal{G}_h\tilde{\rho}^{n+1},$$

where

$$\tilde{\psi}^n = -\frac{\chi}{2}\mathcal{L}_1^{-1}\mathcal{L}_2\tilde{\phi}^n - \frac{\chi^2}{4}\mathcal{L}_1^{-1}\tilde{\rho}^n - \frac{\chi}{2}\tilde{\phi}^n - \frac{\chi^2}{4\theta}\Delta t\tilde{\rho}^n - \frac{\chi}{2}\mathcal{L}_1^{-1}\tau_\phi^{n+\frac{1}{2}}.$$

Subsequently, the following bounds could be derived:

$$\begin{split} &\|\mathcal{L}_{1}^{-1}\mathcal{L}_{2}\tilde{\phi}^{n}\|_{2} \leq \|\tilde{\phi}^{n}\|_{2}, \ \|\frac{\chi}{2}\mathcal{L}_{1}^{-1}\mathcal{L}_{2}\tilde{\phi}^{n} + \frac{\chi}{2}\tilde{\phi}^{n}\|_{2} \leq \chi \|\tilde{\phi}^{n}\|_{2}, \ \|\mathcal{L}_{1}^{-1}\tau_{\phi}^{n+\frac{1}{2}}\|_{2} \leq \theta^{-1}\Delta t \|\tau_{\phi}^{n+\frac{1}{2}}\|_{2}, \\ &\|\mathcal{L}_{1}^{-1}\tilde{\rho}^{n}\|_{2} \leq \theta^{-1}\Delta t \|\tilde{\rho}^{n}\|_{2}, \ \|\frac{\chi^{2}}{4}\mathcal{L}_{1}^{-1}\tilde{\rho}^{n} + \frac{\chi^{2}}{4\theta}\Delta t \tilde{\rho}^{n}\|_{2} \leq \frac{\chi^{2}}{2\theta}\Delta t \|\tilde{\rho}^{n}\|_{2}, \\ &\text{so that} \ \|\tilde{\psi}^{n}\|_{2} \leq \chi \|\tilde{\phi}^{n}\|_{2} + \frac{\chi^{2}}{2\theta}\Delta t \|\tilde{\rho}^{n}\|_{2} + \frac{\chi}{2\theta}\Delta t \|\tau_{\phi}^{n+\frac{1}{2}}\|_{2} \leq C(\Delta t^{\frac{15}{4}} + h^{\frac{15}{4}}), \end{split}$$
 (5.30)

in which the inequalities $\|\mathcal{L}_1^{-1}\mathcal{L}_2 f\|_2 \leq \|f\|_2$, $\|\mathcal{L}_1^{-1}f\|_2 \leq \theta^{-1}\Delta t\|f\|_2$ (the detailed proof is provided in Appendix B), and the a-priori assumption (5.14), have been repeatedly applied in the derivation. Of course, an application of inverse inequality indicates that

$$\|\tilde{\psi}^n\|_{\infty} \le \frac{C\|\tilde{\psi}^n\|_2}{h^{\frac{3}{2}}} \le \frac{C(\Delta t^{\frac{15}{4}} + h^{\frac{15}{4}})}{h^{\frac{3}{2}}} \le C(\Delta t^{\frac{9}{4}} + h^{\frac{9}{4}}) \le h, \quad \text{since } \lambda_1 h \le \Delta t \le \lambda_2 h. \tag{5.31}$$

As a consequence, an application of the rough bound control (5.21) (in Lemma 5.4) gives

$$\langle \tilde{\rho}^{n+1}, \gamma \tilde{S}^{n+\frac{1}{2}} + \tilde{\psi}^n \rangle \ge \frac{C^*}{6} \gamma L^* h^3 - \check{C}_2(\gamma^2 \| \tilde{\rho}^n \|_2^2 + \| \tilde{\psi}^n \|_2^2). \tag{5.32}$$

Moreover, the monotonicity estimate (4.2) of the operator \mathcal{G}_h (in Lemma 4.2) implies that

$$\left\langle \tilde{\rho}^{n+1}, \mathcal{G}_h \tilde{\rho}^{n+1} \right\rangle \ge 0.$$
 (5.33)

In turn, a combination of (5.32) and (5.33) leads to

$$\langle \tilde{\rho}^{n+1}, \tilde{v}^{n+\frac{1}{2}} \rangle \ge \frac{C^*}{6} \gamma L^* h^3 - \check{C}_2(\gamma^2 \|\tilde{\rho}^n\|_2^2 + \|\tilde{\psi}^n\|_2^2).$$
 (5.34)

Step 3. A combination of (5.34) with (5.29) reveals that

$$\frac{C^*}{6}\gamma L^*h^3 + \frac{\varepsilon^*\Delta t}{8} \|\nabla_h \tilde{v}^{n+\frac{1}{2}}\|_2^2 \leq \frac{2}{\varepsilon^*\Delta t} \|\tilde{\rho}^n\|_{-1,h}^2 + \frac{2\Delta t}{\varepsilon^*} \|\tau_{\rho}^{n+\frac{1}{2}}\|_{-1,h}^2 + \check{C}_2 \|\tilde{\psi}^n\|_2^2 \\
+ (\check{C}_2 \gamma^2 + 1) \|\tilde{\rho}^n\|_2^2 + \hat{C}_1 \Delta t (\|\tilde{\rho}^{n-1}\|_2^2 + \Delta t^8), \text{ if } 3\hat{C}_1 \Delta t \leq 1. \tag{5.35}$$

The following bounds for the right hand side terms are available, based on the a-priori assumption (5.14), the preliminary estimate (5.30), as well as the higher order truncation error accuracy:

$$\frac{2}{\varepsilon^* \Delta t} \|\tilde{\rho}^n\|_{-1,h}^2 \leq \frac{2C}{\varepsilon^* \Delta t} \|\tilde{\rho}^n\|_2^2 \leq C(\Delta t^{\frac{13}{2}} + h^{\frac{13}{2}}),
\check{C}_2 \|\tilde{\psi}^n\|_2^2, \ (\check{C}_2 \gamma^2 + 1) \|\tilde{\rho}^n\|_2^2 \leq C(\Delta t^{\frac{15}{2}} + h^{\frac{15}{2}}),
\frac{2\Delta t}{\varepsilon^*} \|\tau_{\rho}^{n+\frac{1}{2}}\|_{-1,h}^2 \leq C\Delta t \|\tau_{\rho}^{n+\frac{1}{2}}\|_2^2 \leq C(\Delta t^9 + \Delta t h^8),
\hat{C}_1 \Delta t \|\tilde{\rho}^{n-1}\|_2^2 \leq C\Delta t (\Delta t^{\frac{11}{2}} + h^{\frac{11}{2}}) \leq C(\Delta t^{\frac{13}{2}} + \Delta t h^{\frac{11}{2}}).$$
(5.36)

Again, the inequality $||f||_{-1,h} \le C||f||_2$ and the linear refinement requirement $\lambda_1 h \le \Delta t \le \lambda_2 h$, have been used. Going back to (5.35), we arrive at

$$\frac{C^*}{6}\gamma L^* h^3 \le C(\Delta t^{\frac{13}{2}} + h^{\frac{13}{2}}).$$

If $L^* \geq 1$, this inequality could make a contradiction, provided that Δt and h are sufficiently small. Therefore, we conclude that $L^* = 0$. In turn, an improved estimate (5.22), as given by Lemma 5.4, becomes available. As a direct consequence, we obtain

$$\langle \tilde{\rho}^{n+1}, \tilde{v}^{n+\frac{1}{2}} \rangle \geq \check{C}_{3} \|\tilde{\rho}^{n+1}\|_{2}^{2} - \check{C}_{2}(\gamma^{2} \|\tilde{\rho}^{n}\|_{2}^{2} + \|\tilde{\psi}^{n}\|_{2}^{2}), \quad \text{so that}$$

$$\check{C}_{3} \|\tilde{\rho}^{n+1}\|_{2}^{2} + \frac{\varepsilon^{*} \Delta t}{8} \|\nabla_{h} \tilde{v}^{n+\frac{1}{2}}\|_{2}^{2} \leq \frac{2}{\varepsilon^{*} \Delta t} \|\tilde{\rho}^{n}\|_{-1,h}^{2} + \frac{2\Delta t}{\varepsilon^{*}} \|\tau_{\rho}^{n+\frac{1}{2}}\|_{-1,h}^{2} + \check{C}_{2} \|\tilde{\psi}^{n}\|_{2}^{2} + \hat{C}_{1} \Delta t^{9} + (\check{C}_{2}\gamma^{2} + 1) \|\tilde{\rho}^{n}\|_{2}^{2} + \hat{C}_{1} \Delta t \|\tilde{\rho}^{n-1}\|_{2}^{2} \leq C(\Delta t^{\frac{13}{2}} + h^{\frac{13}{2}}).$$

$$(5.37)$$

In particular, we see that

$$\|\tilde{\rho}^{n+1}\|_{2} \le C(\Delta t^{\frac{13}{4}} + h^{\frac{13}{4}}) \le \Delta t^{3} + h^{3},\tag{5.38}$$

under the linear refinement requirement $\lambda_1 h \leq \Delta t \leq \lambda_2 h$. This inequality is exactly the rough error estimate (5.23), and the proof of Proposition 5.5 is completed.

With the rough error estimate (5.23) at hand, we are able to establish the $W_h^{1,\infty}$ bound of the numerical solution for the density variable. A direct application of 3-D inverse inequality gives

$$\|\tilde{\rho}^{n+1}\|_{\infty} \leq \frac{C\|\tilde{\rho}^{n+1}\|_{2}}{h^{\frac{3}{2}}} \leq C(\Delta t^{\frac{3}{2}} + h^{\frac{3}{2}}) \leq \frac{\varepsilon^{*}}{2},$$

$$\|\nabla_{h}\tilde{\rho}^{n+1}\|_{\infty} \leq \frac{2\|\tilde{\rho}^{n+1}\|_{\infty}}{h} \leq C(\Delta t^{\frac{1}{2}} + h^{\frac{1}{2}}) \leq 1,$$
(5.39)

under the same linear refinement requirement. In turn, the following separation is valid at time step t_{n+1} :

$$\frac{\varepsilon^*}{2} \le \rho^{n+1} \le C^* + \frac{\varepsilon^*}{2} = \check{C}_0. \tag{5.40}$$

This $\|\cdot\|_{\infty}$ bound will play a very important role in the refined error estimate. Moreover, a maximum norm bound also becomes available for $\nabla_h \rho^{n+1}$:

$$\|\nabla_h \rho^{n+1}\|_{\infty} \le \|\nabla_h \check{\rho}^{n+1}\|_{\infty} + \|\nabla_h \check{\rho}^{n+1}\|_{\infty} \le C^* + 1 = \tilde{C}_0. \tag{5.41}$$

Meanwhile, the following bound, in terms of the discrete temporal derivative for the numerical solution at time step t_{n+1} , will be used in the refined error estimate:

$$\|\tilde{\rho}^{n+1} - \tilde{\rho}^n\|_{\infty} \le \|\tilde{\rho}^{n+1}\|_{\infty} + \|\tilde{\rho}^n\|_{\infty} \le 2C(\Delta t^{\frac{3}{2}} + h^{\frac{3}{2}}) \le \Delta t,$$

$$\|\rho^{n+1} - \rho^n\|_{\infty} \le \|\check{\rho}^{n+1} - \check{\rho}^n\|_{\infty} + \|\tilde{\rho}^{n+1} - \tilde{\rho}^n\|_{\infty} \le (C^* + 1)\Delta t = \tilde{C}_0 \Delta t.$$
(5.42)

In particular, the following observation is made

$$\|\rho^{n+1} - \hat{\rho}^{n+\frac{1}{2}}\|_{\infty} \le \|(\rho^{n+1} - \rho^n) - \frac{1}{2}(\rho^n - \rho^{n-1})\|_{\infty} + C\Delta t^4$$

$$\le \|\rho^{n+1} - \rho^n\|_{\infty} + \frac{1}{2}\|\rho^n - \rho^{n-1}\|_{\infty} + C\Delta t^4 \le \frac{3}{2}\tilde{C}_0\Delta t.$$
(5.43)

Meanwhile, by the fact that $\frac{\varepsilon^*}{2} \leq \rho^{n+1}$, $\hat{\rho}^{n+\frac{1}{2}} \leq \tilde{C}_0$, it is clear that

$$\frac{3}{4} \le \frac{\hat{\rho}^{n+\frac{1}{2}}}{\rho^{n+1}} \le \frac{5}{4}, \quad \text{at a point-wise level, provided that } \Delta t \text{ is sufficiently small.}$$
 (5.44)

5.3 A refined error estimate

The rough error estimate (5.23) is not able to go through an induction argument. Therefore, a refined error estimate is needed to accomplish a closed loop of convergence analysis. Because of the Crank-Nicolson-style temporal discretization in the numerical design, the following preliminary estimate is necessary to control the nonlinear errors associated with the logarithmic diffusion part. The technical details of the proof are provided in Appendix C.

Proposition 5.6 Assume that the a-priori $\|\cdot\|_{\infty}$ estimate (5.16)-(5.19) and the rough $\|\cdot\|_{\infty}$ estimates (5.40)-(5.44) hold for the numerical solution at the previous and next time steps, respectively. There exist positive constants \tilde{C}_1 , M_1 , dependent only on ε^* , C^* , γ , \tilde{C}_0 and $|\Omega|$ such that

$$\gamma \left\langle \hat{\rho}^{n+\frac{1}{2}} \nabla_h \tilde{S}^{n+\frac{1}{2}}, \nabla_h (\tilde{\rho}^{n+1} + \tilde{\rho}^n) \right\rangle \ge \frac{\gamma}{4} \|\nabla_h (\tilde{\rho}^{n+1} + \tilde{\rho}^n)\|_2^2 - \tilde{C}_1(\|\tilde{\rho}^{n+1}\|_2^2 + \|\tilde{\rho}^n\|_2^2) - M_1 h^8.$$
(5.45)

Proposition 5.7 Assume that the a-priori $\|\cdot\|_{\infty}$ estimate (5.19) hold for the numerical solution at the previous time steps. There exists a positive constant C, independent of h and Δt , such that

$$\|\tilde{\rho}^{n+1}\|_{2} + \|\tilde{\phi}^{n+1}\|_{2} + \|\nabla_{h}\tilde{\phi}^{n+1}\|_{2} \le C(\Delta t^{4} + h^{4}),$$

$$\Delta t \sum_{k=1}^{n} \|\nabla_{h}(\tilde{\rho}^{k+1} + \tilde{\rho}^{k})\|_{2}^{2} + \Delta t \sum_{k=1}^{n} \|\Delta_{h}(\tilde{\phi}^{k+1} + \tilde{\phi}^{k})\|_{2}^{2} \le C(\Delta t^{8} + h^{8}).$$

Proof Now we look at the refined error estimate. Taking a discrete inner product with (5.10) by $(\tilde{\rho}^{n+1} + \tilde{\rho}^n)$ gives

$$\frac{1}{\Delta t} (\|\tilde{\rho}^{n+1}\|_{2}^{2} - \|\tilde{\rho}^{n}\|_{2}^{2}) + \left\langle \hat{\rho}^{n+\frac{1}{2}} \nabla_{h} \tilde{v}^{n+\frac{1}{2}}, \nabla_{h} (\tilde{\rho}^{n+1} + \tilde{\rho}^{n}) \right\rangle
= -\left\langle \tilde{\hat{\rho}}^{n+\frac{1}{2}} \nabla_{h} \mathcal{V}^{n+\frac{1}{2}}, \nabla_{h} (\tilde{\rho}^{n+1} + \tilde{\rho}^{n}) \right\rangle + \left\langle \tau_{\rho}^{n+\frac{1}{2}}, \tilde{\rho}^{n+1} + \tilde{\rho}^{n} \right\rangle.$$
(5.46)

The first term on the right hand side could be analyzed in a standard way:

$$\begin{split} -\left\langle \tilde{\rho}^{n+\frac{1}{2}} \nabla_{h} \mathcal{V}^{n+\frac{1}{2}}, \nabla_{h} (\tilde{\rho}^{n+1} + \tilde{\rho}^{n}) \right\rangle \leq & \|\nabla_{h} \mathcal{V}^{n+\frac{1}{2}}\|_{\infty} \cdot \|\tilde{\rho}^{n+\frac{1}{2}}\|_{2} \cdot \|\nabla_{h} (\tilde{\rho}^{n+1} + \tilde{\rho}^{n})\|_{2} \\ \leq & C^{*} (\frac{3}{2} \|\tilde{\rho}^{n}\|_{2} + \frac{1}{2} \|\tilde{\rho}^{n-1}\|_{2} + \Delta t^{4}) \|\nabla_{h} (\tilde{\rho}^{n+1} + \tilde{\rho}^{n})\|_{2} \\ \leq & \frac{(C^{*})^{2}}{\gamma} (24 \|\tilde{\rho}^{n}\|_{2}^{2} + 8\gamma \|\tilde{\rho}^{n-1}\|_{2}^{2} + 8\Delta t^{8}) \\ & + \frac{\gamma}{16} \|\nabla_{h} (\tilde{\rho}^{n+1} + \tilde{\rho}^{n})\|_{2}^{2}. \end{split}$$

$$(5.47)$$

The Cauchy inequality is applied to bound the local truncation error term:

$$\langle \tau_{\rho}^{n+\frac{1}{2}}, \tilde{\rho}^{n+1} + \tilde{\rho}^{n} \rangle \leq \|\tau_{\rho}^{n+\frac{1}{2}}\|_{2} \cdot \|\tilde{\rho}^{n+1} + \tilde{\rho}^{n}\|_{2} \leq \frac{1}{2} \|\tau_{\rho}^{n+\frac{1}{2}}\|_{2}^{2} + (\|\tilde{\rho}^{n+1}\|_{2}^{2} + \|\tilde{\rho}^{n}\|_{2}^{2}). \tag{5.48}$$

For the nonlinear term on the left hand side, we separate it into three parts:

$$\left\langle \hat{\rho}^{n+\frac{1}{2}} \nabla_{h} \tilde{v}^{n+\frac{1}{2}}, \nabla_{h} (\tilde{\rho}^{n+1} + \tilde{\rho}^{n}) \right\rangle
= \gamma \left\langle \hat{\rho}^{n+\frac{1}{2}} \nabla_{h} \tilde{S}^{n+\frac{1}{2}}, \nabla_{h} (\tilde{\rho}^{n+1} + \tilde{\rho}^{n}) \right\rangle - \frac{\chi}{2} \left\langle \hat{\rho}^{n+\frac{1}{2}} \nabla_{h} (\tilde{\phi}^{n+1} + \tilde{\phi}^{n}), \nabla_{h} (\tilde{\rho}^{n+1} + \tilde{\rho}^{n}) \right\rangle
+ \frac{\chi^{2} \Delta t}{4\theta} \left\langle \hat{\rho}^{n+\frac{1}{2}} \nabla_{h} (\tilde{\rho}^{n+1} - \tilde{\rho}^{n}), \nabla_{h} (\tilde{\rho}^{n+1} + \tilde{\rho}^{n}) \right\rangle.$$
(5.49)

The second part could be controlled by a direct application of the Cauchy inequality:

$$\frac{\chi}{2} \left\langle \hat{\rho}^{n+\frac{1}{2}} \nabla_{h} (\tilde{\phi}^{n+1} + \tilde{\phi}^{n}), \nabla_{h} (\tilde{\rho}^{n+1} + \tilde{\rho}^{n}) \right\rangle
\leq \frac{\chi}{2} \|\hat{\rho}^{n+\frac{1}{2}}\|_{\infty} \cdot \|\nabla_{h} (\tilde{\phi}^{n+1} + \tilde{\phi}^{n})\|_{2} \cdot \|\nabla_{h} (\tilde{\rho}^{n+1} + \tilde{\rho}^{n})\|_{2}
\leq \frac{\chi \check{C}_{0}}{2} \cdot \|\nabla_{h} (\tilde{\phi}^{n+1} + \tilde{\phi}^{n})\|_{2} \cdot \|\nabla_{h} (\tilde{\rho}^{n+1} + \tilde{\rho}^{n})\|_{2}
\leq \frac{2\chi^{2} \check{C}_{0}^{2}}{\gamma} (\|\nabla_{h} \tilde{\phi}^{n+1}\|_{2}^{2} + \|\nabla_{h} \tilde{\phi}^{n}\|_{2}^{2}) + \frac{\gamma}{16} \|\nabla_{h} (\tilde{\rho}^{n+1} + \tilde{\rho}^{n})\|_{2}^{2}.$$
(5.50)

In terms of the third part on the right hand side of (5.49), we begin with a point-wise vector identity: $\nabla_h(\tilde{\rho}^{n+1} - \tilde{\rho}^n) \cdot \nabla_h(\tilde{\rho}^{n+1} + \tilde{\rho}^n) = |\nabla_h\tilde{\rho}^{n+1}|^2 - |\nabla_h\tilde{\rho}^n|^2$. This in turn leads to

$$\left\langle \hat{\rho}^{n+\frac{1}{2}} \nabla_{h} (\tilde{\rho}^{n+1} - \tilde{\rho}^{n}), \nabla_{h} (\tilde{\rho}^{n+1} + \tilde{\rho}^{n}) \right\rangle
= \left\langle \hat{\rho}^{n+\frac{1}{2}}, |\nabla_{h} \tilde{\rho}^{n+1}|^{2} - |\nabla_{h} \tilde{\rho}^{n}|^{2} \right\rangle
= \left\langle \hat{\rho}^{n+\frac{1}{2}}, |\nabla_{h} \tilde{\rho}^{n+1}|^{2} \right\rangle - \left\langle \hat{\rho}^{n-\frac{1}{2}}, |\nabla_{h} \tilde{\rho}^{n}|^{2} \right\rangle - \left\langle \hat{\rho}^{n+\frac{1}{2}} - \hat{\rho}^{n-\frac{1}{2}}, |\nabla_{h} \tilde{\rho}^{n}|^{2} \right\rangle.$$
(5.51)

Moreover, for the last term in the rewritten expansion, an application of the preliminary estimate (5.19) implies that

$$\left\langle \hat{\rho}^{n+\frac{1}{2}} - \hat{\rho}^{n-\frac{1}{2}}, |\nabla_h \tilde{\rho}^n|^2 \right\rangle \le \|\hat{\rho}^{n+\frac{1}{2}} - \hat{\rho}^{n-\frac{1}{2}}\|_{\infty} \cdot \|\nabla_h \tilde{\rho}^n\|_2^2 \le 2\tilde{C}_0 \Delta t \|\nabla_h \tilde{\rho}^n\|_2^2. \tag{5.52}$$

Subsequently, a combination of (5.51) and (5.52) yields

$$\frac{\chi^{2}\Delta t}{4\theta} \left\langle \hat{\rho}^{n+\frac{1}{2}} \nabla_{h} (\tilde{\rho}^{n+1} - \tilde{\rho}^{n}), \nabla_{h} (\tilde{\rho}^{n+1} + \tilde{\rho}^{n}) \right\rangle \\
\geq \frac{1}{4} \chi^{2} \theta^{-1} \Delta t \left(\left\langle \hat{\rho}^{n+\frac{1}{2}}, |\nabla_{h} \tilde{\rho}^{n+1}|^{2} \right\rangle - \left\langle \hat{\rho}^{n-\frac{1}{2}}, |\nabla_{h} \tilde{\rho}^{n}|^{2} \right\rangle \right) - \frac{1}{2} \chi^{2} \tilde{C}_{0} \theta^{-1} \Delta t^{2} \|\nabla_{h} \tilde{\rho}^{n}\|_{2}^{2}. \tag{5.53}$$

Meanwhile, the nonlinear diffusion error estimate (5.45) is valid, as stated in Proposition 5.6. A substitution of (5.45), (5.50), and (5.53) into (5.49) results in

$$\left\langle \hat{\rho}^{n+\frac{1}{2}} \nabla_{h} \tilde{v}^{n+\frac{1}{2}}, \nabla_{h} (\tilde{\rho}^{n+1} + \tilde{\rho}^{n}) \right\rangle
\geq \frac{1}{4} \chi^{2} \theta^{-1} \Delta t \left(\left\langle \hat{\rho}^{n+\frac{1}{2}}, |\nabla_{h} \tilde{\rho}^{n+1}|^{2} \right\rangle - \left\langle \hat{\rho}^{n-\frac{1}{2}}, |\nabla_{h} \tilde{\rho}^{n}|^{2} \right\rangle \right) + \frac{3\gamma}{16} \|\nabla_{h} (\tilde{\rho}^{n+1} + \tilde{\rho}^{n})\|_{2}^{2} - M_{1} h^{8}
- \tilde{C}_{1} (\|\tilde{\rho}^{n+1}\|_{2}^{2} + \|\tilde{\rho}^{n}\|_{2}^{2}) - \frac{2\chi^{2} \tilde{C}_{0}^{2}}{\gamma} (\|\nabla_{h} \tilde{\phi}^{n+1}\|_{2}^{2} + \|\nabla_{h} \tilde{\phi}^{n}\|_{2}^{2}) - \frac{1}{2} \chi^{2} \tilde{C}_{0} \theta^{-1} \Delta t^{2} \|\nabla_{h} \tilde{\rho}^{n}\|_{2}^{2}.$$
(5.54)

Its combination with (5.46)-(5.48) reveals that

$$\frac{1}{\Delta t} (\|\tilde{\rho}^{n+1}\|_{2}^{2} - \|\tilde{\rho}^{n}\|_{2}^{2}) + \frac{1}{4}\chi^{2}\theta^{-1}\Delta t(\langle\hat{\rho}^{n+\frac{1}{2}}, |\nabla_{h}\tilde{\rho}^{n+1}|^{2}\rangle - \langle\hat{\rho}^{n-\frac{1}{2}}, |\nabla_{h}\tilde{\rho}^{n}|^{2}\rangle) + \frac{\gamma}{8}\|\nabla_{h}(\tilde{\rho}^{n+1} + \tilde{\rho}^{n})\|_{2}^{2} \\
\leq (\tilde{C}_{1} + 1)\|\tilde{\rho}^{n+1}\|_{2}^{2} + (\tilde{C}_{1} + \frac{1}{2}\chi^{2}\tilde{C}_{0}\theta^{-1}\hat{C}_{3}^{2} + 24\frac{(C^{*})^{2}}{\gamma} + 1)\|\tilde{\rho}^{n}\|_{2}^{2} + 8\frac{(C^{*})^{2}}{\gamma}\|\tilde{\rho}^{n-1}\|_{2}^{2} \\
+ \frac{2\chi^{2}\tilde{C}_{0}^{2}}{\gamma}(\|\nabla_{h}\tilde{\phi}^{n+1}\|_{2}^{2} + \|\nabla_{h}\tilde{\phi}^{n}\|_{2}^{2}) + \frac{1}{2}\|\tau_{\rho}^{n+\frac{1}{2}}\|_{2}^{2} + \frac{8(C^{*})^{2}}{\gamma}\Delta t^{8} + M_{1}h^{8}, \tag{5.55}$$

in which an inverse inequality and $\Delta t \|\nabla_h \tilde{\rho}^n\|_2 \leq \hat{C}_3 \|\tilde{\rho}^n\|_2$ (under the linear refinement requirement $\lambda_1 h \leq \Delta t \leq \lambda_2 h$) has been used.

The analysis for the numerical error evolutionary equation (5.11) takes a much simpler form, because of its linear nature. Taking a discrete inner product with (5.11) by $(\tilde{\phi}^{n+1} + \tilde{\phi}^n)$ gives

$$\frac{\theta}{\Delta t} (\|\tilde{\phi}^{n+1}\|_{2}^{2} - \|\tilde{\phi}^{n}\|_{2}^{2}) + \frac{\mu}{2} \|\nabla_{h}(\tilde{\phi}^{n+1} + \tilde{\phi}^{n})\|_{2}^{2} + \frac{\alpha}{2} \|\tilde{\phi}^{n+1} + \tilde{\phi}^{n}\|_{2}^{2}
= \frac{\chi}{2} \langle \tilde{\rho}^{n+1} + \tilde{\rho}^{n}, \tilde{\phi}^{n+1} + \tilde{\phi}^{n} \rangle + \langle \tau_{\phi}^{n+\frac{1}{2}}, \tilde{\phi}^{n+1} + \tilde{\phi}^{n} \rangle
\leq \frac{\chi}{2} (\|\tilde{\rho}^{n+1}\|_{2}^{2} + \|\tilde{\rho}^{n}\|_{2}^{2}) + (\frac{\chi}{2} + 1) (\|\tilde{\phi}^{n+1}\|_{2}^{2} + \|\tilde{\phi}^{n}\|_{2}^{2}) + \frac{1}{2} \|\tau_{\phi}^{n+\frac{1}{2}}\|_{2}^{2},$$
(5.56)

in which the Cauchy inequality has been repeatedly applied. Meanwhile, we need a further H^1 error estimate for the density variable, to balance the terms $\|\nabla_h \tilde{\phi}^{n+1}\|_2^2$ and $\|\nabla_h \tilde{\phi}^n\|_2^2$ on the right

hand side of (5.55). Taking a discrete inner product with (5.11) by $-\Delta_h(\tilde{\phi}^{n+1} + \tilde{\phi}^n)$ indicates

$$\frac{\theta}{\Delta t} (\|\nabla_h \tilde{\phi}^{n+1}\|_2^2 - \|\nabla_h \tilde{\phi}^n\|_2^2) + \frac{\mu}{2} \|\Delta_h (\tilde{\phi}^{n+1} + \tilde{\phi}^n)\|_2^2 + \frac{\alpha}{2} \|\nabla_h (\tilde{\phi}^{n+1} + \tilde{\phi}^n)\|_2^2
= -\frac{\chi}{2} \langle \tilde{\rho}^{n+1} + \tilde{\rho}^n, \Delta_h (\tilde{\phi}^{n+1} + \tilde{\phi}^n) \rangle - \langle \tau_{\phi}^{n+\frac{1}{2}}, \Delta_h (\tilde{\phi}^{n+1} + \tilde{\phi}^n) \rangle
\leq \chi^2 \mu^{-1} (\|\tilde{\rho}^{n+1}\|_2^2 + \|\tilde{\rho}^n\|_2^2) + 2\mu^{-1} \|\tau_{\phi}^{n+\frac{1}{2}}\|_2^2 + \frac{\mu}{4} \|\Delta_h (\tilde{\phi}^{n+1} + \tilde{\phi}^n)\|_2^2.$$
(5.57)

This is equivalent to

$$\frac{\theta}{\Delta t} (\|\nabla_h \tilde{\phi}^{n+1}\|_2^2 - \|\nabla_h \tilde{\phi}^n\|_2^2) + \frac{\mu}{4} \|\Delta_h (\tilde{\phi}^{n+1} + \tilde{\phi}^n)\|_2^2 + \frac{\alpha}{2} \|\nabla_h (\tilde{\phi}^{n+1} + \tilde{\phi}^n)\|_2^2
\leq \chi^2 \mu^{-1} (\|\tilde{\rho}^{n+1}\|_2^2 + \|\tilde{\rho}^n\|_2^2) + 2\mu^{-1} \|\tau_{\phi}^{n+\frac{1}{2}}\|_2^2.$$
(5.58)

Therefore, a combination of (5.55), (5.56) and (5.58) leads to

$$\begin{split} &\frac{1}{\Delta t} \Big(\|\tilde{\rho}^{n+1}\|_{2}^{2} - \|\tilde{\rho}^{n}\|_{2}^{2} + \theta(\|\tilde{\phi}^{n+1}\|_{2}^{2} - \|\tilde{\phi}^{n}\|_{2}^{2} + \|\nabla_{h}\tilde{\phi}^{n+1}\|_{2}^{2} - \|\nabla_{h}\tilde{\phi}^{n}\|_{2}^{2}) \Big) \\ &+ \frac{1}{4} \chi^{2} \theta^{-1} \Delta t (\langle \hat{\rho}^{n+\frac{1}{2}}, |\nabla_{h}\tilde{\rho}^{n+1}|^{2} \rangle - \langle \hat{\rho}^{n-\frac{1}{2}}, |\nabla_{h}\tilde{\rho}^{n}|^{2} \rangle) \\ &+ \frac{\gamma}{8} \|\nabla_{h} (\tilde{\rho}^{n+1} + \tilde{\rho}^{n})\|_{2}^{2} + \frac{\mu}{4} \|\Delta_{h} (\tilde{\phi}^{n+1} + \tilde{\phi}^{n})\|_{2}^{2} \\ &\leq (\tilde{C}_{1} + 1 + \frac{\chi}{2} + \chi^{2} \mu^{-1}) \|\tilde{\rho}^{n+1}\|_{2}^{2} + (\tilde{C}_{1} + \frac{1}{2} \chi^{2} \tilde{C}_{0} \theta^{-1} \hat{C}_{3}^{2} + 24 \frac{(C^{*})^{2}}{\gamma} + 1 + \frac{\chi}{2} + \chi^{2} \mu^{-1}) \|\tilde{\rho}^{n}\|_{2}^{2} \\ &+ 8 \frac{(C^{*})^{2}}{\gamma} \|\tilde{\rho}^{n-1}\|_{2}^{2} + (\frac{\chi}{2} + 1) (\|\tilde{\phi}^{n+1}\|_{2}^{2} + \|\tilde{\phi}^{n}\|_{2}^{2}) + \frac{2\chi^{2} \tilde{C}_{0}^{2}}{\gamma} (\|\nabla_{h}\tilde{\phi}^{n+1}\|_{2}^{2} + \|\nabla_{h}\tilde{\phi}^{n}\|_{2}^{2}) \\ &+ \frac{1}{2} \|\tau_{\phi}^{n+\frac{1}{2}}\|_{2}^{2} + \frac{1}{2} \|\tau_{\rho}^{n+\frac{1}{2}}\|_{2}^{2} + 2\mu^{-1} \|\tau_{\phi}^{n+\frac{1}{2}}\|_{2}^{2} + 8 \frac{(C^{*})^{2}}{\gamma} \Delta t^{8} + M_{1}h^{8}. \end{split} \tag{5.59}$$

In turn, the following quantity is introduced:

$$\mathcal{F}^{n+1} := \|\tilde{\rho}^{n+1}\|_{2}^{2} + \theta(\|\tilde{\phi}^{n+1}\|_{2}^{2} + \|\nabla_{h}\tilde{\phi}^{n+1}\|_{2}^{2}) + \frac{1}{4}\chi^{2}\theta^{-1}\Delta t^{2}\langle\hat{\rho}^{n+\frac{1}{2}}, |\nabla_{h}\tilde{\rho}^{n+1}|^{2}\rangle. \tag{5.60}$$

Then we obtain

$$\frac{1}{\Delta t} (\mathcal{F}^{n+1} - \mathcal{F}^n) + \frac{\gamma}{8} \|\nabla_h (\tilde{\rho}^{n+1} + \tilde{\rho}^n)\|_2^2 + \frac{\mu}{4} \|\Delta_h (\tilde{\phi}^{n+1} + \tilde{\phi}^n)\|_2^2
\leq \tilde{C}_2 (\mathcal{F}^{n+1} + \mathcal{F}^n + \mathcal{F}^{n-1}) + \frac{1}{2} \|\tau_{\rho}^{n+\frac{1}{2}}\|_2^2 + 2\mu^{-1} \|\tau_{\phi}^{n+\frac{1}{2}}\|_2^2 + \frac{1}{2} \|\tau_{\phi}^{n+\frac{1}{2}}\|_2^2
+ 8 \frac{(C^*)^2}{\gamma} \Delta t^8 + M_1 h^8,$$
(5.61)

where

$$\tilde{C}_2 = \max\Big(\tilde{C}_1 + \frac{1}{2}\chi^2\tilde{C}_0\theta^{-1}\hat{C}_3^2 + 24\frac{(C^*)^2}{\gamma} + 1 + \frac{\chi}{2} + \chi^2\mu^{-1}, (\frac{\chi}{2} + 1)\theta^{-1}, \frac{2\chi^2\check{C}_0^2\theta^{-1}}{\gamma}\Big).$$

Consequently, an application of the discrete Gronwall inequality gives the desired higher order convergence estimate [46]:

$$\mathcal{F}^{n+1} \leq C(\Delta t^{8} + h^{8}), \quad \|\tilde{\rho}^{n+1}\|_{2} + \|\tilde{\phi}^{n+1}\|_{2} + \|\nabla_{h}\tilde{\phi}^{n+1}\|_{2} \leq C(\mathcal{F}^{n+1})^{\frac{1}{2}} \leq C(\Delta t^{4} + h^{4}),$$

$$\Delta t \sum_{k=1}^{n} \|\nabla_{h}(\tilde{\rho}^{k+1} + \tilde{\rho}^{k})\|_{2}^{2} + \Delta t \sum_{k=1}^{n} \|\Delta_{h}(\tilde{\phi}^{k+1} + \tilde{\phi}^{k})\|_{2}^{2} \leq C(\Delta t^{8} + h^{8}),$$

$$(5.62)$$

in which the fourth order truncation error accuracy $\|\tau_{\rho}^{n+\frac{1}{2}}\|_2$, $\|\tau_{\phi}^{n+\frac{1}{2}}\|_2 \leq C(\Delta t^4 + h^4)$ has been applied. This finishes the refined error estimate.

5.4 Recovery of the a-priori assumption (5.14)

With the help of the higher order error estimate, we see that the a-priori assumption (5.14) is satisfied at t_{n+1} :

$$\|\tilde{\rho}^{n+1}\|_{2}, \|\tilde{\phi}^{n+1}\|_{2} \le C(\Delta t^{4} + h^{4}) \le \Delta t^{\frac{15}{4}} + h^{\frac{15}{4}},$$
 (5.63)

provided that Δt and h are sufficiently small. The recovery for $\|\tilde{\rho}^n\|_2$ and $\|\tilde{\rho}^{n-1}\|_2$ would be more straightforward. Therefore, an induction analysis could be effectively applied and the higher order convergence analysis is complete. Subsequently, a combination of (5.62) with (5.4) leads to the convergence estimate (5.3). The proof of Theorem 5.1 is completed.

6 Numerical results

6.1 Accuracy test

We now test numerical accuracy of the proposed scheme (3.1-3.2) in solving the PKS system

$$\begin{cases} \partial_t \rho = \Delta \rho - \nabla \cdot (\rho \nabla \phi) + f_1, \\ \theta \partial_t \phi = \Delta \phi - \phi + \rho + f_2, \end{cases}$$
 (6.1)

in computational domains $\Omega = (0,1)^2$ and $\Omega = (0,1)^3$. For 2D simulations, the source terms f_1 and f_2 are determined by the following exact solution

$$\begin{cases} \rho_e(x, y, t) = 0.1e^{-t}\cos(\pi x)\cos(\pi y) + 0.2, \\ \phi_e(x, y, t) = 0.1e^{-t}\cos(\pi x)\cos(\pi y) + 0.2. \end{cases}$$
(6.2)

In the 3D simulation, the source terms f_1 and f_2 are determined by the following exact solution

$$\begin{cases} \rho_e(x, y, z, t) = 0.1e^{-t}\cos(\pi x)\cos(\pi y)\cos(\pi z) + 0.2, \\ \phi_e(x, y, z, t) = 0.1e^{-t}\cos(\pi x)\cos(\pi y)\cos(\pi z) + 0.2. \end{cases}$$
(6.3)

The initial conditions are obtained by evaluating the exact solution at T=0. We consider homogeneous Neumann boundary condition (1.2) for both ρ and ϕ . We first test numerical accuracy of the proposed scheme utilizing various spatial step size h with a fixed mesh ratio $\Delta t = h/10$. Figure 1 displays the ℓ^{∞} errors and convergence orders for the density of living organisms and chemical signals at a final time T=0.1. We observe that the numerical error

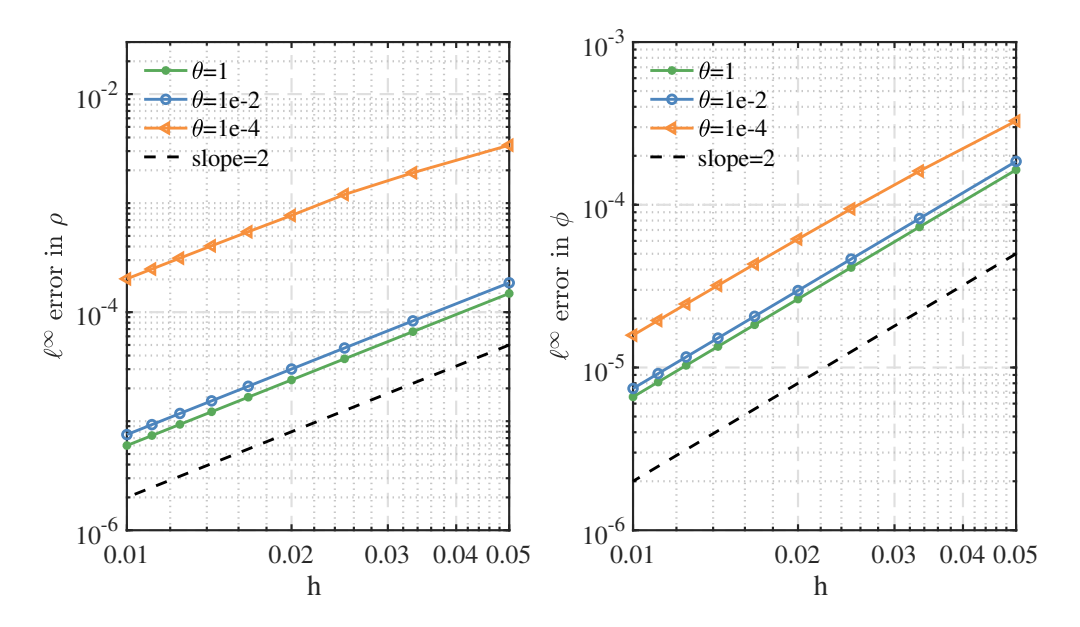


Figure 1: Numerical errors (in ℓ^{∞}) of ρ and ϕ computed by the second-order accurate scheme (3.1)-(3.2) at a final time T=0.1 in 2D simulations, with a mesh ratio $\Delta t=h/10$. Various values of θ are considered: $\theta=1, \theta=1e-2$, and $\theta=1e-4$.

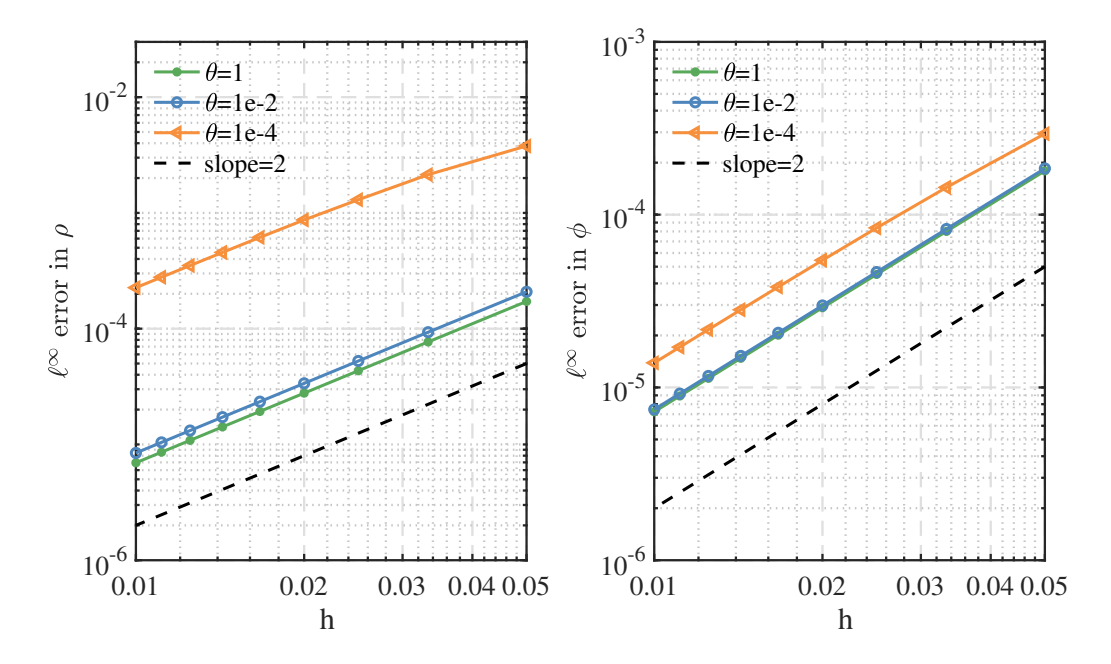


Figure 2: Numerical errors (in ℓ^{∞}) of ρ and ϕ computed by the second-order accurate scheme (3.1)-(3.2) at a final time T=0.1 in the 3D simulation, with a mesh ratio $\Delta t=h/10$. Various values of θ are used: $\theta=1, \theta=1e-2, \text{ and } \theta=1e-4.$

decreases as the mesh refines and that second order convergence rates are clearly observed for both ρ and ϕ . This verifies the second-order accuracy for the proposed numerical scheme (3.1-3.2), in both temporal and spatial discretization. In the 3D simulation, as the mesh refines from $h = \frac{1}{20}$ to $h = \frac{1}{100}$, the ℓ^{∞} errors displayed in Figure 2 decrease at a second-order convergence rate as well, for both the density of living organisms and chemical signals. Also, we observe from the figures that smaller values of θ result in larger ℓ^{∞} errors, particularly for $\theta = 1e - 4$. However, the second-order convergence rate can be robustly maintained across all tested values of θ . Notice that the mesh ratio is chosen for the sake of numerical accuracy test, not for stability or positivity.

6.2 Blowup phenomena

6.2.1 Blowup in the center

In this case, we demonstrate the performance of the proposed scheme in preserving mass conservation, energy dissipation, and solution positivity in a two-dimensional domain $\Omega = (0,1)^2$. The parameters are taken as: $\gamma = 1$, $\chi = 1$, $\theta = 1$, $\mu = 1$, and $\alpha = 1$. The homogeneous boundary conditions are imposed for both ρ and ϕ . The initial data is prescribed as follows:

$$\begin{cases} \rho^{0}(x,y) = 1000e^{-100\left[(x-\frac{1}{2})^{2} + (y-\frac{1}{2})^{2}\right]}, \\ \phi^{0}(x,y) = e^{-100\left[(x-\frac{1}{2})^{2} + (y-\frac{1}{2})^{2}\right]}, \end{cases}$$
(6.4)

which mimics concentrated living organisms and chemical signals of high peak values initially distribute at the center of the domain. According to the mathematical analysis in [26], the

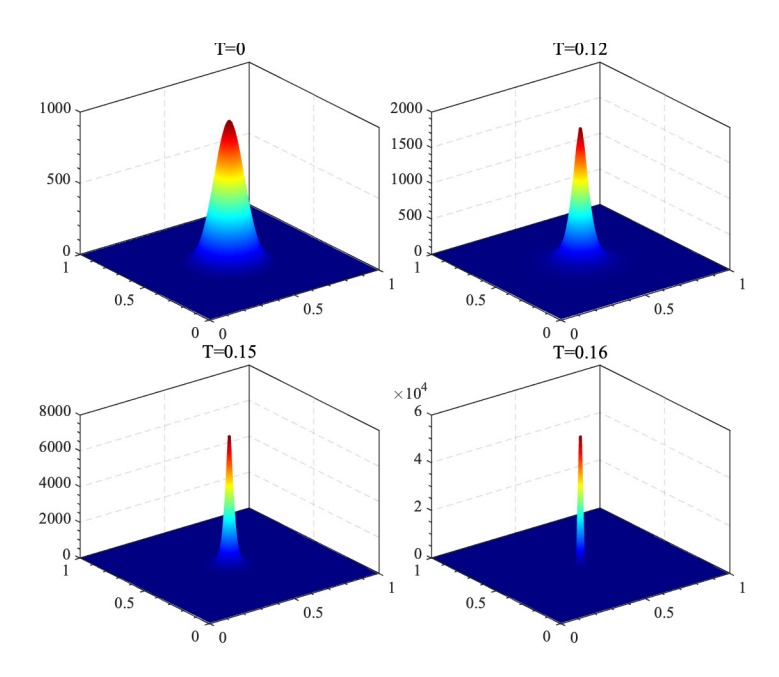


Figure 3: Evolution of density ρ at time instants: $T=0,\,0.12,\,0.15,\,$ and 0.16, with $\Delta t=10^{-5}$ and $h=10^{-2}$.

analytic solution to the classical PKS system is expected to develop a blowup at the center of

the domain in finite time, with initial mass $\|\rho^0\|_1 \approx 31.4159 > 8\pi$. Indeed, Figure 3 displays numerical results on singularity formation at a sequence of time instants: T = 0, 0.12, 0.15, and 0.16, with a time step size $\Delta t = 10^{-5}$. It is observed that the numerical solution of the living organism density evolves into blowup at the center of the domain, leading to a shrinking support for the organism density.

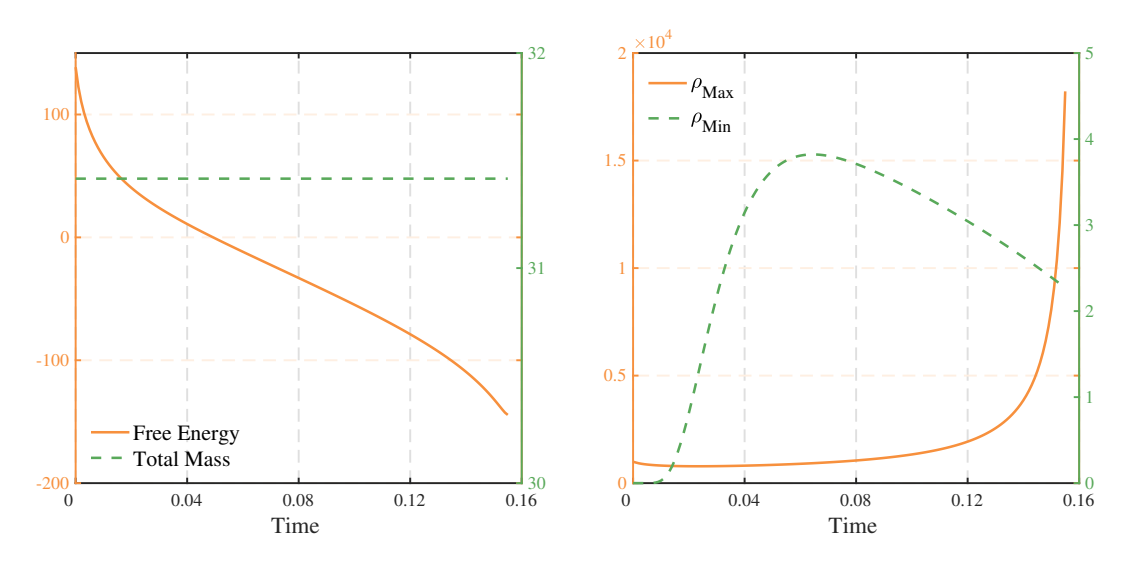


Figure 4: Time evolution of the discrete energy F_h , mass of ρ , and the maximum and minimum values of ρ for the case with blowup at the center.

We next demonstrate the robustness of the proposed numerical scheme in preserving the desired properties in such blowup evolution, which poses a challenging task on numerical stability. With homogeneous Neumann boundary conditions, the physical system possesses mass conservation and free-energy dissipation. From the left panel of Figure 4, one can see that the free energy (4.1) monotonically decreases and the total mass of ρ remains constant robustly as time evolves. The right panel of Figure 4 displays the time evolution of $\rho_{\text{Min}} := \text{Min}_{i,j} \ \rho_{i,j}$ and $\rho_{\text{Max}} := \text{Max}_{i,j} \ \rho_{i,j}$, the minimum and maximum values of ρ over the computational mesh, respectively. It is observed that the proposed numerical scheme is positivity-preserving and the maximum value of ρ grows exponentially as time evolves in the singularity formation.

6.2.2 Effect of mobility

In this case, we assess the performance of the proposed numerical scheme (3.1-3.2) in simulating the PKS system with various mobility functions $\eta(\rho)$ (cf. (2.3)-(2.5)). The simulations are conducted in a two-dimensional domain $\Omega=(0,1)^2$ with the same initial conditions and parameters given in the previous section. In terms of the mobility parameters, we set $\kappa=1e-4$ in the bounded-mobility system (2.4), and M=2000 in saturation-concentration choice (2.5). Figure 5 illustrates (a) the bounded-mobility system in the first row, and (b) the saturation-concentration system in the second row. The first column shows the density distribution ρ at T=0.15. Both modified models effectively capture the chemotaxis phenomenon, characterized by cell aggregation. In contrast to the plot for the PKS system with a classical mobility, displayed in Figure 3, one

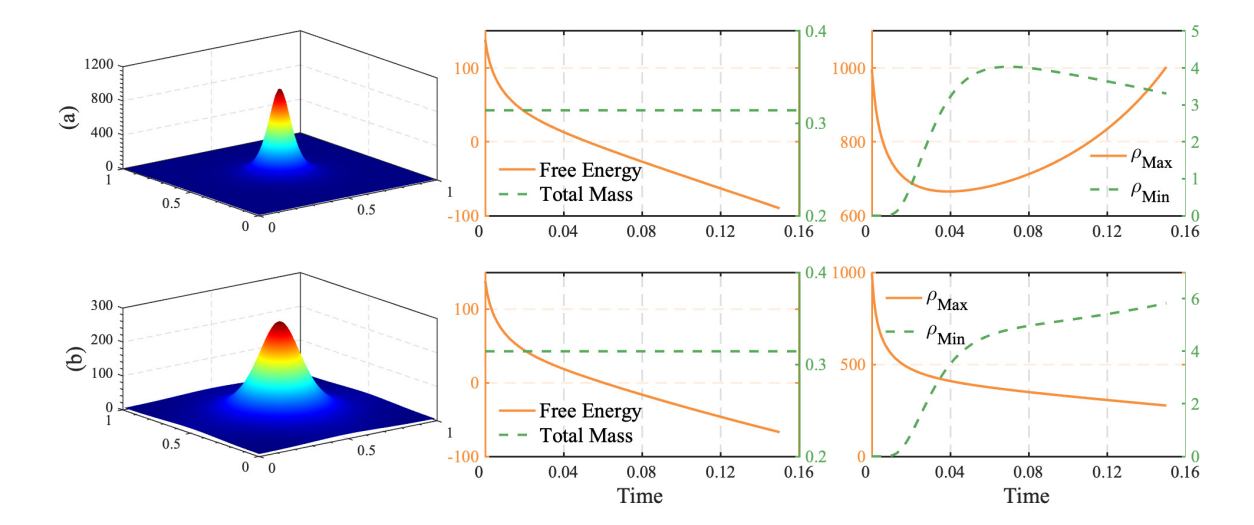


Figure 5: The first column shows the density distribution ρ at T=0.15, the second column gives the evolution of the free energy and total mass, and the third column presents the maximum and minimum concentration over the computational mesh. The first row (a) shows the bounded-mobility system and the second row (b) depicts the saturation-concentration system.

can observe that the modified mobility gives bounded solutions without exhibiting blowup. The second column depicts the evolution of discrete free energy (solid orange) and total mass (dashed green). As expected, the discrete free energy monotonically decreases and total mass remains constant as time evolves. The third column illustrates the evolution of the maximum density values ρ_{Max} (solid orange) and minimum density values ρ_{Min} (dashed green), demonstrating that the numerical solution remains positive over time.

6.2.3 Blowup at the corner

The proposed second-order accurate scheme (3.1-3.2) is applied to probe blowup formation away from the peak position of initial densities. We consider the same IBVPs as in Section 6.2.1, while the center of initial data is shifted to (0.75, 0.75):

$$\begin{cases} \rho^{0}(x,y) = 1000e^{-100((x-0.75)^{2}+(y-0.75)^{2})}, \\ \phi^{0}(x,y) = e^{-100((x-0.75)^{2}+(y-0.75)^{2})}. \end{cases}$$

Again, the solution of ρ may blow up in a finite time due to the fact that $\|\rho^0\|_1 \approx 31.4033 > 8\pi$ [31]. Figure 6 displays spatial density profiles of living organisms at four different time instants. It has been proved in [26] that the solution is expected to blow up at the boundary of the domain in this case. It is clearly observed that the behavior of the computed solution matches our expectation: the living organisms first move towards the boundary and then concentrate due to zero-flux boundary conditions, eventually forming solution blow up at the corner. Similar to the previous example, the free energy (4.1) depicted in Figure 7 gradually decreases over time and the total mass of ρ remains at a constant value perfectly. Regarding the energy functional F_h , a significant decline in magnitude occurs before blowup and continuing decrease can be seen during

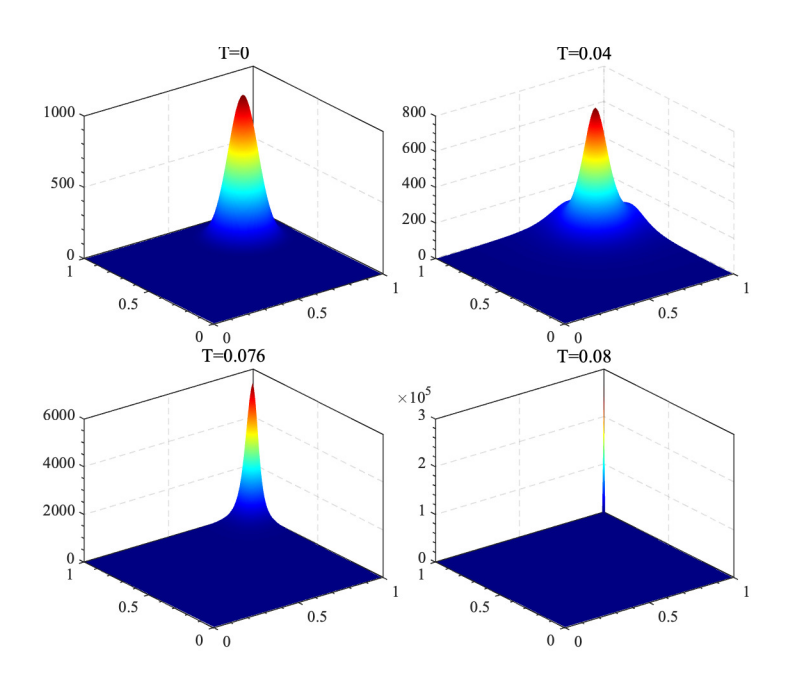


Figure 6: Time evolution of ρ at a sequence of time instants: $T=0,\,0.04,\,0.076,\,$ and 0.08, with $\Delta t=10^{-5}$ and h=1/100.

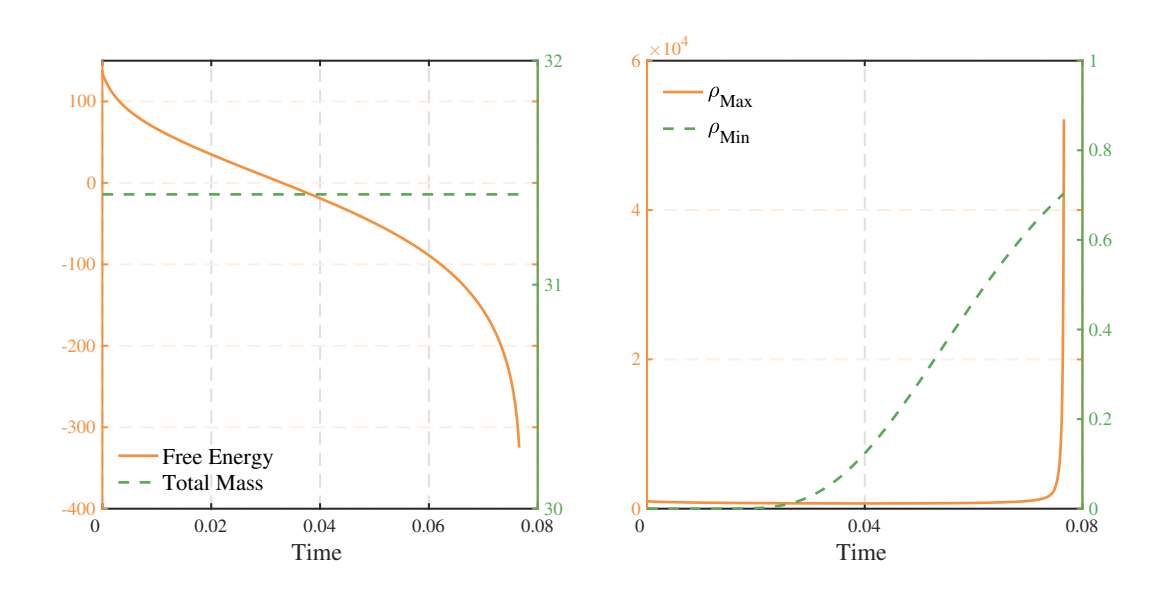


Figure 7: Time evolution of the discrete energy F_h , mass of ρ , and the minimum and maximum values of ρ for the case with blowup at the corner.

the singularity formation. Additionally, the density of living organism always remains positive, and the maximum value of density increases exponentially over time, indicating a solution blowup.

6.2.4 Blowup in 3D

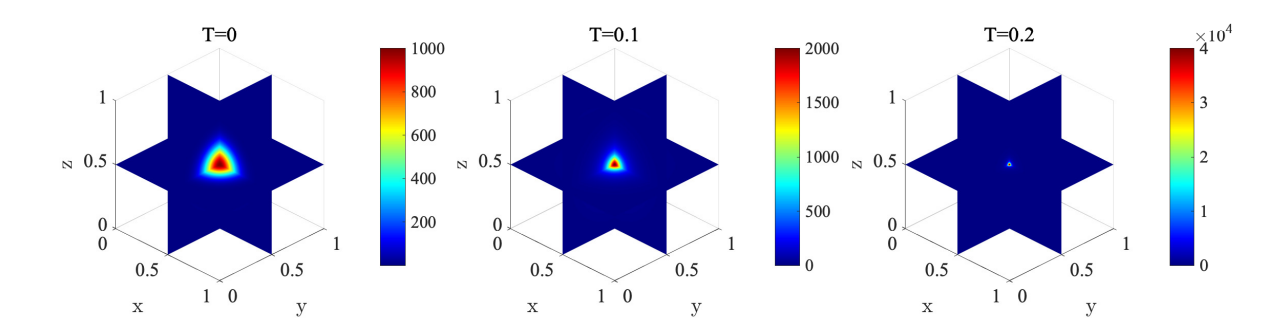


Figure 8: Cross-section snapshots of the density ρ at time instances $T=0,\,0.01,\,$ and 0.02, with $\Delta t=10^{-5}$ and $h=\frac{1}{100}$.

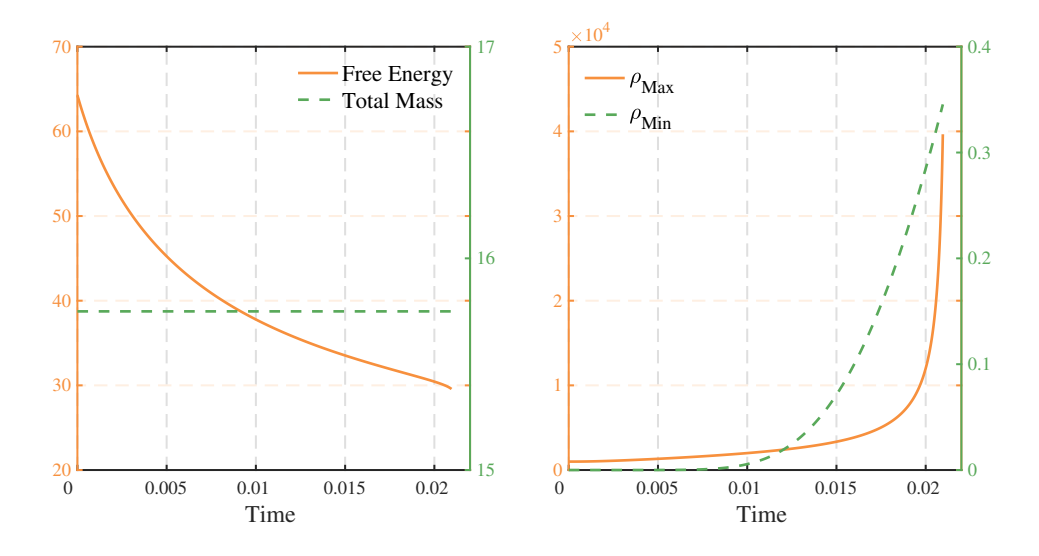


Figure 9: Time evolution of the discrete energy F_h , mass of ρ , and the minimum and maximum values of ρ in the case of 3D blowup.

To further illustrate the 3D solution behavior, we conduct a blowup test for the PKS system over a cubic domain $\Omega = (0,1)^3$. The initial data is given by

$$\begin{cases} \rho^0(x,y,z) = 1000 \mathrm{e}^{-50\left[(x-\frac{1}{2})^2 + (y-\frac{1}{2})^2 + (z-\frac{1}{2})^2\right]}, \\ \phi^0(x,y,z) = \mathrm{e}^{-50\left[(x-\frac{1}{2})^2 + (y-\frac{1}{2})^2 + (z-\frac{1}{2})^2\right]}. \end{cases}$$

Figure 8 shows cross-section snapshots of the density ρ at time instances $T=0,\,0.01,\,$ and 0.02, using a spatial resolution of $h=\frac{1}{100}$. The extracted cross-section slices at the planes $x=0.5,\,$

y = 0.5, and z = 0.5 demonstrate that the solution is spherically symmetric and concentrates more and more at the center, exhibiting a 3D blowup phenomenon.

Figure 9 presents the time evolution of the free energy, total mass of ρ , maximum value ρ_{Max} , and minimum value of ρ_{Min} over the computational mesh with $h = \frac{1}{100}$ and $\Delta t = 10^{-5}$. Similar to the 2D examples, the free energy (4.1) gradually decreases over time and the total mass of ρ remains at a perfect constant value. Furthermore, the density of living organism consistently stays positive, and the maximum value of density grows exponentially over time, indicating a solution blowup.

7 Conclusions

This work has proposed a novel second-order accurate numerical scheme for the PKS system with various mobilities for the description of chemotaxis. The variational structure of the PDE system has been used to facilitate the numerical design. The singular part in the chemical potential is discretized by a modified Crank-Nicolson approach, which leads to a nonlinear and singular numerical system. The unique solvability and positivity-preserving property have been theoretically established, in which the convexity of the nonlinear and singular term plays an important role. Moreover, a careful nonlinear analysis has proved a dissipation property of the original free energy functional, instead of a modified energy reported in many existing works for a multi-step numerical scheme. This makes the original energy stability analysis remarkable for the second-order discretization. In addition, this study has provided an optimal rate convergence analysis and error estimate for the proposed second order scheme, in which several highly non-standard techniques have been included. With a careful linearization expansion, the higher-order asymptotic expansion (up to fourth order accuracy in both time and space) has been performed. In turn, we are able to derive a rough error estimate, so that the ℓ^{∞} bound for the density variable, as well as its temporal derivative, becomes available. Subsequently, a refined error estimate has been performed and the desired convergence estimate for ρ is accomplished, in the $\ell^{\infty}(0,T;l^2) \cap \ell^2(0,T;H_h^1)$ norm. A few numerical results have confirmed the accuracy and robustness of the numerical scheme in preserving desired properties in simulations of chemotaxis. Given the numerical performance of the proposed scheme in terms of the structure preservation, it is of interest to see whether the scheme is able to numerically predict the blowup time. This deserves a further study in our future work.

A Proof of Lemma 5.4

By the fact that $S^{n+\frac{1}{2}}=\ln \rho^{n+1}+\frac{5\rho^n}{6\rho^{n+1}}-\frac{\rho^n}{6(\rho^{n+1})^2}-\frac{2}{3}$, we see that the term $\tilde{S}^{n+\frac{1}{2}}$ could be decomposed into two parts: $\tilde{S}^{n+\frac{1}{2}}=\tilde{S}_1^{n+\frac{1}{2}}+\tilde{S}_2^{n+\frac{1}{2}}$, where

$$\begin{split} \tilde{S}_{1}^{n+\frac{1}{2}} &= \check{S}^{n+\frac{1}{2}} - \left(\ln\check{\rho}^{n+1} + \frac{5\rho^{n}}{6\check{\rho}^{n+1}} - \frac{(\rho^{n})^{2}}{6(\check{\rho}^{n+1})^{2}} - \frac{2}{3}\right) = \left(\frac{5}{6\check{\rho}^{n+1}} - \frac{\check{\rho}^{n} + \rho^{n}}{6(\check{\rho}^{n+1})^{2}}\right) \tilde{\rho}^{n}, \\ \tilde{S}_{2}^{n+\frac{1}{2}} &= \ln\check{\rho}^{n+1} + \frac{5\rho^{n}}{6\check{\rho}^{n+1}} - \frac{(\rho^{n})^{2}}{6(\check{\rho}^{n+1})^{2}} - \frac{2}{3} - S^{n+\frac{1}{2}} = \left[\frac{1}{\xi^{n+1}} - \frac{5\rho^{n}}{6(\xi^{n+1})^{2}} + \frac{(\rho^{n})^{2}}{3(\xi^{n+1})^{3}}\right] \tilde{\rho}^{n+1}, \end{split} \tag{A.1}$$

and ξ^{n+1} is between $\check{\rho}^{n+1}$ and ρ^{n+1} , with an application of intermediate value theorem.

Recalling the phase separation property (5.7), regularity requirement (5.8), and a-priori $\|\cdot\|_{\infty}$ estimate (5.16) at the previous time step, we have

$$\left|\frac{5}{6\check{\rho}^{n+1}} - \frac{\check{\rho}^n + \rho^n}{6(\check{\rho}^{n+1})^2}\right| \leq \max\left(\frac{5}{6\check{\rho}^{n+1}}, \quad \frac{\check{\rho}^n + \rho^n}{6(\check{\rho}^{n+1})^2}\right) \leq \max\left(\frac{5}{6\varepsilon^*}, \quad \frac{C^* + \check{C}_0}{6(\varepsilon^*)^2}\right) := \hat{C}_2.$$

Therefore, the following inequality is available:

$$\langle \tilde{S}_{1}^{n+\frac{1}{2}}, \tilde{\rho}^{n+1} \rangle = h^{3} \sum_{i,j,k=1}^{N} \left(\frac{5}{6 \check{\rho}_{i,j,k}^{n+1}} - \frac{\check{\rho}_{i,j,k}^{n} + \rho_{i,j,k}^{n}}{6 (\check{\rho}_{i,j,k}^{n+1})^{2}} \right) \tilde{\rho}_{i,j,k}^{n} \cdot \tilde{\rho}_{i,j,k}^{n+1} \geq -\hat{C}_{2} h^{3} \sum_{i,j,k=1}^{N} |\tilde{\rho}_{i,j,k}^{n}| \cdot |\tilde{\rho}_{i,j,k}^{n+1}|. \tag{A.2}$$

In terms of $\tilde{S}_2^{n+\frac{1}{2}}$, we begin with the following observation:

$$\frac{1}{\xi^{n+1}} - \frac{5\rho^n}{6(\xi^{n+1})^2} + \frac{(\rho^n)^2}{3(\xi^{n+1})^3} = \frac{2(\rho^n - \frac{5}{4}\xi^{n+1})^2 + \frac{23}{8}(\xi^{n+1})^2}{6(\xi^{n+1})^3} \ge \frac{23}{48\xi^{n+1}}.$$
 (A.3)

This in turn implies that

$$\langle \tilde{S}_{2}^{n+\frac{1}{2}}, \tilde{\rho}^{n+1} \rangle \ge h^{3} \sum_{i,j,k=1}^{N} \frac{23}{48\xi_{i,j,k}^{n+1}} |\tilde{\rho}_{i,j,k}^{n+1}|^{2}.$$
 (A.4)

Its combination with (A.2) yields

$$\langle \tilde{S}^{n+\frac{1}{2}}, \tilde{\rho}^{n+1} \rangle \ge h^{3} \sum_{i,j,k=1}^{N} \left(\frac{23}{48\xi_{i,j,k}^{n+1}} |\tilde{\rho}_{i,j,k}^{n+1}|^{2} - \hat{C}_{2} |\tilde{\rho}_{i,j,k}^{n}| \cdot |\tilde{\rho}_{i,j,k}^{n+1}| \right), \quad \text{and}$$

$$\langle \gamma \tilde{S}^{n+\frac{1}{2}} + \tilde{\psi}^{n}, \tilde{\rho}^{n+1} \rangle \ge h^{3} \sum_{i,j,k=1}^{N} \left(\frac{23\gamma}{48\xi_{i,j,k}^{n+1}} |\tilde{\rho}_{i,j,k}^{n+1}|^{2} - (\hat{C}_{2}\gamma |\tilde{\rho}_{i,j,k}^{n}| + |\tilde{\psi}_{i,j,k}^{n}|) |\tilde{\rho}_{i,j,k}^{n+1}| \right).$$
(A.5)

At a fixed grid point (i, j, k) that is not in \mathbb{K} , i.e., $0 < \rho_{i,j,k}^{n+1} < 2C^* + 1$, the following estimate is available:

$$\frac{1}{\xi_{i,j,k}^{n+1}} \ge \min\left(\frac{1}{\check{\rho}_{i,j,k}^{n+1}}, \ \frac{1}{\rho_{i,j,k}^{n+1}}\right) \ge \frac{1}{2C^* + 1}.$$

Subsequently, the following inequality is valid for $0 < \rho_{i,j,k}^{n+1} < 2C^* + 1$:

$$\frac{23\gamma}{48\xi_{i,j,k}^{n+1}} |\tilde{\rho}_{i,j,k}^{n+1}|^2 - (\hat{C}_2\gamma|\tilde{\rho}_{i,j,k}^n| + |\tilde{\psi}_{i,j,k}^n|) |\tilde{\rho}_{i,j,k}^{n+1}|
\geq \frac{23\gamma}{48(2C^*+1)} |\tilde{\rho}_{i,j,k}^{n+1}|^2 - \left(\frac{23\gamma}{96(2C^*+1)} |\tilde{\rho}_{i,j,k}^{n+1}|^2 + \frac{48\gamma\hat{C}_2^2(2C^*+1)}{23} |\tilde{\rho}_{i,j,k}^n|^2 \right)
+ \frac{48(2C^*+1)}{23\gamma} |\tilde{\psi}_{i,j,k}^n|^2 \right)
= \frac{23\gamma}{96(2C^*+1)} |\tilde{\rho}_{i,j,k}^{n+1}|^2 - \frac{48\gamma\hat{C}_2^2(2C^*+1)}{23} |\tilde{\rho}_{i,j,k}^n|^2 - \frac{48(2C^*+1)}{23\gamma} |\tilde{\psi}_{i,j,k}^n|^2.$$
(A.6)

On the other hand, if (i, j, k) is in \mathbb{K} , i.e., $\rho_{i,j,k}^{n+1} \geq 2C^* + 1$, we have $\tilde{\rho}_{i,j,k}^{n+1} = \tilde{\rho}_{i,j,k}^{n+1} - \rho_{i,j,k}^{n+1} < 0$, so that the following inequalities are valid:

$$\begin{split} \tilde{\rho}_{i,j,k}^{n+1} &\leq C^* \leq \frac{C^*}{2C^*+1}(2C^*+1) \leq \frac{C^*\rho_{i,j,k}^{n+1}}{2C^*+1}, \\ |\tilde{\rho}_{i,j,k}^{n+1}| &= |\tilde{\rho}_{i,j,k}^{n+1} - \rho_{i,j,k}^{n+1}| \geq |\rho_{i,j,k}^{n+1}| - \frac{C^*\rho_{i,j,k}^{n+1}}{2C^*+1} \geq \frac{(C^*+1)}{2C^*+1}\rho_{i,j,k}^{n+1}, \\ \frac{|\tilde{\rho}_{i,j,k}^{n+1}|}{\xi_{i,j,k}^{n+1}} &\geq \frac{|\tilde{\rho}_{i,j,k}^{n+1}|}{\rho_{i,j,k}^{n+1}} \geq \frac{(C^*+1)}{2C^*+1}. \end{split}$$

Subsequently, the following inequality could be derived:

$$\frac{23\gamma}{48\xi_{i,j,k}^{n+1}} |\tilde{\rho}_{i,j,k}^{n+1}|^2 - (\hat{C}_2\gamma|\tilde{\rho}_{i,j,k}^n| + |\tilde{\psi}_{i,j,k}^n|) |\tilde{\rho}_{i,j,k}^{n+1}|
\geq \frac{23(C^*+1)\gamma}{48(2C^*+1)} |\tilde{\rho}_{i,j,k}^{n+1}| - (\gamma\hat{C}_2 \cdot C(\Delta t^{\frac{9}{4}} + h^{\frac{9}{4}}) + h) |\tilde{\rho}_{i,j,k}^{n+1}|
\geq \frac{\gamma}{6} |\tilde{\rho}_{i,j,k}^{n+1}| \geq \frac{\gamma}{6} (C^*+1) \geq \frac{C^*\gamma}{6},$$
(A.7)

where the $\|\cdot\|_{\infty}$ estimate (5.15) and the assumption that $\|\tilde{\psi}^n\|_{\infty} \leq h$ have been recalled in the second step, and the fact that $\frac{23(C^*+1)\gamma}{48(2C^*+1)} - (\gamma\hat{C}_2\cdot C(\Delta t^{\frac{9}{4}} + h^{\frac{9}{4}}) + h) \geq \frac{\gamma}{6}$ has been used in the last step.

As a result, a substitution of the point-wise inequalities (A.6) and (A.7) into (A.5) results in the desired estimate (5.21), by taking $\check{C}_2 = \frac{48\hat{C}_2^2(2C^*+1)}{23\gamma}$. Moreover, if $|\mathbb{K}| = 0$, the improved nonlinear estimate in (5.22) could be derived, based on (A.6), by taking $\check{C}_3 = \frac{23\gamma}{96(2C^*+1)}$. Therefore, the proof of Lemma 5.4 is completed.

B Proof of the bounds for $\|\mathcal{L}_1^{-1}\|_2$ and $\|\mathcal{L}_1^{-1}\mathcal{L}_2\|_2$

Recall the definitions

$$\mathcal{L}_1 = \frac{\theta}{\Delta t} + \frac{\alpha}{2} - \frac{\mu}{2} \Delta_h, \quad \mathcal{L}_2 = \frac{\theta}{\Delta t} - \frac{\alpha}{2} + \frac{\mu}{2} \Delta_h,$$

where $\alpha > 0$, $\mu > 0$, and Δ_h is a negative semi-definite discrete Laplacian operator with homogenous Neumann boundary conditions. For any $\eta \in \mathring{\mathfrak{C}}$, there exists $u \in \mathring{\mathfrak{C}}$ such that $\mathscr{L}_1 u = \eta$. Since $\frac{\alpha}{2} - \frac{\mu}{2} \Delta_h$ is positive definite, it follows that

$$\langle u, \mathcal{L}_1 u \rangle \ge \frac{\theta}{\Delta t} ||u||_2^2.$$

It follows from $\mathcal{L}_1^{-1}\eta = u$ that

$$\frac{\theta}{\Delta t} \|\mathcal{L}_1^{-1}\eta\|_2^2 \le \left\langle \mathcal{L}_1^{-1}\eta, \eta \right\rangle \le \|\mathcal{L}_1^{-1}\eta\|_2 \cdot \|\eta\|_2.$$

Therefore, $\|\mathcal{L}_1^{-1}\eta\|_2 \leq \frac{\Delta t}{\theta} \|\eta\|_2$, which implies that $\|\mathcal{L}_1^{-1}\|_2 \leq \frac{\Delta t}{\theta}$.

Denote by $u = \mathcal{L}_1^{-1}\mathcal{L}_2 \eta \in \mathring{\mathfrak{C}}$, where $\eta \in \mathring{\mathfrak{C}}$. By $\mathcal{L}_1 u = \mathcal{L}_2 \eta$, one has

$$-\frac{\theta}{\Delta t}(u-\eta) = \left(\frac{\alpha}{2} - \frac{\mu}{2}\Delta_h\right)(u+\eta).$$

It follows from the negative semi-definiteness of Δ_h that

$$-\frac{\theta}{\Delta t} \langle u + \eta, u - \eta \rangle = \left\langle u + \eta, \left(\frac{\alpha}{2} - \frac{\mu}{2} \Delta_h \right) (u + \eta) \right\rangle \ge \frac{\alpha}{2} \langle u + \eta, u + \eta \rangle.$$

Therefore, we see that

$$\left(\frac{\alpha}{2} + \frac{\theta}{\Delta t}\right)\langle u, u \rangle + \left(\frac{\alpha}{2} - \frac{\theta}{\Delta t}\right)\langle \eta, \eta \rangle \leq -\alpha \langle u, \eta \rangle \leq \frac{\alpha}{2} \langle u, u \rangle + \frac{\alpha}{2} \langle \eta, \eta \rangle,$$

which leads to $\langle u, u \rangle \leq \langle \eta, \eta \rangle$, i.e., $\|\mathcal{L}_1^{-1}\mathcal{L}_2\eta\|_2 \leq \|\eta\|_2$. This completes the proof of $\|\mathcal{L}_1^{-1}\mathcal{L}_2\|_2 \leq 1$.

C Proof of Proposition 5.6

By the numerical error expansion formula (5.12), the following decomposition is available for $\tilde{S}^{n+\frac{1}{2}}$, at a point-wise level:

$$\tilde{S}^{n+\frac{1}{2}} = J_1 + J_2 + J_3 + J_4 + J_5, \quad \text{with}
J_1 = \ln(\check{\rho}^{n+1}) - \ln(\rho^{n+1}), \quad J_2 = -\frac{1}{2\rho^{n+1}} (\check{\rho}^{n+1} - \check{\rho}^n), \quad J_3 = \frac{\check{\rho}^{n+1}}{2\check{\rho}^{n+1}\rho^{n+1}} (\check{\rho}^{n+1} - \check{\rho}^n), \quad (C.1)
J_4 = -\frac{\check{\rho}^{n+1} - \check{\rho}^n + \rho^{n+1} - \rho^n}{6(\rho^{n+1})^2} (\check{\rho}^{n+1} - \check{\rho}^n), \quad J_5 = \frac{(\check{\rho}^{n+1} + \rho^{n+1})\check{\rho}^{n+1}}{6(\check{\rho}^{n+1})^2 (\rho^{n+1})^2} (\check{\rho}^{n+1} - \check{\rho}^n)^2.$$

Meanwhile, at each cell, from $(i, j, k) \rightarrow (i + 1, j, k)$, the following expansion identity is always valid:

$$D_x(fg)_{i+1/2,j,k} = (A_x f)_{i+1/2,j,k} \cdot (D_x g)_{i+1/2,j,k} + (A_x g)_{i+1/2,j,k} \cdot (D_x f)_{i+1/2,j,k}.$$
(C.2)

We first look at the D_xJ_3 term. Because of the point-wise bounds, $\varepsilon^* \leq \check{\rho}^{n+1} \leq C^*$, $\frac{\varepsilon^*}{2} \leq \rho^{n+1} \leq \check{C}_0$, and $\|\nabla_h\rho^{n+1}\|_{\infty} \leq \check{C}_0$ as given by (5.7), (5.40), and (5.41), respectively, the following estimates could be derived:

$$0 < A_x(\frac{1}{\check{\rho}^{n+1}}) \le (\varepsilon^*)^{-1}, \ 0 < A_x(\frac{1}{\rho^{n+1}}) \le 2(\varepsilon^*)^{-1}, \ 0 < A_x(\frac{1}{\check{\rho}^{n+1}\rho^{n+1}}) \le 2(\varepsilon^*)^{-2}, \tag{C.3}$$

$$|D_x(\frac{1}{\check{\rho}^{n+1}})| \le (\varepsilon^*)^{-2} |D_x\check{\rho}^{n+1}| \le C^*(\varepsilon^*)^{-2}, \ |D_x(\frac{1}{\rho^{n+1}})| \le 4(\varepsilon^*)^{-2} |D_x\rho^{n+1}| \le 4\tilde{C}_0(\varepsilon^*)^{-2}, \ (C.4)$$

$$|D_{x}(\frac{1}{\check{\rho}^{n+1}\rho^{n+1}})| \leq A_{x}(\frac{1}{\check{\rho}^{n+1}}) \cdot |D_{x}(\frac{1}{\rho^{n+1}})| + A_{x}(\frac{1}{\rho^{n+1}}) \cdot |D_{x}(\frac{1}{\check{\rho}^{n+1}})|$$

$$\leq (\varepsilon^{*})^{-3}(2C^{*} + 4\tilde{C}_{0}),$$
(C.5)

in which inequalities (5.8) and (5.41) have also been applied. Subsequently, a further application of (C.2) leads to

$$\left| A_{x} \left(\frac{\tilde{\rho}^{n+1}}{2\tilde{\rho}^{n+1}\rho^{n+1}} \right) \right| \leq \frac{1}{2} \cdot 2(\varepsilon^{*})^{-2} A_{x} |\tilde{\rho}^{n+1}| = (\varepsilon^{*})^{-2} A_{x} |\tilde{\rho}^{n+1}|,
\left| D_{x} \left(\frac{\tilde{\rho}^{n+1}}{2\tilde{\rho}^{n+1}\rho^{n+1}} \right) \right| \leq \frac{1}{2} A_{x} \left(\frac{1}{\tilde{\rho}^{n+1}\rho^{n+1}} \right) \cdot |D_{x}\tilde{\rho}^{n+1}| + \frac{1}{2} |D_{x} \left(\frac{1}{\tilde{\rho}^{n+1}\rho^{n+1}} \right)| \cdot |A_{x}\tilde{\rho}^{n+1}|
\leq (\varepsilon^{*})^{-2} |D_{x}\tilde{\rho}^{n+1}| + (\varepsilon^{*})^{-3} (C^{*} + 2\tilde{C}_{0}) A_{x} |\tilde{\rho}^{n+1}|.$$
(C.6)

Meanwhile, the regularity assumption (5.8) (for the constructed profile $\check{\rho}$) implies that

$$|\check{\rho}^{n+1} - \check{\rho}^n| \le C^* \Delta t$$
, $|D_x(\check{\rho}^{n+1} - \check{\rho}^n)| \le C^* \Delta t$, at a point-wise level. (C.7)

Consequently, a combination of (C.6) and (C.7) reveals that

$$|D_{x}J_{3}| \leq \left| A_{x} \left(\frac{\tilde{\rho}^{n+1}}{2\tilde{\rho}^{n+1}\rho^{n+1}} \right) \right| \cdot |D_{x}(\check{\rho}^{n+1} - \check{\rho}^{n})| + \left| D_{x} \left(\frac{\tilde{\rho}^{n+1}}{2\check{\rho}^{n+1}\rho^{n+1}} \right) \right| \cdot A_{x}|\check{\rho}^{n+1} - \check{\rho}^{n}|$$

$$\leq (\varepsilon^{*})^{-2}C^{*}\Delta t \left(|D_{x}\tilde{\rho}^{n+1}| + ((\varepsilon^{*})^{-1}(C^{*} + 2\tilde{C}_{0}) + 1)A_{x}|\tilde{\rho}^{n+1}| \right).$$
(C.8)

Notice that we have dropped the $|\cdot|_{i+1/2,j,k}$ subscript notation on the right hand side terms, for simplicity of presentation, since all these inequalities are derived at a point-wise level.

Similar bounds could be derived for $|D_xJ_4|$ and $|D_xJ_5|$ terms:

$$\begin{split} 0 &< A_x (\frac{1}{(\rho^{n+1})^2}) \leq 4(\varepsilon^*)^{-2}, \quad |D_x (\frac{1}{(\rho^{n+1})^2})| \leq 16(\varepsilon^*)^{-3} |D_x \rho^{n+1}| \leq 16 \bar{C}_0 (\varepsilon^*)^{-3}, \\ |\bar{\rho}^{n+1} - \bar{\rho}^n|, |D_x (\bar{\rho}^{n+1} - \bar{\rho}^n)| \leq C^* \Delta t, \quad |\rho^{n+1} - \rho^n| \leq \bar{C}_0 \Delta t, \\ |A_x (\bar{\rho}^{n+1} - \bar{\rho}^n + \rho^{n+1} - \rho^n)| \leq (C^* + \bar{C}_0) \Delta t, \quad |D_x (\bar{\rho}^{n+1} - \bar{\rho}^n + \rho^{n+1} - \rho^n)| \leq C^* \Delta t + 2\bar{C}_0, \\ |A_x (\frac{\bar{\rho}^{n+1} - \bar{\rho}^n + \rho^{n+1} - \rho^n)| \leq (C^* + \bar{C}_0) \Delta t, \quad |D_x (\bar{\rho}^{n+1} - \bar{\rho}^n + \rho^{n+1} - \rho^n)| \leq C^* \Delta t + 2\bar{C}_0, \\ |A_x (\frac{\bar{\rho}^{n+1} - \bar{\rho}^n + \rho^{n+1} - \rho^n}{(\rho^{n+1})^2})| \leq (C^* + \bar{C}_0) \Delta t \cdot 4(\varepsilon^*)^{-2} = 4(\varepsilon^*)^{-2} (C^* + \bar{C}_0) \Delta t, \\ |D_x (\frac{\bar{\rho}^{n+1} - \bar{\rho}^n + \rho^{n+1} - \rho^n}{(\rho^{n+1})^2})| \leq (C^* + \bar{C}_0) \Delta t \cdot 16\bar{C}_0 (\varepsilon^*)^{-3} + (C^* \Delta t + 2\bar{C}_0) \cdot 4(\varepsilon^*)^{-2} \\ \leq 4(\varepsilon^*)^{-2} \Delta t \Big(C^* + 4\tilde{C}_0 (\varepsilon^*)^{-1} (\tilde{C}_0 + C^*)\Big) + 8(\varepsilon^*)^{-2} \tilde{C}_0 \leq 8(\varepsilon^*)^{-2} \tilde{C}_0 + 1, \\ |D_x J_4| \leq \frac{1}{6} |A_x (\frac{\bar{\rho}^{n+1} - \bar{\rho}^n + \rho^{n+1} - \rho^n}{(\rho^{n+1})^2})| \cdot |D_x (\bar{\rho}^{n+1} - \bar{\rho}^n)| \\ + \frac{1}{6} |D_x (\frac{\bar{\rho}^{n+1} - \bar{\rho}^n + \rho^{n+1} - \rho^n}{(\rho^{n+1})^2})| \cdot |A_x |\bar{\rho}^{n+1} - \bar{\rho}^n| \\ \leq \frac{2}{3} (\varepsilon^*)^{-2} (C^* + \tilde{C}_0) \Delta t (|D_x \bar{\rho}^{n+1}| + |D_x \bar{\rho}^n|) + \frac{1}{6} (8(\varepsilon^*)^{-2} \tilde{C}_0 + 1) (A_x |\bar{\rho}^{n+1}| + A_x |\bar{\rho}^n|) \\ 0 \leq (\bar{\rho}^{n+1} - \bar{\rho}^n)^2 \leq (C^*)^2 \Delta t^2, \\ 0 < A_x (\frac{1}{(\bar{\rho}^{n+1})^2 (\rho^{n+1})^2}) \leq (\varepsilon^*)^{-2} \cdot 4(\varepsilon^*)^{-2} = 4(\varepsilon^*)^{-4}, \\ |D_x (\bar{\rho}^{n+1} - \bar{\rho}^{n+2})^2 (D_x |\bar{\rho}^{n+1}| + 2|D_x \bar{\rho}^{n+1}| + 2|D_x \bar{\rho}^{n+1}|) \leq 8(C^* + 2\tilde{C}_0)(\varepsilon^*)^{-5}, \\ |A_x (\bar{\rho}^{n+1} + \rho^{n+1})| \leq C^* + \tilde{C}_0, \quad |D_x (\bar{\rho}^{n+1} + \rho^{n+1})| \leq |D_x \bar{\rho}^{n+1}| + |D_x \bar{\rho}^{n+1$$

$$|A_{x}(\frac{(\check{\rho}^{n+1} + \rho^{n+1})(\check{\rho}^{n+1} - \check{\rho}^{n})^{2}}{(\check{\rho}^{n+1})^{2}(\rho^{n+1})^{2}})| \leq 4(\varepsilon^{*})^{-4}(C^{*} + \check{C}_{0})(C^{*})^{2}\Delta t^{2},$$

$$|D_{x}(\frac{(\check{\rho}^{n+1} + \rho^{n+1})(\check{\rho}^{n+1} - \check{\rho}^{n})^{2}}{(\check{\rho}^{n+1})^{2}(\rho^{n+1})^{2}})|$$

$$\leq 8(\varepsilon^{*})^{-5}(C^{*} + \check{C}_{0})(C^{*} + 2\tilde{C}_{0} + 1) \cdot (C^{*})^{2}\Delta t^{2} + 4(\varepsilon^{*})^{-4}(C^{*} + \check{C}_{0}) \cdot 2(C^{*})^{2}\Delta t^{2}$$

$$\leq 8(\varepsilon^{*})^{-5}(C^{*})^{2}\Delta t^{2}(C^{*} + \check{C}_{0})(C^{*} + 2\tilde{C}_{0} + 2),$$

$$|D_{x}J_{5}| \leq \frac{1}{6}|A_{x}(\frac{(\check{\rho}^{n+1} + \rho^{n+1})(\check{\rho}^{n+1} - \check{\rho}^{n})^{2}}{(\check{\rho}^{n+1})^{2}(\rho^{n+1})^{2}})| \cdot |D_{x}\tilde{\rho}^{n+1}|$$

$$+ \frac{1}{6}|D_{x}(\frac{(\check{\rho}^{n+1} + \rho^{n+1})(\check{\rho}^{n+1} - \check{\rho}^{n})^{2}}{(\rho^{n+1})^{2}(\rho^{n+1})^{2}})| \cdot A_{x}|\tilde{\rho}^{n+1}|$$

$$\leq \frac{2}{3}(\varepsilon^{*})^{-4}(C^{*})^{2}\Delta t^{2}(C^{*} + \check{C}_{0})\left(2(\varepsilon^{*})^{-1}(C^{*} + 2\tilde{C}_{0} + 2) \cdot A_{x}|\tilde{\rho}^{n+1}| + |D_{x}\tilde{\rho}^{n+1}|\right)$$

$$\leq \Delta t(|D_{x}\tilde{\rho}^{n+1}| + A_{x}|\tilde{\rho}^{n+1}|).$$
(C.10)

Notice that the phase separation property (5.7), regularity assumption (5.8) for the constructed profile, a-priori estimate (5.16)-(5.19), and the rough $\|\cdot\|_{\infty}$ estimates (5.40)-(5.44) for the numerical solution, have been repeatedly applied in the above derivation.

In fact, the finite difference operations for the J_3 , J_4 and J_5 terms could be viewed as higherorder perturbations in the nonlinear expansion of $D_x \tilde{S}^{n+\frac{1}{2}}$, and the two leading terms, namely $D_x J_1$ and $D_x J_2$, turn out to play a dominant role in the nonlinear error estimate. Now we focus on the $D_x J_1$ term. Within a single mesh cell $(i, j, k) \to (i + 1, j, k)$, the following expansion is straightforward, based on the mean value theorem:

$$D_{x}(\ln \check{\rho}^{n+1} - \ln \rho^{n+1})_{i+1/2,j,k} = \frac{1}{h}(\ln \check{\rho}_{i+1,j,k}^{n+1} - \ln \check{\rho}_{i,j,k}^{n+1}) - \frac{1}{h}(\ln \rho_{i+1,j,k}^{n+1} - \ln \rho_{i,j,k}^{n+1})$$

$$= \frac{1}{\xi_{\check{\rho}}} D_{x} \check{\rho}_{i+1/2,j,k}^{n+1} - \frac{1}{\xi_{\rho}} D_{x} \rho_{i+1/2,j,k}^{n+1}$$

$$= \left(\frac{1}{\xi_{\check{\rho}}} - \frac{1}{\xi_{\rho}}\right) D_{x} \check{\rho}_{i+1/2,j,k}^{n+1} + \frac{1}{\xi_{\rho}} D_{x} \check{\rho}_{i+1/2,j,k}^{n+1}, \tag{C.11}$$

where

$$\frac{1}{\xi_{\check{\rho}}} = \frac{\ln \check{\rho}_{i+1,j,k}^{n+1} - \ln \check{\rho}_{i,j,k}^{n+1}}{\check{\rho}_{i+1,j,k}^{n+1} - \check{\rho}_{i,j,k}^{n+1}}, \qquad \frac{1}{\xi_{\rho}} = \frac{\ln \rho_{i+1,j,k}^{n+1} - \ln \rho_{i,j,k}^{n+1}}{\rho_{i+1,j,k}^{n+1} - \rho_{i,j,k}^{n+1}}.$$
(C.12)

Meanwhile, for any a > 0 and b > 0, a careful Taylor expansion of $\ln x$ around a middle point $x_0 = \frac{a+b}{2}$ reveals that

$$\frac{\ln b - \ln a}{b - a} = \frac{1}{x_0} + \frac{(b - a)^2}{12x_0^3} + \frac{(b - a)^4}{160} \left(\frac{1}{\eta_1^5} + \frac{1}{\eta_2^5}\right),\tag{C.13}$$

in which η_1 is between a and x_0 , η_2 is between x_0 and b. It is observed that, only the even order terms appear in (C.13), due to the symmetric expansion around $x_0 = \frac{a+b}{2}$. This fact will greatly simplify the nonlinear analysis. In turn, a more precise representation for $\frac{1}{\xi_{\rho}}$ and $\frac{1}{\xi_{\rho}}$, as given

in (C.12), becomes available:

$$\frac{1}{\xi_{\check{\rho}}} = \frac{1}{A_x \check{\rho}_{i+1/2,j,k}^{n+1}} + \frac{h^2 (D_x \check{\rho}_{i+1/2,j,k}^{n+1})^2}{12 (A_x \check{\rho}_{i+1/2,j,k}^{n+1})^3} + \frac{h^4 (D_x \check{\rho}_{i+1/2,j,k}^{n+1})^4}{160} \left(\frac{1}{\eta_{\check{\rho},1}^5} + \frac{1}{\eta_{\check{\rho},2}^5}\right),
\frac{1}{\xi_{\check{\rho}}} = \frac{1}{A_x \rho_{i+1/2,j,k}^{n+1}} + \frac{h^2 (D_x \rho_{i+1/2,j,k}^{n+1})^2}{12 (A_x \rho_{i+1/2,j,k}^{n+1})^3} + \frac{h^4 (D_x \rho_{i+1/2,j,k}^{n+1})^4}{160} \left(\frac{1}{\eta_{\check{\rho},1}^5} + \frac{1}{\eta_{\check{\rho},2}^5}\right),
\eta_{\check{\rho},1} \text{ is between } \check{\rho}_{i,j,k}^{n+1} \text{ and } A_x \check{\rho}_{i+1/2,j,k}^{n+1}, \eta_{\check{\rho},2} \text{ is between } A_x \check{\rho}_{i+1/2,j,k}^{n+1} \text{ and } \check{\rho}_{i+1,j,k}^{n+1},
\eta_{\rho,1} \text{ is between } \rho_{i,j,k}^{n+1} \text{ and } A_x \rho_{i+1/2,j,k}^{n+1}, \eta_{\rho,2} \text{ is between } A_x \rho_{i+1/2,j,k}^{n+1} \text{ and } \rho_{i+1,j,k}^{n+1}.$$
(C.14)

Then we obtain a detailed expansion of $\frac{1}{\xi_{\tilde{\rho}}} - \frac{1}{\xi_{\rho}}$, which is needed in the analysis for (C.12):

$$\frac{1}{\xi_{\tilde{\rho}}} - \frac{1}{\xi_{\rho}} = \frac{-(A_{x}\tilde{\rho})_{i+1/2,j,k}^{n+1}}{A_{x}\check{\rho}_{i+1/2,j,k}^{n+1} \cdot A_{x}\rho_{i+1/2,j,k}^{n+1}} + \frac{h^{2}(D_{x}\rho_{i+1/2,j,k}^{n+1} + D_{x}\check{\rho}_{i+1/2,j,k}^{n+1})D_{x}\tilde{\rho}_{i+1/2,j,k}^{n+1}}{12(A_{x}\rho_{i+1/2,j,k}^{n+1})^{3}} - \frac{h^{2}(D_{x}\check{\rho}_{i+1/2,j,k}^{n+1})^{2}(A_{x}\tilde{\rho}_{i+1/2,j,k}^{n+1})}{12(A_{x}\check{\rho}_{i+1/2,j,k}^{n+1})^{3}(A_{x}\rho_{i+1/2,j,k}^{n+1})^{3}} - \frac{(C.15)}{(A_{x}\check{\rho}_{i+1/2,j,k}^{n+1})^{2} + A_{x}\check{\rho}_{i+1/2,j,k}^{n+1} \cdot A_{x}\rho_{i+1/2,j,k}^{n+1} + (A_{x}\rho_{i+1/2,j,k}^{n+1})^{2})}{160} + \frac{h^{4}(D_{x}\check{\rho}_{i+1/2,j,k}^{n+1})^{4}}{160} \left(\frac{1}{\eta_{\tilde{\rho},1}^{5}} + \frac{1}{\eta_{\tilde{\rho},2}^{5}}\right) - \frac{h^{4}(D_{x}\rho_{i+1/2,j,k}^{n+1})^{4}}{160} \left(\frac{1}{\eta_{\tilde{\rho},1}^{5}} + \frac{1}{\eta_{\tilde{\rho},2}^{5}}\right).$$

On the other hand, because of the following bounds at (i + 1/2, j, k) and time step t_{n+1} :

$$\varepsilon^* \leq A_x \check{\rho} \leq C^*, \quad |D_x \check{\rho}| \leq C^*, \quad \frac{\varepsilon^*}{2} \leq A_x \rho \leq \check{C}_0, \quad |D_x \rho| \leq \tilde{C}_0,
\varepsilon^* \leq \eta_{\check{\rho},1}, \, \eta_{\check{\rho},2} \leq C^*, \quad \frac{\varepsilon^*}{2} \leq \eta_{\rho,1}, \, \eta_{\rho,2} \leq \check{C}_0, \tag{C.16}$$

the following estimates could be derived:

$$\left| \frac{A_x \tilde{\rho}}{A_x \tilde{\rho} \cdot A_x \rho} \right| \leq 2(\varepsilon^*)^{-2} |A_x \tilde{\rho}|,
\left| \frac{h^2 (D_x \rho + D_x \tilde{\rho}) D_x \tilde{\rho}}{12 (A_x \rho)^3} \right| \leq \frac{h^2}{12} \cdot 8(\varepsilon^*)^{-3} \cdot (C^* + \tilde{C}_0) |D_x \tilde{\rho}| = \frac{2h^2}{3} (\varepsilon^*)^{-3} (C^* + \tilde{C}_0) |D_x \tilde{\rho}|,
\left| \frac{h^2 (D_x \tilde{\rho})^2 (A_x \tilde{\rho})}{12 (A_x \tilde{\rho})^3 (A_x \rho)^3} \cdot \left((A_x \tilde{\rho})^2 + A_x \tilde{\rho} \cdot A_x \rho + (A_x \rho)^2 \right) \right|
\leq \frac{h^2}{12} \cdot 8(\varepsilon^*)^{-6} \cdot (C^* + \tilde{C}_0)^2 \cdot (C^*)^2 |A_x \tilde{\rho}| = \frac{2}{3} (\varepsilon^*)^{-6} (C^* + \tilde{C}_0)^2 (C^*)^2 h^2 |A_x \tilde{\rho}|,
\left| \frac{h^4 (D_x \tilde{\rho})^4}{160} \left(\frac{1}{\eta_{\rho,1}^5} + \frac{1}{\eta_{\rho,2}^5} \right) \right| \leq \frac{h^4}{160} \cdot (C^*)^4 \cdot 2(\varepsilon^*)^{-5} = \frac{(C^*)^4 (\varepsilon^*)^{-5}}{80} h^4,
\left| \frac{h^4 (D_x \rho)^4}{160} \left(\frac{1}{\eta_{\rho,1}^5} + \frac{1}{\eta_{\rho,2}^5} \right) \right| \leq \frac{h^4}{160} \cdot (\tilde{C}_0)^4 \cdot 64(\varepsilon^*)^{-5} = \frac{2(\tilde{C}_0)^4 (\varepsilon^*)^{-5}}{5} h^4.$$
(C.17)

Again, we have dropped the $|\cdot|_{i+1/2,j,k}^{n+1}$ script notation in the analysis, for simplicity of presentation, and all these inequalities are derived at a point-wise level. Subsequently, a substitution of (C.17) into (C.15) yields

$$\left| \frac{1}{\xi_{\tilde{\rho}}} - \frac{1}{\xi_{\rho}} \right| \le (2(\varepsilon^*)^{-2} + 1)|A_x \tilde{\rho}_{i+1/2,j,k}^{n+1}| + h|D_x \tilde{\rho}_{i+1/2,j,k}^{n+1}| + \frac{2(\tilde{C}_0 + C^*)^4(\varepsilon^*)^{-5}}{5} h^4, \tag{C.18}$$

provided that h is sufficiently small.

In terms of the second expansion term on the right hand side of (C.11), we observe an $O(h^2)$ Taylor expansion to obtain $\frac{1}{\xi_0}$, in a similar formula as in (C.14):

$$\frac{1}{\xi_{\rho}} = \frac{1}{A_x \rho_{i+1/2,j,k}^{n+1}} + \frac{h^2 (D_x \rho_{i+1/2,j,k}^{n+1})^2}{24} \left(\frac{1}{\eta_{\rho,3}^3} + \frac{1}{\eta_{\rho,4}^3}\right),\tag{C.19}$$

 $\eta_{\rho,3} \text{ is between } \rho_{i,j,k}^{n+1} \text{ and } A_x \rho_{i+1/2,j,k}^{n+1}, \ \eta_{\rho,4} \text{ is between } A_x \rho_{i+1/2,j,k}^{n+1} \text{ and } \rho_{i+1,j,k}^{n+1}.$

Again, the remaining expansion terms could be bounded as follows

$$\frac{\varepsilon^*}{2} \le A_x \rho \le \check{C}_0, \quad |D_x \rho| \le \tilde{C}_0, \quad \frac{\varepsilon^*}{2} \le \eta_{\rho,3}, \quad \eta_{\rho,4} \le \check{C}_0, \quad \text{so that}
\left| \frac{h^2 (D_x \rho)^2}{24} \left(\frac{1}{\eta_{\rho,3}^3} + \frac{1}{\eta_{\rho,4}^3} \right) \right| \le \frac{h^2}{24} \cdot (\tilde{C}_0)^2 \cdot 16(\varepsilon^*)^{-3} = \frac{2(\tilde{C}_0)^2 (\varepsilon^*)^{-3}}{3} h^2 \le h,$$
(C.20)

provided that h is sufficiently small.

As a result, a substitution of (C.18)-(C.20) into (C.11) reveals the following fact, at a pointwise level:

$$(D_{x}J_{1})_{i+1/2,j,k} = \frac{D_{x}\tilde{\rho}_{i+1/2,j,k}^{n+1}}{A_{x}\rho_{i+1/2,j,k}^{n+1}} + \zeta_{1}^{n+\frac{1}{2}}, \quad \text{with}$$

$$|\zeta_{1}^{n+\frac{1}{2}}| \leq (2(\varepsilon^{*})^{-2} + 1)C^{*}|A_{x}\tilde{\rho}_{i+1/2,j,k}^{n+1}| + (C^{*} + 1)h|D_{x}\tilde{\rho}_{i+1/2,j,k}^{n+1}|$$

$$+ \frac{2C^{*}(\tilde{C}_{0} + C^{*})^{4}(\varepsilon^{*})^{-5}}{5}h^{4}.$$
(C.21)

Notice that the $W_h^{1,\infty}$ bound for $\check{\rho}$, $\|D_x\check{\rho}^{n+1}\|_{\infty} \leq C^*$, has been applied.

The analysis for the D_xJ_2 part is more straightforward. An application of identity (C.2) gives

$$D_x J_2 = -\frac{1}{2} A_x \left(\frac{1}{\rho^{n+1}}\right) \cdot D_x (\tilde{\rho}^{n+1} - \tilde{\rho}^n) - \frac{1}{2} D_x \left(\frac{1}{\rho^{n+1}}\right) \cdot A_x (\tilde{\rho}^{n+1} - \tilde{\rho}^n). \tag{C.22}$$

The second term could be bounded as follows

$$|D_{x}(\frac{1}{\rho^{n+1}})| \leq 4\tilde{C}_{0}(\varepsilon^{*})^{-2}, \quad \text{so that}$$

$$\left|D_{x}(\frac{1}{\rho^{n+1}}) \cdot A_{x}(\tilde{\rho}^{n+1} - \tilde{\rho}^{n})\right| \leq 4\tilde{C}_{0}(\varepsilon^{*})^{-2}(|A_{x}\tilde{\rho}^{n+1}| + |A_{x}\tilde{\rho}^{n}|). \tag{C.23}$$

In terms of the first part on the right hand side of (C.22), we need to estimate the difference between $A_x(\frac{1}{\rho^{n+1}})$ and $\frac{1}{A_x\rho^{n+1}}$. Similarly, for any $a>0,\ b>0$, a careful Taylor expansion of $\frac{1}{x}$

around a middle point $x_0 = \frac{a+b}{2}$ reveals that

$$\frac{1}{2} \left(\frac{1}{a} + \frac{1}{b} \right) = \frac{1}{x_0} + \frac{(b-a)^2}{8} \left(\frac{1}{\eta_1^3} + \frac{1}{\eta_2^3} \right), \tag{C.24}$$

in which η_1 is between a and x_0 , η_2 is between x_0 and b. In turn, by setting $a = \rho_{i,j,k}^{n+1}$, $b = \rho_{i+1,j,k}^{n+1}$, we see that

$$A_x(\frac{1}{\rho^{n+1}})_{i+1/2,j,k} - \frac{1}{A_x \rho_{i+1/2,j,k}^{n+1}} = \frac{h^2 (D_x \rho_{i+1/2,j,k}^{n+1})^2}{8} \left(\frac{1}{\eta_{\rho,5}^3} + \frac{1}{\eta_{\rho,6}^3}\right),\tag{C.25}$$

 $\eta_{
ho,5}$ is between $ho_{i,j,k}^{n+1}$ and $A_x
ho_{i+1/2,j,k}^{n+1}, \, \eta_{
ho,6}$ is between $A_x
ho_{i+1/2,j,k}^{n+1}$ and $ho_{i+1,j,k}^{n+1}$.

A bound for the remainder term is available:

$$|D_{x}\rho^{n+1}| \leq \tilde{C}_{0}, \quad \frac{\varepsilon^{*}}{2} \leq \eta_{\rho,5}, \, \eta_{\rho,6} \leq \tilde{C}_{0}, \quad \text{so that}$$

$$\left|\frac{h^{2}(D_{x}\rho_{i+1/2,j,k}^{n+1})^{2}}{8} \left(\frac{1}{\eta_{0.5}^{3}} + \frac{1}{\eta_{0.6}^{3}}\right)\right| \leq \frac{h^{2}}{8} \cdot (\tilde{C}_{0})^{2} \cdot 16(\varepsilon^{*})^{-3} \leq h, \tag{C.26}$$

provided that h is sufficiently small. Therefore, a substitution of (C.23), (C.25), and (C.26) into (C.22) leads to

$$(D_x J_2)_{i+1/2,j,k} = -\frac{D_x(\tilde{\rho}^{n+1} - \tilde{\rho}^n)_{i+1/2,j,k}}{2A_x \rho_{i+1/2,j,k}^{n+1}} + \zeta_2^{n+\frac{1}{2}}, \quad \text{with}$$

$$|\zeta_2^{n+\frac{1}{2}}| \le 2\tilde{C}_0(\varepsilon^*)^{-2} (|A_x \tilde{\rho}_{i+1/2,j,k}^{n+1}| + |A_x \tilde{\rho}_{i+1/2,j,k}^n|) + \frac{h}{2} (|D_x \tilde{\rho}_{i+1/2,j,k}^{n+1}| + |D_x \tilde{\rho}_{i+1/2,j,k}^n|). \tag{C.27}$$

Finally, a combination of (C.8), (C.9), (C.10), (C.21), and (C.27) results in

$$(D_{x}\tilde{S}^{n+\frac{1}{2}})_{i+1/2,j,k} = \frac{D_{x}(\tilde{\rho}^{n+1} + \tilde{\rho}^{n})_{i+1/2,j,k}}{2A_{x}\rho_{i+1/2,j,k}^{n+1}} + \zeta^{n+\frac{1}{2}},$$

$$|\zeta^{n+\frac{1}{2}}| \leq \check{C}_{1}(A_{x}|\tilde{\rho}_{i+1/2,j,k}^{n+1}| + A_{x}|\tilde{\rho}_{i+1/2,j,k}^{n}|) + (\check{C}_{2}h + \check{C}_{3}\Delta t)(|D_{x}\tilde{\rho}_{i+1/2,j,k}^{n+1}| + |D_{x}\tilde{\rho}_{i+1/2,j,k}^{n}|)$$

$$+ \frac{2C^{*}(\tilde{C}_{0} + C^{*})^{4}(\varepsilon^{*})^{-5}}{5}h^{4},$$

$$(C.28)$$

provided that Δt and h are sufficiently small, with

$$\check{C}_1 = \frac{1}{6} (8(\varepsilon^*)^{-2} \tilde{C}_0 + 1) + (2(\varepsilon^*)^{-2} + 1)C^* + 2\tilde{C}_0(\varepsilon^*)^{-2} + 1,
\check{C}_2 = C^* + \frac{3}{2}, \quad \check{C}_3 = \frac{5}{3} (\varepsilon^*)^{-2} (C^* + \tilde{C}_0) + 1.$$
(C.29)

In particular, it is observed that the following identity has played a crucial role in the combined form of (C.28):

$$D_x \tilde{\rho}^{n+1} - \frac{1}{2} D_x (\tilde{\rho}^{n+1} - \tilde{\rho}^n) = \frac{1}{2} D_x (\tilde{\rho}^{n+1} + \tilde{\rho}^n). \tag{C.30}$$

As a consequence, the point-wise estimate (C.28) implies that

$$\left\langle \hat{\rho}^{n+\frac{1}{2}} D_x \tilde{S}^{n+\frac{1}{2}}, D_x (\tilde{\rho}^{n+1} + \tilde{\rho}^n) \right\rangle = \left\langle \frac{\hat{\rho}^{n+\frac{1}{2}}}{2A_x \rho^{n+1}} D_x (\tilde{\rho}^{n+1} + \tilde{\rho}^n), D_x (\tilde{\rho}^{n+1} + \tilde{\rho}^n) \right\rangle + \left\langle \hat{\rho}^{n+\frac{1}{2}} \zeta^{n+\frac{1}{2}}, D_x (\tilde{\rho}^{n+1} + \tilde{\rho}^n) \right\rangle.$$
(C.31)

Meanwhile, the point-wise ratio bound (5.44) reveals that

$$\left\langle \frac{\hat{\rho}^{n+\frac{1}{2}}}{2A_x \rho^{n+1}} D_x(\tilde{\rho}^{n+1} + \tilde{\rho}^n), D_x(\tilde{\rho}^{n+1} + \tilde{\rho}^n) \right\rangle \ge \frac{3}{8} \|D_x(\tilde{\rho}^{n+1} + \tilde{\rho}^n)\|_2^2. \tag{C.32}$$

In terms of the second term on the right hand side of (C.31), a direct application of the Cauchy inequality indicates that

$$\langle \hat{\rho}^{n+\frac{1}{2}} \zeta^{n+\frac{1}{2}}, D_x(\tilde{\rho}^{n+1} + \tilde{\rho}^n) \rangle \ge -\frac{1}{8} \|D_x(\tilde{\rho}^{n+1} + \tilde{\rho}^n)\|_2^2 - 2\|\hat{\rho}^{n+\frac{1}{2}} \zeta^{n+\frac{1}{2}}\|_2^2. \tag{C.33}$$

A further application of the Cauchy inequality gives

$$\|\hat{\rho}^{n+\frac{1}{2}}\zeta^{n+\frac{1}{2}}\|_{2}^{2} \leq 7\tilde{C}_{0}^{2}\check{C}_{1}^{2}(\|\tilde{\rho}^{n+1}\|_{2}^{2} + \|\tilde{\rho}^{n}\|_{2}^{2}) + 7\tilde{C}_{0}^{2}(\check{C}_{2}^{2}h^{2} + \check{C}_{3}^{2}\Delta t^{2})(\|D_{x}\tilde{\rho}^{n+1}\|_{2}^{2} + \|D_{x}\tilde{\rho}^{n}\|_{2}^{2})$$

$$+ \frac{28(\tilde{C}_{0}C^{*})^{2}(\tilde{C}_{0} + C^{*})^{8}(\varepsilon^{*})^{-10}}{25}h^{8}$$

$$\leq 7(\tilde{C}_{0}^{2}\check{C}_{1}^{2} + \tilde{C}_{0}^{2}\check{C}_{2}^{2}\hat{C}_{4}^{2} + \tilde{C}_{0}^{2}\check{C}_{2}^{2}\hat{C}_{3}^{2})(\|\tilde{\rho}^{n+1}\|_{2}^{2} + \|\tilde{\rho}^{n}\|_{2}^{2})$$

$$+ \frac{28(\tilde{C}_{0}C^{*})^{2}(\tilde{C}_{0} + C^{*})^{8}(\varepsilon^{*})^{-10}}{25}h^{8},$$
(C.34)

in which the inverse inequalities, $\Delta t \|\nabla_h f\|_2 \leq \hat{C}_3 \|f\|_2$ and $h\|\nabla_h f\|_2 \leq \hat{C}_4 \|f\|_2$ (with the linear refinement requirement $\lambda_1 h \leq \Delta t \leq \lambda_2 h$), have been applied. Therefore, a substitution of (C.32)-(C.34) into (C.31) yields

$$\gamma \langle \hat{\rho}^{n+\frac{1}{2}} D_x \tilde{S}^{n+\frac{1}{2}}, D_x (\tilde{\rho}^{n+1} + \tilde{\rho}^n) \rangle \geq \frac{\gamma}{4} \|D_x (\tilde{\rho}^{n+1} + \tilde{\rho}^n)\|_2^2 - \check{C}_5 (\|\tilde{\rho}^{n+1}\|_2^2 + \|\tilde{\rho}^n\|_2^2) - Q^{(0)} h^8,$$

with

$$\check{C}_5 = 14\gamma (\tilde{C}_0^2 \check{C}_1^2 + \tilde{C}_0^2 \check{C}_2^2 \hat{C}_4^2 + \tilde{C}_0^2 \check{C}_2^2 \hat{C}_3^2), \quad Q^{(0)} = \frac{56\gamma (\tilde{C}_0 C^*)^2 (\tilde{C}_0 + C^*)^8 (\varepsilon^*)^{-10}}{25}.$$

The nonlinear diffusion error estimates in the y and z directions could be performed in the same manner. This completes the proof of Proposition 5.6, by taking $\tilde{C}_1 = 3\tilde{C}_5$ and $M_1 = 3Q^{(0)}$.

Acknowledgements. This work is supported in part by the National Natural Science Foundation of China 12101264, Natural Science Foundation of Jiangsu Province BK20210443, High level personnel project of Jiangsu Province 1142024031211190 (J. Ding), National Science Foundation DMS-2012269 and DMS-2309548 (C. Wang), and National Natural Science Foundation of China 12171319 (S. Zhou).

References

- [1] H. Abels and M. Wilke. Convergence to equilibrium for the Cahn-Hilliard equation with a logarithmic free energy. *Nonlinear Anal.*, 67:3176–3193, 2007.
- [2] D. Acosta-Soba, F. Guillén-González, and J. Rodríguez-Galván. An unconditionally energy stable and positive upwind DG scheme for the Keller–Segel model. *J. Sci. Comput.*, 97(1):18, 2023.
- [3] S. Badia, J. Bonilla, and J. V. Gutiérrez-Santacreu. Bound-preserving finite element approximations of the Keller–Segel equations. *Math. Models Methods Appl. Sci.*, 33(03):609–642, 2023.
- [4] M. Bessemoulin-Chatard and A. Jüngel. A finite volume scheme for a Keller-Segel model with additional cross-diffusion. *IMA J. Numer. Anal.*, 34(1):96–122, 2012.
- [5] A. Blanchet, E. A. Carlen, and J. A. Carrillo. Functional inequalities, thick tails and asymptotics for the critical mass Patlak–Keller–Segel model. *J. Funct. Anal.*, 262:2142–2230, 2010.
- [6] A. Blanchet, J. A. Carrillo, D. Kinderlehrer, M. Kowalczyk, P. Laurencçot, and S. Lisini. A hybrid variational principle for the Keller-Segel system in ℝ². ESIAM: M2AN, 49(6):1553– 1576, 2015.
- [7] A. Blanchet, J. Dolbeault, and B. Perthame. Two-dimensional Keller-Segel model: Optimal critical mass and qualitative properties of the solutions. *Electron J. Differ. Equ.*, 44:1–33, 2006.
- [8] V. Calvez and L. Corrias. The parabolic-parabolic Keller-Segel model in \mathbb{R}^2 . Commun. Math. Sci., 6:417–447, 2008.
- [9] W. Chen, J. Jing, C. Wang, and X. Wang. A positivity preserving, energy stable finite difference scheme for the Flory-Huggins-Cahn-Hilliard-Navier-Stokes system. J. Sci. Comput., 92, 2022.
- [10] W. Chen, J. Jing, C. Wang, X. Wang, and S. M. Wise. A modified Crank-Nicolson numerical scheme for the Flory-Huggins Cahn-Hilliard model. *Commun. Comput. Phys.*, 31(1):60–93, 2022.
- [11] W. Chen, C. Wang, X. Wang, and S. M. Wise. Positivity-preserving, energy stable numerical schemes for the Cahn-Hilliard equation with logarithmic potential. *J. Comput. Phys. X*, 3:100031, 2019.
- [12] A. Chertock and A. Kurganov. A second-order positivity preserving central-upwind scheme for chemotaxis and haptotaxis models. *Numer. Math.*, 111(2):169–205, 2008.
- [13] W. Cong and J.-G. Liu. Uniform L^{∞} boundedness for a degenerate parabolic-parabolic Keller-Segel model. Discrete Contin. Dyn. Syst. Ser. B, 22:307–338, 2017.
- [14] A. Debussche and L. Dettori. On the Cahn-Hilliard equation with a logarithmic free energy. *Nonlinear Anal.*, 24:1491–1514, 1995.

- [15] J. Ding, C. Wang, and S. Zhou. Optimal rate convergence analysis of a second order numerical scheme for the Poisson–Nernst–Planck system. *Numer. Math. Theor. Meth. Appl.*, 12:607–626, 2019.
- [16] Y. Dolak and C. Schmeiser. The Keller–Segel model with logistic sensitivity function and small diffusivity. SIAM J. Appl. Math., 66(1):286–308, 2005.
- [17] J. Dolbeault and B. Perthame. Optimal critical mass in the two dimensional Keller-Segel model in \mathbb{R}^2 . C. R. Math. Acad. Sci. Paris, 339(9):611–616, 2004.
- [18] L. Dong, C. Wang, S. M. Wise, and Z. Zhang. A positivity-preserving, energy stable scheme for a ternary Cahn-Hilliard system with the singular interfacial parameters. *J. Comput. Phys.*, 442:110451, 2021.
- [19] L. Dong, C. Wang, H. Zhang, and Z. Zhang. A positivity-preserving, energy stable and convergent numerical scheme for the Cahn–Hilliard equation with a Flory–Huggins–deGennes energy. *Commun. Math. Sci.*, 17(4):921–939, 2019.
- [20] L. Dong, C. Wang, H. Zhang, and Z. Zhang. A positivity-preserving second-order BDF scheme for the Cahn-Hilliard equation with variable interfacial parameters. Commun. Comput. Phys., 28(3):967–998, 2020.
- [21] Y. Epshteyn. Upwind-difference potentials method for Patlak-Keller-Segel chemotaxis model. J. Sci. Comput., 53:689–713, 2012.
- [22] Y. Epshteyn and A. Izmirlioglu. Fully discrete analysis of a discontinuous finite element method for the Keller-Segel chemotaxis model. J. Sci. Comput., 40(1-3):211–256, 2009.
- [23] Y. Epshteyn and A. Kurganov. New interior penalty discontinuous galerkin methods for the Keller-Segel chemotaxis model. SIAM J. Numer. Anal., 47(1):386–408, 2008.
- [24] F. Filbet. A finite volume scheme for the Patlak–Keller–Segel chemotaxis model. *Numer. Math.*, 104:457–488, 2006.
- [25] J. Guo, C. Wang, S. M. Wise, and X. Yue. An H^2 convergence of a second-order convex-splitting, finite difference scheme for the three-dimensional Cahn-Hilliard equation. *Commun. Math. Sci.*, 14:489–515, 2016.
- [26] M. A. Herrero and J. J. L. Velázquez. A blow-up mechanism for a chemotaxis model. *Ann. Sc. Norm. Super.*, 24:633–683, 1997.
- [27] T. Hillen and K. Painter. Global existence for a parabolic chemotaxis model with prevention of overcrowding. Adv. in Appl. Math., 26(4):280–301, 2001.
- [28] T. Hillen and K. Painter. A user's guide to PDE models for chemotaxis. *J. Math. Biol.*, 58:183–217, 2009.
- [29] D. Horstmann. From 1970 until now: the Keller-Segel model in chemotaxis and its consequences I. Jahresber. *Deutsch. Math.-Verein.*, 105:103–165, 2003.

- [30] D. Horstmann. From 1970 until now: the Keller-Segel model in chemotaxis and its consequences II. Jahresber. *Deutsch. Math.-Verein.*, 106:51–69, 2004.
- [31] D. Horstmann and G. Wang. Blow-up in a chemotaxis model without symmetry assumptions. European J. Appl. Math., 12:159–177, 2001.
- [32] F. Huang and J. Shen. Bound/positivity preserving and energy stable scalar auxiliary variable schemes for dissipative systems: applications to Keller-Segel and Poisson-Nernst-Planck equations. SIAM J. Sci. Comput., 43:A1832–A1857, 2021.
- [33] W. Jäger and S. Luckhaus. On explosions of solutions to a system of partial differential equations modelling chemotaxis. *Trans. Amer. Math. Soc.*, 329:819–824, 1992.
- [34] E. Keller and L. Segel. Traveling bands of chemotactic bacteria: a theoretical analysis. *J. Theoret. Biol.*, 30(2):235–48, 1971.
- [35] H. Kozono and Y. Sugiyama. Global strong solution to the semi-linear Keller-Segel system of parabolic-parabolic type with small data in scale invariant spaces. *J. Differ. Equ.*, 246(7):2890–2904, 2009.
- [36] A. Kurganov and M. Lukáčová-Medvidov. Numerical study of two-species chemotaxis models. Discrete Contin. Dyn. Syst. Ser. B, 19(1), 2014.
- [37] C. Liu, C. Wang, S. Wise, X. Yue, and S. Zhou. A positivity-preserving, energy stable and convergent numerical scheme for the Poisson–Nernst-Planck system. *Math. Comput.*, 90(331):2071–2106, 2021.
- [38] C. Liu, C. Wang, S. M. Wise, X. Yue, and S. Zhou. A second order accurate numerical method for the Poisson-Nernst-Planck system in the energetic variational formulation. J. Sci. Comput., 97:23, 2023.
- [39] J.-G. Liu, L. Wang, and Z. Zhou. Positivity-preserving and asymptotic preserving method for 2D Keller-Segal equations. *Math. Comput.*, 87(311):1165–1189, 2016.
- [40] J.-G. Liu and J. Wang. Refined hyper-contractivity and uniqueness for the Keller-Segel equations. *Appl. Math. Lett.*, 52:212–219, 2016.
- [41] T. Nagai. Blowup of nonradial solutions to parabolic–elliptic systems modeling chemotaxis in two-dimensional domains. *J. Inequal. Appl.*, 2001:970292, 2001.
- [42] T. Nagai, T. Senba, and K. Yoshida. Application of the Trudinger-Moser inequality to a parabolic system of chemotaxis. *Funkcial. Ekvac.*, 40:411–433, 1997.
- [43] C. S. Patlak. Random walk with persistence and external bias. *Bull. Math. Biophys*, 15:311–338, 1953.
- [44] B. Perthame. Transport Equations in Biology. Frontiers in Mathematicas, Birkhäuser Basel, 2007.
- [45] J. Shen and J. Xu. Unconditionally bound preserving and energy dissipative schemes for a class of Keller-Segel equations. SIAM J. Numer. Anal., 58:1674–1695, 2020.

- [46] V. Thomée. Galerkin finite element methods for parabolic problems. Springer Science & Business Media, 2006.
- [47] J. Velázquez. Point dynamics in a singular limit of the Keller–Segel model 1: Motion of the concentration regions. SIAM J. Appl. Math., 64(4):1198–1223, 2004.
- [48] J. Velázquez. Point dynamics in a singular limit of the Keller–Segel model 2: Formation of the concentration regions. SIAM J. Appl. Math., 64(4):1224–1248, 2004.
- [49] C. Wang and S. M. Wise. An energy stable and convergent finite-difference scheme for the modified phase field crystal equation. SIAM J. Numer. Anal., 49:945–969, 2011.
- [50] S. Wang, S. Zhou, S. Shi, and W. Chen. Fully decoupled and energy stable BDF schemes for a class of Keller-Segel equations. J. Comput. Phys., 449:110799, 2022.
- [51] M. Winkler. Aggregation vs global diffusive behavior in higher-dimensional Keller-Segel model. J. Differ. Equ., 248(12):2889–2905, 2010.
- [52] M. Winkler. Finite-time blow-up in the higher-dimensional parabolic-parabolic Keller-Segel system. J. Math. Pures Appl., 100(5):748-767, 2013.
- [53] S. M. Wise, C. Wang, and J. Lowengrub. An energy stable and convergent finite-difference scheme for the phase field crystal equation. SIAM J. Numer. Anal., 47:2269–2288, 2009.
- [54] M. Yuan, W. Chen, C. Wang, S. M. Wise, and Z. Zhang. An energy stable finite element scheme for the three-component Cahn-Hilliard-Type model for macromolecular microsphere composite hydrogels. J. Sci. Comput., 87, 2021.
- [55] J. Zhang, C. Wang, S. M. Wise, and Z. Zhang. Structure-preserving, energy stable numerical schemes for a liquid thin film coarsening model. *SIAM J. Sci. Comput.*, 43:A1248–A1272, 2020.
- [56] G. Zhou and N. Saito. Finite volume methods for a Keller–Segel system: discrete energy, error estimates and numerical blow-up analysis. *Numer. Math.*, 135(1):265–311, 2017.